SMAC MIMETIC COMPOUND TREATMENT INDUCES TUMOUR REGRESSION AND SKELETAL MUSCLE WASTING

Jennifer Vineham

Thesis submitted to the
Faculty of Graduate and Postdoctoral Studies
In partial fulfillment of the requirements
For the M.Sc. degree in Cellular and Molecular Medicine

Department of Cellular and Molecular Medicine
Faculty of Medicine
University of Ottawa

ABSTRACT

Of all of the cancer patients throughout the world, approximately 50% of them are affected to some degree by cachexia. This syndrome involves significant skeletal muscle wasting, loss of adipose tissue and overall decrease in body weight in patients, particularly those with lung, pancreatic and gastric cancers. Cancer-induced cachexia is characterized by the presence of increased cytokines, notably TNF-α, IL-1β and IL-6. Most patients suffering of cancer-induced cachexia experience increased toxicity in response to chemotherapy, leading to fewer rounds of treatment and thus impeding the patients' chances for recovery. More research into effective treatments for cancer-induced cachexia would therefore be indispensable.

The inhibitor of apoptosis proteins (IAPs) have emerged as important cancer targets, primarily because of their roles as caspase inhibitors and regulators of NF-κB signalling. Small molecule IAP antagonists known as Smac mimetic compounds (SMCs) are currently in stage I/II clinical trials. They function by targeting cIAP1 and cIAP2 (and to a lesser extent, XIAP) resulting in a cytokine mediated death response in cancer cells. SMCs induce the production of TNF-α, a cytokine with which SMCs can potently synergize. However, limited efficacy occurs in some cancer cell lines (presumably because TNF-α cannot be induced in an autocrine fashion) and an exogenous source of the cytokine, such as that induced by using an oncolytic virus, is required. Notably, TNF-α (initially known as "cachectin") is known to play a significant role in the induction of skeletal muscle atrophy. We therefore wanted to examine the effects of TNF-α induction by SMC and oncolytic virus co-treatment on both tumour regression and skeletal muscle in tumour bearing mice.

We investigated the effects of SMC treatment on Lewis Lung Carcinoma (LLC) and B16F10 melanoma cell lines, both of which have been shown to be established cachectic cancer cell lines. Our *in-vitro* analysis of LLC and B16F10 cells revealed that LLC cells are sensitive to SMC and TNF-α co-treatment whereas B16F10 cancer cells remain resistant. SMC treatment, in combination with an oncolytic virus, VSVΔ51, increased tumour regression and survival time in LLC tumour bearing mice. Based on findings from previous studies, we investigated the role of cellular FLICE-like inhibitory protein (c-FLIP) in the resistance of the B16F10 melanoma cell line to SMC treatment. We were able to determine that the down-regulation of c-FLIP sensitizes the B16F10 cells to SMC and TNF-α induced cell death.

In extending these findings, we found that SMC treatment alone can cause skeletal muscle wasting in the tibialis anterior muscle of LLC tumour bearing mice. However, the atrophic response was observed to be minimal as documented by a slight but significant decrease (approximately 10%) in muscle fibre cross-sectional area. Moreover, no biochemical evidence of muscle atrophy, as visualized by changes in the expression of myosin heavy chain (MHC) and Muscle RING Finger protein 1 (MuRF1), was found. Regardless, we speculate that the impact of SMC treatment on muscle wasting would be transient and reversible, and propose that the benefits of such a combination immunotherapy would greatly outweigh the risks.

TABLE OF CONTENTS

Chapter 2: Materials and Methods

Chapter 4: Discussion

LIST OF TABLES

LIST OF FIGURES

LIST OF ABBREVIATIONS

Akt	Protein kinase B
AVPI	Alanine-valine-proline-isoleucine
BAFF	B cell-activating factor
Bcl-2	B-cell lymphoma 2
BIR	Baculoviral IAP repeat
c/EBPβ	CCAAT/enhancer binding protein β
cIAP1/2	Cellular inhibitor of apoptosis-1/2
c-FLIP	Cellular FLICE (FADD-like interleukin 1β-converting enzyme) inhibitory protein
CM	Conditioned media
CpG	CpG oligodeoxynucleotide
DMD	Duchenne muscular dystrophy
DMEM	Dulbecco's modified Eagle medium
DMSO	Dimethyl sulfoxide
DR-4/5	Death receptor 4/5
ERK	Extracellular signal-regulated kinase
FADD	Fas-associated death domain
FBS	Fetal bovine serum
GAPDH	Glyceraldehyde phosphate dehydrogenase
HSV	Herpes simplex virus
IAP	Inhibitor of apoptosis
IFN-β/γ	Interferon-β/γ

IKKα/β/γ	Inhibitor of IκB kinase-α/β/γ
IL-1β/6	Interleukin-1β/6
IRF	IFN response factor
IT	Intratumeral
IV	Intravenous
LLC	Lewis lung carcinoma
MAFbx	Muscle atrophy F-box
Mcl-1	Myeloid cell leukemia sequence 1
MHC	Myosin heavy chain
MuRF1	Muscle RING Finger protein 1
NEMO	NF-κB essential modulator
NF-κB	Nuclear factor-κB
NIK	NF-κB interacting protein
NK	Natural killer
OCTC	Optimal cutting temperature compound
PARP	Poly (ADP-ribose) polymerase
PBS	Phosphate-buffered saline
PI3K	Phosphatidylinositol 3-kinase
PIF	Proteolysis-inducing factor
Poly(I:C)	Polyinosine-polycytidylic
RASSF1A	Ras-association domain-containing protein 1 isoform A
RING	Really interesting new gene
RIP1	Receptor-interacting protein-1

RLR	RIG-I-like receptor
RT-PCR	Reverse transcription polymerase chain reaction
siRNA	Short interfering RNA
SMC	Smac-mimetic compound
TA	Tibialis anterior
TBS-T	Tris-phosphate buffered saline with tween
TLR	Toll-like receptor
TNF	Tumour necrosis factor
TNF-R1	TNF receptor 1
TRADD	TNF-receptor1-associated death domain
TRAF	TNF receptor associated factor
TRAIL	TNF-related apoptosis-inducing ligand
TRAIL-R1/2	TRAIL receptor 1/2
TWEAK	TNF-like weak inducer of apoptosis
VSV	Vesicular stomatitis virus
XIAP	X-linked inhibitor of apoptosis

ACKNOWLEDGEMENTS

I would first and foremost like to thank Dr. Robert Korneluk for giving me the chance to fulfill my Master of Science degree. This challenge has provided me with an exceptional learning opportunity and an occasion for personal growth. Dr. Korneluk, you have been such a supportive and encouraging supervisor; I am grateful to have had the occasion to learn from a true role model in the scientific community.

Thank you as well to my TAC committee members, Drs. Nadine Wiper-Bergeron and Luc Sabourin, for their guidance and suggestions along the way. A special thank you is for Janelle Holbrook who was my mentor when I started as a summer student and who has largely contributed to the experiments in my thesis. Thank you as well to the other members of my lab, past and present, who answered all of my questions, helped with experiments and provided ideas: Dr. Emeka Enwere, Dr. Herman Cheung, Dr. Eric Lacasse, Dr. Andrew Smith, Nathalie Earl, Martine St-Jean, Jeff Nuyens, Caroline Beauregard, Nadine Adam and notably Dr. Shawn Beug, a great scientist with whom I appreciate having had the chance to learn from. I also appreciate the hard work of our lab co-ordinator Lynn Kelly. Thank you as well to our funding agencies, the Canadian Institutes of Health Research, the Ottawa Regional Cancer Foundation, the Children's Hospital of Eastern Ontario Foundation and the Muscular Dystrophy Association.

Thank you to my family, to my Mom, Paulette, my Dad, Terry, and my brother, Kyle, for their support along the way. But most importantly, thank you to my fiancé, Habib Abou-Hamad, without whom I most definitely would not be where I am today. Thank you for always believing in me and for motivating me to bring forward the best in myself. I am so proud of everything that I have accomplished.

CHAPTER 1: INTRODUCTION

1.1 The Inhibitors of Apoptosis

1.11 Characterization of the Inhibitors of Apoptosis

The human family of inhibitors of apoptosis (IAPs) were discovered nearly twenty years ago and since then eight members have been identified (Figure 1, Liston *et al*., 1996). The most studied are the X-linked inhibitor of apoptosis (XIAP) as well as the cellular inhibitors of apoptosis-1 and -2 (cIAP-1 and -2). These IAPs are both suppressors of programmed cell death and regulators of signal transduction pathways (Gyrd-Hansen *et al*., 2008). The IAPs suppress apoptosis caused by different stimuli such as growth factor withdrawal or radiation. This gene family is characterized by each member containing three N-terminal baculoviral IAP repeat (BIR) domains, which regulate the activity of initiator and effector caspases (Fulda and Vucic, 2012). XIAP has the ability to directly inhibit caspases whereas cIAP1 and 2 primarily inhibit caspases via an indirect method. The IAPs also control signalling by acting as ubiquitin E3 ligases via their C-terminal Really Interesting New Gene (RING) domain (Wu *et al*., 2007).

1.12 The IAPs Suppress Programmed Cell Death

The IAPs were first discovered to be suppressors of programmed cell death (reviewed in Gyrd-Hansen *et al*., 2008). Programmed cell death is the pre-determined end point of a cell in a multicellular organism. This process encompasses different pathways of cell death including apoptosis and the more recently described processes of necroptosis and autophagy. Most characterized is apoptosis, a cell death process initially identified by the morphological changes to the cell. During apoptosis, a cell will first undergo shrinkage and membrane blebbing followed by chromatin condensation and

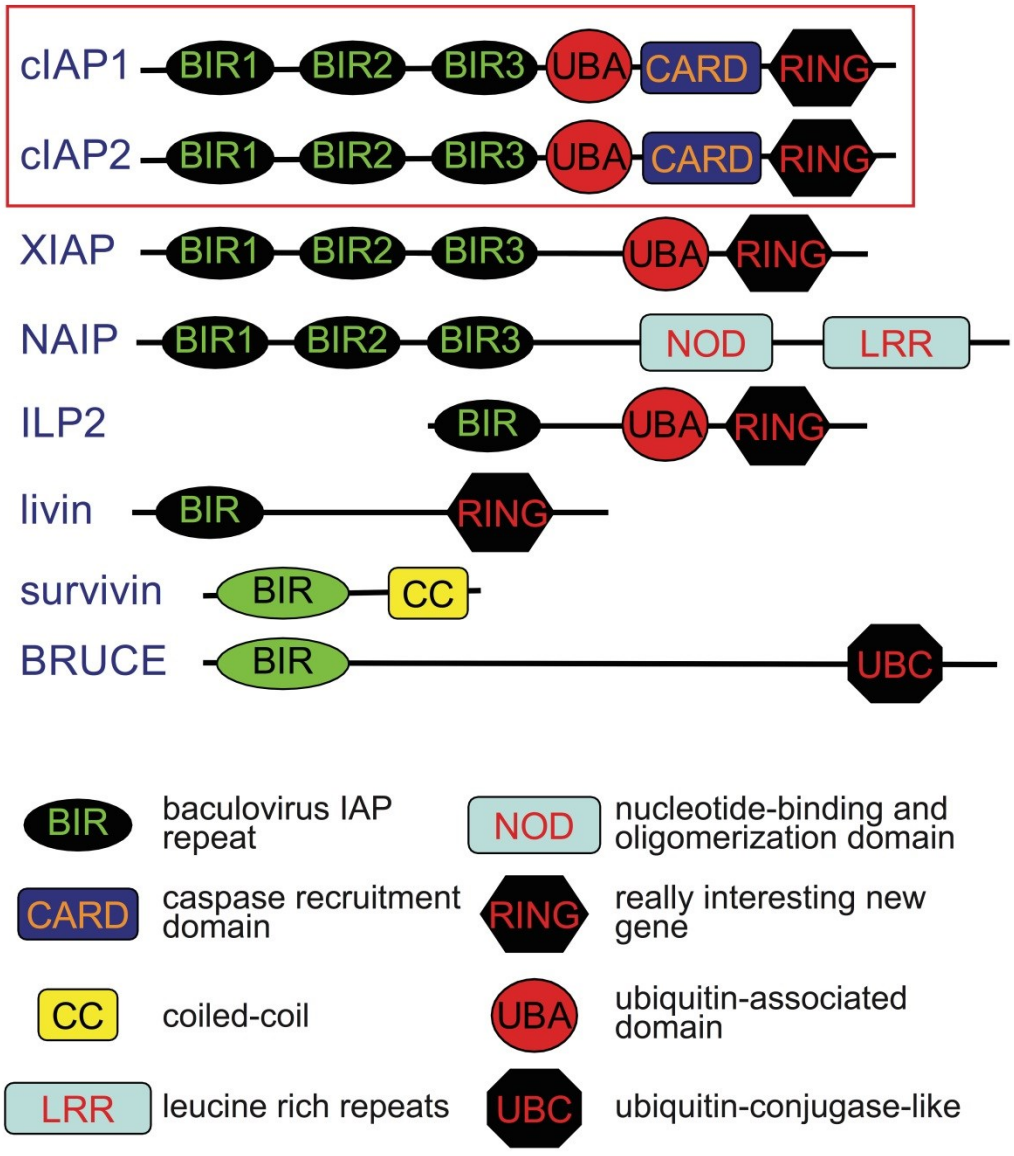

Figure 1. Characteristics of the human family of inhibitors of apoptosis.

Each member of the IAP gene family contains at least one canonical BIR domain. These are important for protein-protein interactions with factors such as caspases and Smac. The RING domain provides IAP family members with E3 ubiquitin ligase activity. Certain IAP members contain a UBA domain which is responsible for binding ubiquitin and polyubiquitinated chains. Finally, IAP members can be found to contain a CARD domain which inhibits the E3 ligase function of the IAPs when in a steady state.

nuclear fragmentation (Micheau, 2003). The process of apoptosis is a very important and normal part of embryonic development and tissue homeostasis (Ranjan *et al*., 2012). Mutations in this pathway can lead to inappropriate inhibition of apoptosis and can thus lead to the growth of unwanted cells that have the ability to become cancerous. Both intrinsic (mitochondria-meditated) and extrinsic (receptor-mediated) apoptotic pathways can lead to cell death, although these occur through very different stimuli and signalling pathways (Figure 2). Regardless, the two pathways often converge on similar downstream pro-apoptotic proteins to cause cell death (Matthews *et al*., 2012; Schultz and Harrington, 2003).

Activation of the intrinsic pathway occurs from cellular stresses such as ultraviolet-irradiation, chemotherapeutic drugs or the removal of growth factors. When any of these occur, the BH3-only proteins initiate intrinsic apoptotic cell death by binding to pro-survival proteins which release Bak and/or Bax. These proteins then form pores and cause holes in the outer mitochondrial membrane, releasing a number of mitochondrial proteins into the cytoplasm including cytochrome c and Smac. Smac can directly bind to and inhibit the IAPs. The apoptosome is formed by the interaction of cytochrome c, pro-caspase-9 and Apaf-1. Once caspase-9 is activated, achieved by its interaction with the apoptosome, it proceeds to activate effector caspases-3 and -7 leading to cell death (Matthews *et al*., 2012; Schultz and Harrington, 2003).

Extrinsic apoptotic pathway activation results when a tumour necrosis factor (TNF) superfamily member binds to its receptor. The human TNF superfamily consists of 19 ligands and 29 receptors. The TNF superfamily is comprised of important factors that play a role in many cellular processes such as the regulation of immune cell function and

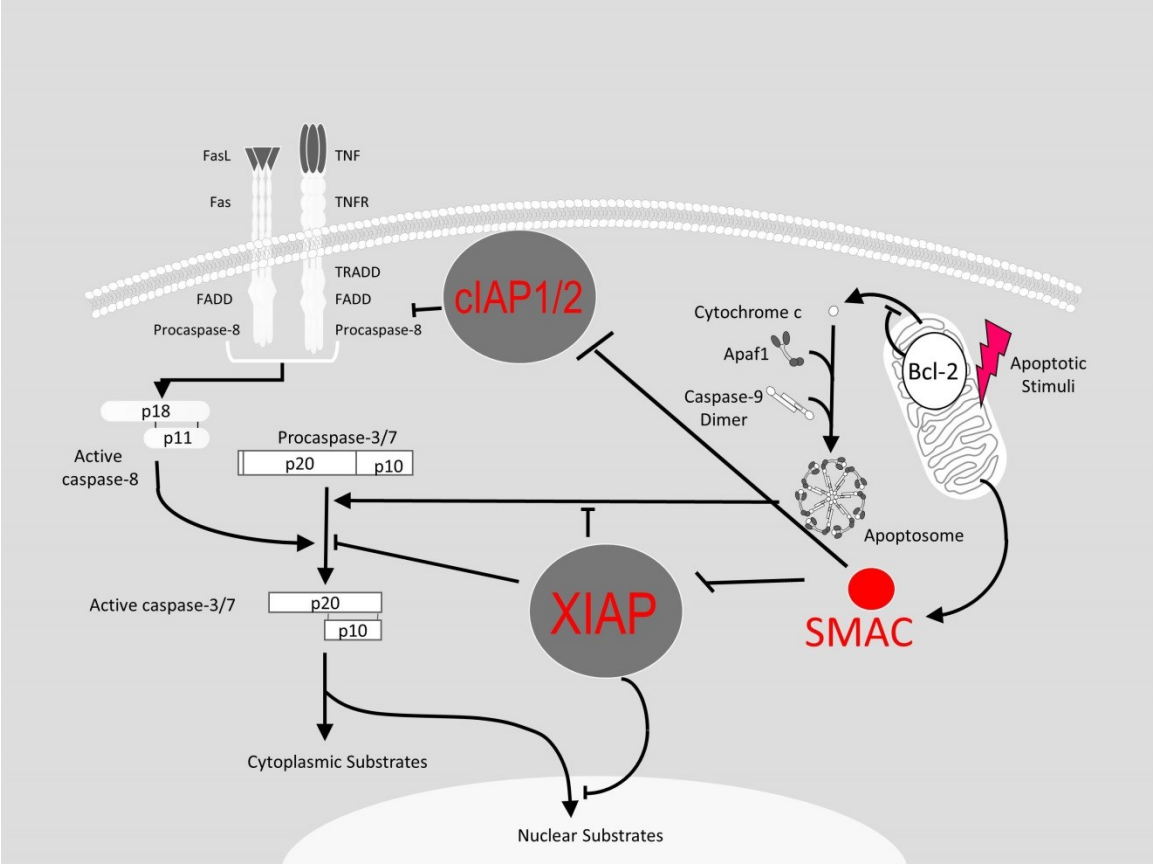

Figure 2. IAP antagonism of the intrinsic and extrinsic apoptotic pathway.

Second mitochondria-derived activator of caspases (SMAC) is released from the mitochondria in response to apoptotic stimuli and inhibits caspase mediated cell death by binding to the BIR3 domain of XIAP and cIAP1/2. The cIAPs predominantly antagonize the extrinsic apoptotic pathway (receptor mediated) whereas XIAP antagonizes later steps in the intrinsic (mitochondria mediated) and extrinsic apoptotic pathway.

apoptosis. They are also known to be involved in cancer and many autoimmune diseases. In fact, TNF superfamily member TNF-α, when first discovered, was called "cachectin" and was proposed to be the main factor that induced cachexia. The TNF superfamily ligands that are involved in the extrinsic pathway of caspase activation all contain a death domain. These domains are responsible for recruiting caspase-interacting proteins (Croft *et al*., 2013). When Fas ligand (FasL), TNF-related apoptosis-inducing ligand (TRAIL) or TNF-α bind to their receptors Fas receptor (FasR), TRAIL receptor 1/death receptor 4 (TRAIL-R1/DR-4), TRAIL receptor 2/death receptor 5 (TRAIL-R2/DR-5) or TNF receptor 1 (TNF-R1), respectively, the receptors will oligomerize at the cell membrane inducing a signal that attracts Fas-associated death domain (FADD) to the complex. Pro-caspase-8 and pro-caspase-10 can then bind to FADD forming the ripoptosome. The formation of the ripoptosome induces the cleavage of caspases-8 and -10 which activates the caspase cascade and in turn cleaves the effector caspase-3 leading to cell death (Matthews *et al*., 2012; Schultz and Harrington, 2003).

1.13 The IAPs Modulate the Nuclear Factor-κB Pathway

In addition to playing a role in the inhibiton of cell death as caspase inhibitors, both cIAP1 and cIAP2 have been discovered to be important modulators of the nuclear factor-κB (NF-κB) pathway (Mahoney *et al*., 2008; reviewed in LaCasse *et al*., 2008). The NF-κB pathway controls many different cellular processes such as cell death, cell growth, inflammation and angiogenesis, to name a few (Tornatore *et al*., 2012). The classical ligand-dependent NF-κB pathway involves the binding of tumour necrosis factor-α (TNF-α) which activates the inhibitor of IκB kinase (IKK) complex, which is composed of IKKα/IKKβ/NF-κB essential modulator (NEMO) subunits. This complex then

phosphorylates the IκB proteins (Ghosh *et al*., 2012). Proteasomal degradation frees the NF-κB/Rel complex, which can then translocate to the nucleus and allow transcription of target genes (Siomek, 2012). Examples of target genes of the classical NF-κB pathway include c-FLIP, Bcl-2 and Bcl-x_L, XIAP and cIAP2 (Piao *et al*., 2012). The alternative NF-κB pathway involves signalling through receptors to activate NF-κB interacting protein (NIK) which then activates the IKKα complex (Sun, 2012). This complex phosphorylates the C-terminal residues of p100. The p100 is then ubiquitinated and processed into p52 allowing a p52/RelB dimer to form and to translocate to the nucleus where transcription of target genes, which have yet to be identified, can occur (Bakkar and Guttridge, 2010).

Both cIAP1 and cIAP2 are important modulators of the NF-κB pathway in that they positively regulate the ligand-dependent canonical NF-κB pathway and negatively regulate the non-canonical NF-κB pathway (Figure 3). For example, the binding of TNF-α to its receptor, TNF-R1, allows for the recruitment of TNF-receptor1-associated death domain (TRADD), TNF receptor associated factor 2 and 5 (TRAF2 and TRAF5), cIAP1 and cIAP2 (Darding *et al*., 2011). The E3 ubiquitin ligase activity of cIAP1/2 regulates the ubiquitination of receptor-interacting protein 1 (RIP1) by adding K63 ubiquitin chains to RIP1. The K63 ubiquitin chains that are added to RIP1 are scaffolds for the assembly of the IKKα-IKKβ-IKKγ complex which in turn activates the classical NF-κB pathway following the pathway previously described (Bertrand *et al*., 2008; reviewed in Beug *et al*., 2012).

In contrast, the alternative pathway is typically suppressed in most cell types due to the constitutive degradation of NIK. The E3 ubiquitin ligase activity of cIAP1/2 results

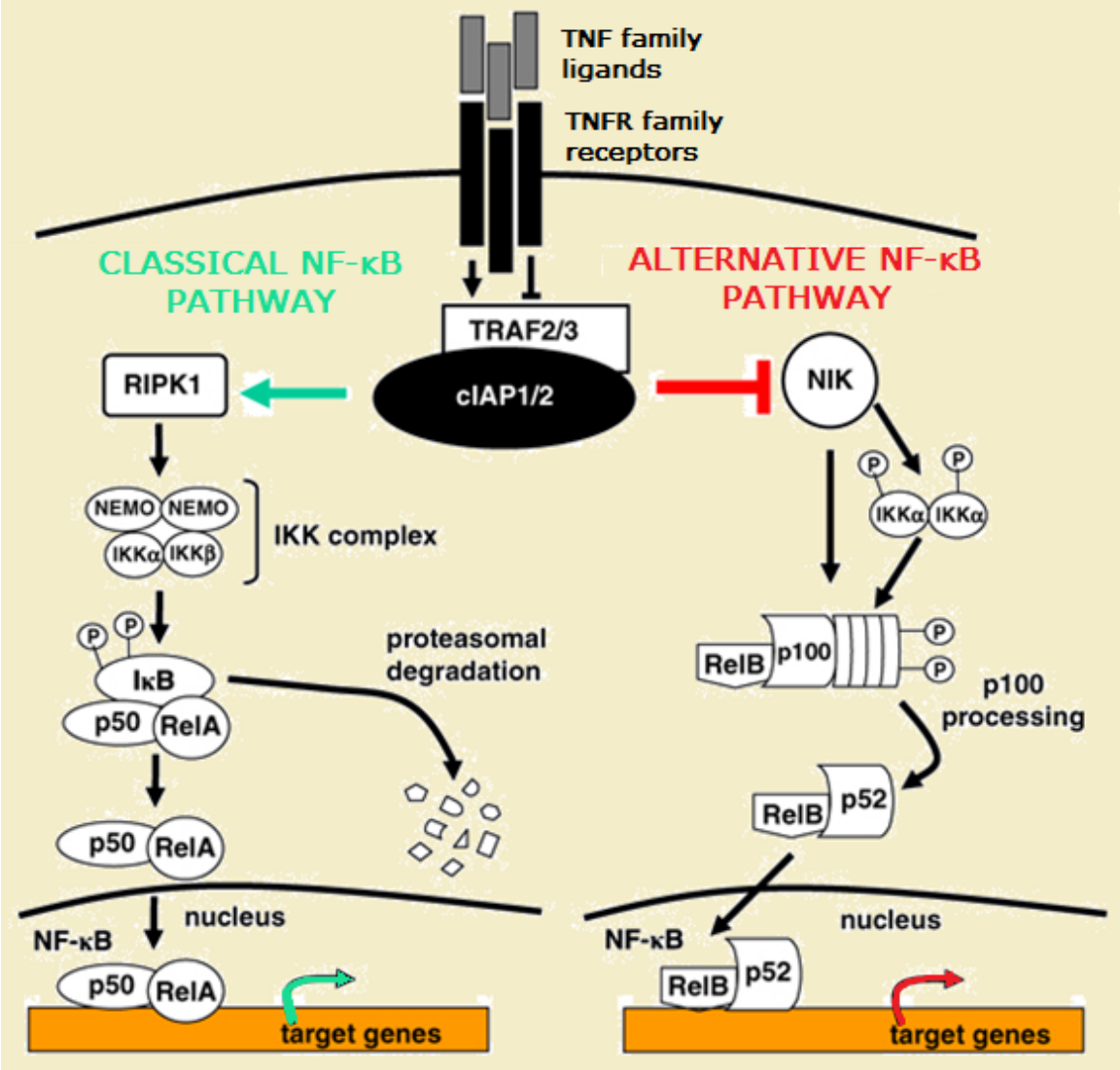

Figure 3. cIAP1/2 regulation of the classical and the alternative NF-κB pathways.

The IAPs positively regulate the classical NF-κB pathway whereas they negatively regulate the alternative NF-κB pathway. The classical pathway is mediated primarily by the binding of TNF-α to TNF receptor 1 (TNF-R1) which stimulates the recruitment of TNF related associated factors (TRAFs) and in turn, cIAP1/2 join the complex. The IAPs add K63-linked polyubiquitin chains to RIP1, which can then signal to activate the IKK complex. In turn, IκB is phosphorylated and subsequently degraded allowing the translocation of p50/RelA into the nucleus, thus producing target genes. Conversely, the alternative pathway is mediated by the binding of TWEAK to its receptor Fn-14. cIAP1/2 target NIK for degradation but SMCs, which induce the proteosomal degradation of the IAPs causes activation of the alternative NF-κB pathway. NIK levels accumulate and IKKα is phosphorylated, which phosphorylates p100 which is then partially processed to p52. The p52/RelB heterodimer then translocates into the nucleus to produce target genes.

in the addition of K48 ubiquitin chains to NIK, leading to its proteosomal degradation. However, when ligands such as B cell-activating factor (BAFF), CD40L or TNF-like weak inducer of apoptosis (TWEAK) bind to their receptors, the cIAPs are degraded, and as a result, NIK levels accumulate. Consequently, this leads to the activation of the alternative pathway (Darding and Meier, 2011; reviewed in Beug *et al*., 2012). Taken together, the depletion of the cIAPs results in the activation of the alternative NF-κB pathway and in this case, TNF-α cannot induce cIAP1/2-mediated RIP1 ubiquitination thereby suppressing classical NF-κB pathway activity. However, de-ubiquitinated RIP1 can then associate with caspase-8 and FADD forming the ripoptosome, thus stimulating the extrinsic apoptotic pathway (Cheung *et al*., 2010).

As described above, the many pathways that the cIAPs induce, results in many different cell fates and outcomes and therefore being able to experimentally modify the expression of the cIAPs is proving to be a very powerful tool in the development of therapeutic drugs.

1.2 IAP Inhibitors

1.21 Smac mimetic Compounds Function as IAP Antagonists

A method to selectively modify IAP expression for experimental purposes has been achieved via Smac mimetic compounds. Smac mimetic compounds, hereafter referred to as SMCs, are small molecule IAP antagonists. SMCs were designed to mimic a tetrapeptide alanine-valine-proline-isoleucine (AVPI) amino acid sequence contained in Smac (Chen and Huerta, 2009). The AVPI sequence allows for the binding to the IAPs via their BIR domains. SMCs come in two distinct classes, either as monomers or as dimers, which contain two AVPI mimetics tethered by a linker. SMCs bind to cIAP1 and

2 with much more affinity than binding to XIAP and are therefore antagonized more effectively (Flygare and Fairbrother, 2010). SMCs work by activating the ubiquitin E3 ligase domain of both cIAP1 and 2, and thereby induce auto-ubiquitination and their subsequent proteosomal degradation. This in turn induces autocrine TNF-α signalling in some cancer cell lines, activating caspase-8 and causing apoptosis of the cells (Wu *et al*., 2007).

There are five different SMC compounds that have been approved for clinical trials. The first SMC that was used in clinical trials was GDC-0152 which was developed by Genentech. The other SMCs include: HGS-1029 (Aegera Therapeutics), TL32711 (TetraLogic Pharmaceuticals), AT-406 (Ascenta Therapeutics), (Wang, 2011; Katragadda *et al*., 2013) and LCL161 (Novartis), (Fulda, 2014). LCL161 is perhaps the most advanced in clinical trial evaluation and is one of the SMCs that we use most often in our studies.

Smac mimetics are most effective when used in combination therapy. Most effective combinations are seen with death ligands such as TNF-α or TRAIL, although combinations with standard chemotherapeutic drugs such as cisplatin and taxol have been widely documented (Probst *et al*., 2010; Xu *et al*., 2011). Krepler and collegues studied the response of different melanoma cell lines to SMC and showed that all 18 cell lines studied were resistant to treatment with either the dimeric SMC, birinapant or TNF-α. Combined treatment with the SMC and TNF-α resulted in the sensitization to death in 12 of the 18 melanoma cell lines. For the six melanoma cell lines that remained resistant against this treatment, it was hypothesized by the authors that the resistance factor may be cellular FLICE (FADD-like interleukin 1β-converting enzyme) inhibitory protein (c-

FLIP), myeloid cell leukemia sequence 1 (Mcl-1) or B-cell lymphoma-2 (Bcl-2), all anti-apoptotic proteins (Krepler *et al*., 2013).

SMC treatment, either as stand-alone or combination therapy has been proven effective against many different human cancer cell lines including hepatocellular carcinoma, breast, colon, prostate and ovarian carcinoma (Zhang *et al*., 2012). More recently, a promising and effective therapy has been reported in which SMCs have been used in combination with oncolytic viruses (Beug *et al*., 2014). Oncolytic viruses are replication-competent viruses that can selectively damage cancerous cells without infecting normal, healthy cells. The viruses take over the cell death machinery of the infected cancer cell and use the resources to replicate, creating new virus particles before killing the cancer cell. The benefit of oncolytic viruses is that they can also induce the death of non-infected cancer cells via indirect methods. They target tumour blood vessels and can also amplify anti-cancer immune responses, thus creating obstacles for non-infected cancer cells which eventually lead to their death. Vesicular stomatitis virus (VSV) (Stojdl *et al*., 2003) and herpes simplex virus (HSV) are oncolytic viruses that can be manipulated to specifically target tumour cells (Russell *et al*., 2012). Overall, oncolytic viruses can induce an increased immune response against cancer cells. Moreover, they are relatively specific in their actions against cancer cells, leaving normal healthy cells unharmed and can target other aspects of tumour growth such as angiogenesis. Based on these factors, it was hypothesized that an oncolytic virus would provide a pro-inflammatory environment which would support and perhaps even enhance the function of Smac mimetics. Dr. Shawn Beug, a post-doctoral fellow in the Korneluk laboratory, used rhabdovirus VSVΔ51 in combination with Smac mimetics and found

that there was significant synergy between the two to the extent that it cured mice from certain cancerous tumours (Beug *et al*., 2014). The combination treatment was found to function with many thousand fold efficiency better than treating with oncolytic virus alone. It was determined that the increase in efficiency occurred because the VSVΔ51 oncolytic virus systemically induced TNF-α, which then synergized with SMC treatment to effectively kill tumour cells (Beug *et al*., 2014).

The responses of cancer cell lines to Smac mimetics appear to hold true whether using different SMC compounds or different cancer cell lines and these responses can be categorized into four main outcomes (Table 1). In a study published by our group, Dr. Cheung found that of the 51 human cancer cell lines he tested, 90% of them were resistant to the stand-alone treatment with SMCs (Cheung *et al*., 2009). When TNF-α or TRAIL was added in combination with SMCs, 48% and 55% of the cell lines became sensitive, respectively. The reason as to why certain cell lines were sensitive to the combination treatment and others were not seemed to be the continued presence of one protein, c-FLIP. For the cell lines with continued resistance in the presence of SMCs and TNF-α/TRAIL, 50% of them became sensitized to SMC and TNF-α/TRAIL co-treatment when c-FLIP was down-regulated. This reveals that a possible target for resistant cancer cell lines is the death factor c-FLIP (Cheung *et al*., 2009).

1.22 c-FLIP is the Resistance Factor in IAP-mediated Caspase Cell Death

c-FLIP is a non-active homologue of caspase-8 that plays a role in apoptosis, necroptosis and autophagic cell death (Silke and Strasser, 2013). c-FLIP has 13 splice variants but only three of these variants result in actual peptides. One of these is c-FLIP$_L$ referred to as the long isoform of 55kDa; another is c-FLIP$_S$, known as the short isoform

Table 1

The Four Categories of Responses of Cell Lines to Smac Mimetics

CATEGORIES	CELL LINES THAT RESPOND	EXAMPLES
1 – RESPOND OUTRIGHT	5%	Breast Cancer Carcinoma • MDA-MB-231 (human)
2 – REQUIRE ADDITION OF TNF-ALPHA OR TRAIL	50%	Lung Carcinoma • LLC (mouse)
3 – REQUIRE C-FLIP KNOCKDOWN AND ADDITION OF TNF-ALPHA OR TRAIL	40%	Melanoma • B16F10 (mouse)
4 – REMAIN UNRESPONSIVE	5%	Neuroblastoma • Lan 1 (human)

Information Extracted From:

Cheung HH, Mahoney DJ, Lacasse EC, Korneluk RG. 2009. Down-regulation of c-FLIP Enhances death of cancer cells by smac mimetic compound. *Cancer Res*, 69:7729-38.

with 26kDa and lastly there is c-FLIP$_R$ containing 24kDa. c-FLIP$_L$ is found in the highest quantity in the heart, skeletal muscle, lymphoid and kidney tissues. c-FLIP$_L$ contains two death effector domains in the amino terminus and possesses a caspase homologous domain at the carboxy terminus. This latter characteristic allows for c-FLIP$_L$ resemblance of capases-8 and -10, however, it is not enzymatically active due to substitutions of the critical amino acids (Safa, 2012; Dutton *et al*., 2006; reviewed in Oztürk *et al*., 2012). c-FLIP$_L$ competes with procaspase-8 for binding to FADD and in this way inhibits the activation of the ripoptosome. The ripoptosome is a large complex made up of caspase-8, FADD, RIP1, RIP3 and in certain cell types, c-FLIP. Once formed, the ripoptosome induces the caspase cascade that leads to cell death. c-FLIP$_L$ can more potently inhibit cell death by Fas and TRAIL induced cell death compared to c-FLIP$_S$. c-FLIP$_S$, instead, works by inhibiting caspase-8 activation by forming a heterodimer and although not directly inhibiting the formation of the ripoptosome, c-FLIP$_S$ still succeeds in inhibiting cell death (Fulda, 2013).

Research has shown that c-FLIP is dysregulated in many different auto-immune diseases (e.g. multiple sclerosis, Alzheimer's disease, diabetes mellitus and rheumatoid arthritis) and certain types of cancer. c-FLIP has been found to be up-regulated in many different cancer types such as gastric adenocarcinoma, melanoma as well as in pancreatic, ovarian and prostate carcinomas (Micheau, 2003; Yang, 2008; Bagnoli *et al*., 2010). For example, the average c-FLIP expression level in patients with squamous cervical carcinoma was reported at 82.1%. This is nearly a seven fold increase compared to the c-FLIP expression level (12.5%) in normal patients (Ili *et al*., 2013). An increased c-FLIP expression level has been largely correlated with more aggressive tumours as well as

poor prognosis (Scudiero *et al*., 2012). This has led to much research in targeting c-FLIP in order to treat cancer.

In one study in which a panel of human ovarian cancer cell lines was analyzed, the expression level of c-FLIP was correlated with other proteins, specifically death receptors 4 and 5 (DR4 and DR5) and caspase-8. Duiker and co-workers concluded that c-FLIP was inhibiting death receptor induced apoptosis (Duiker *et al*., 2010). Many studies have found that a reduction in the level of c-FLIP protein expression correlated with an increase in sensitivity to TRAIL-induced cell death (Geserick *et al*., 2008; White *et al*., 2006; Brooks and Sayers, 2005). The reason that c-FLIP is more easily targeted in certain cell lines over others remains yet to be investigated (Perego *et al*., 2006).

The proposed mechanism is that if c-FLIP is down-regulated, it can no longer inhibit the ripoptosome and RIP1 can associate with FADD and caspase-8 allowing for caspase mediated cell death. Also knocking down c-FLIP via siRNA in certain cancer cell lines has been found to induce apoptosis (Cheung *et al*., 2010). The fact that the activation of the classical NF-κB pathway induces the expression of c-FLIP suggests that this pathway could be targeted in the hopes of reducing c-FLIP levels and thus again allowing for cell death to occur (Micheau *et al*., 2001).

1.3 The Impact of SMCs on Skeletal Muscle

1.31 Skeletal Muscle Development and the Potential for SMC Therapy

SMCs target cIAP1 and cIAP2 for degradation in the presence of cytokines, most notably TNF-α, and this loss of cIAP expression in cancer cells can lead to their apoptotic or necroptotic death (Wu *et al*., 2007). However, TNF-α is also known to be a major mediator of skeletal muscle atrophy (Petersen *et al*., 2007). Therefore, we wanted to

investigate the extent of wasting in skeletal muscle of LLC tumour bearing mice that were treated with SMC.

Skeletal muscle is known for its major role in allowing movement and producing force. Often forgotten is its role as a metabolism regulator. Skeletal muscle also stores glycogen and allows for amino acid catabolism (Yusuf and Brand-Saberi, 2012). Adult skeletal muscle is the result of a process known as myogenesis followed by cell fusion (Figure 4). The first step in the development of adult skeletal muscle begins with the differentiation of a $Pax3^{+}/Pax7^{+}$ progenitor population into satellite cells. Satellite cells are the muscle specific stem cells and will differentiate into myoblasts. These then further differentiate into mononuclear myocytes. Mononuclear myocytes will either fuse with pre-existing multi-nucleated myofibres or with other mononuclear myoctyes to form myotubes, which are immature myofibres. These eventually grow to become multinucleated contractile muscle fibres (Tran *et al*., 2013; reviewed in Buckingham *et al*., 2003 and Enwere *et al*., 2014). There are slow-twitch muscle fibres, such as the soleus muscle, that are characterized as being the category of muscles responsible for the continuous daily activity. There are also fast-twitch muscle fibres, such as the tibialis anterior muscle, which contain a variety of different types of fast-twitch muscles but all of which largely contribute to the movement and contractions of muscles used when performing more strenuous exercise. In response to different stimuli, the fast-twitch muscle fibres generally show a greater degree of atrophy than do slow-twitch muscle fibres (Schiaffino and Reggiani, 2011).

Primary myoblasts are widely used in *in-vitro* experiments as they most closely mimic the skeletal muscle environment. Primary myoblasts that are treated with either

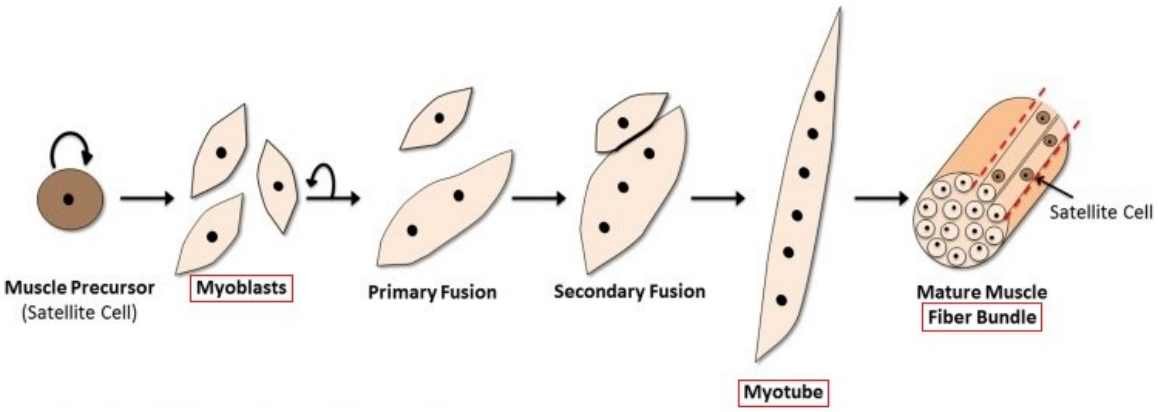

Figure 4. Skeletal myogenesis: from satellite cell to muscle fibre.

Upon stimulation, satellite cells, quiescent myogenic precursor cells, proliferate and differentiate into myoblasts. These myoblasts undergo primary fusion, the fusion of multiple myoblasts together to create multinucleated myocytes or myotubes. Finally, myoblasts fuse to existing myotubes during secondary fusion and these myotubes then align to form muscle fibres. Notably, the NF-κB pathway is known to regulate specific aspects of the differentiation process. The activation of the classical NF-κB is responsible for the proliferation of myoblasts whereas the activation of the alternative NF-κB pathway allows for primary fusion to begin.

Figure adapted from: Enwere EK, Lacasse EC, Adam NJ, Korneluk RG. 2014. Role of the TWEAK-Fn14-cIAP1-NF-κB Signaling Axis in the Regulation of Myogenesis and Muscle Homeostasis. *Front Immunol*, 5:34. Review.

C26 conditioned media (CM), a murine adenocarcinoma, or PC-3 CM, a human prostate carcinoma, both of which induce cachexia, experience a significant decrease in myosin heavy chain (MHC), myogenin and MyoD levels, all of which are muscle specific proteins. Myotubes treated with C26 CM experience a significant decrease in size compared to controls. PC-3 CM treatment of primary myoblasts inhibits differentiation of the muscle cells. Cytokines such as interleukin-1β (IL-1β), PIF (proteolysis-inducing factor) and TNF-α were found to be expressed in the conditioned media from the cancer cell lines and these are suggested to be primarily responsible for the atrophic phenotypes. (Johns *et al*., 2012; Tan *et al*., 2011; Jiang and Clemens, 2006).

Originally, TNF-α, was actually known as 'cachectin'. Cachectin was found to induce skeletal muscle atrophy in mice (Oliff *et al*., 1987) and inhibit myocyte differentiation (Guttridge *et al*., 2000; Ruan *et al*., 2002). Based on these studies, one could propose that SMC treatment, which on its own can induce TNF-α would induce or even exacerbate skeletal muscle atrophy, especially in cancers that are highly cachectic such as lung, pancreatic and gastric cancers. However, recent new findings may suggest that another outcome is possible.

One particular form of muscular dystrophy that has been extensively studied is Duchenne muscular dystrophy (DMD) which is caused by the loss of function of the protein dystrophin. The DMD murine model is the *Mdx* mouse, which harbors a nonsense point mutation in the dystrophin gene resulting in a truncated and unstable protein. In addition, *Mdx* mutant mice have three fold less satellite cells (Yusuf and Brand-Saberi, 2012). In a recent publication from our laboratory, Dr. Enwere studied *Mdx* mutant mice in the capacity of the NF-κB pathway (Enwere *et al*., 2013). He

generated a line of double mutant cIAP1 null/mdx mice and found that these mice sustained less damage to their muscles in the absence of cIAP1. Specifically, the loss of cIAP1 resulted in fewer damaged nuclei, reduced macrophage infiltration and better functioning contractile properties in mdx solei. The muscles themselves also showed increased endurance in response to exercise (Enwere *et al*., 2013).

Therefore, it may be that SMCs, which induce a high production of TNF-α, could have an atrophic effect on skeletal muscle. On the other hand, SMCs, which down-regulate the IAPs and lead to protective state in muscle, could result in resistance to the atrophic state caused by cancer-induced cachexia. Finally, SMC treatment of cancer patients could have absolutely no effect on skeletal muscle atrophy. In any event, the impact of SMC treatment on muscle in cancer-induced cachexia is an area worth studying.

1.32 Characteristics of Cancer-induced Cachexia

Skeletal muscle atrophy is defined as a decrease in the amount of protein content in the muscle, a decrease in the fibre diameter and a general increase in weakness of the muscles. The loss of protein is due to an increase in protein degradation and to a decrease in protein synthesis (Jackman and Kandarian, 2004).

Cachexia is mostly characterized by significant weight loss, severe muscle mass atrophy along with a drastic decrease in body fat. Many diseases or chronic conditions have been found to induce cachexia (Nedergaard *et al*., 2013; reviewed in Tisdale, 2005). These include AIDS, diabetes, renal failure, chronic obstructive pulmonary disease, sepsis, congestive heart failure and cancer (Op den Kamp *et al*., 2013). When cachexia is present due to cancer in the body it is referred to as cancer-induced cachexia. The

cancers that have been shown to be most associated with cachexia are gastric, pancreatic and lung cancers. Of all the Canadian patients with cancer, approximately 30% of deaths are attributed to the cachexia itself (Tan and Fearon, 2008). An indication of cancer-induced cachexia in the body is the presence of copious amounts of pro-inflammatory cytokines, most notably, TNF-α, interferon-γ (IFN-γ), IL-1β and IL-6 (Moses *et al*., 2009; Acharyya *et al*., 2004) (Reviewed in Acharyya and Guttridge, 2007).

The cachectic state lowers the body's response to chemotherapy and radiation causing even more toxicity effects in patients, which underscores the importance of understanding this syndrome and determining the molecular and biochemical basis for cancer-induced cachexia (Acharyya *et al*., 2004) (Reviewed in Acharyya and Guttridge, 2007).

1.33 Pathways Involved in Cancer-induced Cachexia

There are a number of factors and pathways that have been characterized as being associated with causing cancer-induced cachexia. Bonetto and co-workers identified factors such as the inflammatory cytokines TNF-α, IL-6, IL-1α/β and IFN-γ as being important inducers of cachexia (Bonetto *et al*., 2012).

Factors and pathways involved in skeletal muscle atrophy are due, in part, to the activation of the ubiquitin- and proteasome-dependent system. More specifically, two muscle specific ubiquitin E3 ligases, Muscle RING Finger protein 1 (MuRF1) and atrogin1/Muscle Atrophy F-box (MAFbx), are shown to be central to the induction of protein degradation during muscle atrophy (Bodine *et al*., 2001; reviewed in Fearon *et al*., 2012). Mice that were lacking the expression of MuRF1 or atrogin1/MAFbx were resistant to atrophy normally caused by denervation (Bonaldo and Sandri, 2013). The

activity of MuRF1 and atrogin1/MAFbx are induced by the activation of the NF-κB pathway and the p38 pathway, respectively. Both muscle specific E3 ligases degrade MHC, a muscle specific protein (Zhang *et al*., 2011).

Acharyya and team found that atrogin1/MAFbx was up-regulated in the muscle of animals bearing LLC cells (Acharyya *et al*., 2004). The presence of cancer cachexia induced by the LLC cells activates the p38 pathway in muscle whereby p38 associates with CCAAT/enhancer binding protein β (C/EBPβ) which becomes phosphorylated and can then activate atrogin1/MAFbx. Atrogin1/MAFbx indirectly decreases the expression of MHC via degradation of MyoD (Zhang *et al*., 2011). Atrogin1/MAFbx interacts with a LXXLL motif found on MyoD which induces the ubiquitination and subsequent degradation of MyoD. Finally, through an indirect method, the degradation of MyoD induces a down-regulation in MHC (Tintignac *et al*., 2005).

The NF-κB pathway plays a prominent role in the signalling pathway leading to muscle atrophy (Cai *et al*., 2004 and reviewed in Jackman *et al*., 2013). This pathway is induced by cachectic factors, such as TNF-α and is important in the induction of mediators like MuRF1 (Ladner *et al*., 2003; Romanick *et al*., 2013). In a similar fashion as atrogin1/MAFbx in the p38 pathway, TNF-α and IFN-γ work in synergy to induce the decrease in MHC levels via the loss of MyoD. MyoD is lost because there is an NF-κB-dependent activation of nitric oxide synthase that sequesters HuR, a MyoD-stabilizing RNA binding protein (Acharyya *et al*., 2004; Guttridge *et al*., 2000). Since Smac mimetics can affect the NF-κB pathway, the impact of these IAP antagonists should be examined in models of cancer cachexia.

1.4 The Cancer Models Chosen for SMC Treatment

1.41 Characteristics of Lung Cancer

Patients with lung cancer have one of the worst prognoses and therapeutic treatments have not advanced as fast compared to other cancer types. Lung cancer is responsible for the most number of deaths in males and the second most deaths in females. Lung cancer continues to have a survival of approximately no more than five years (Qin *et al*., 2012). Amongst lung cancer patients, non-small-cell-lung cancer accounts for 85% of cases while small-cell-lung-cancer patients make up the remaining 15%. Treatment options include: surgery, chemotherapy, radiation and more recently, targeted therapies (Pietanza and Ladanyi, 2012). However, many of these drug treatments cause a variety of undesirable side effects (Ricciardi *et al*., 2009). In order to study lung cancer, a very popular model that is employed is the mouse Lewis Lung Carcinoma (LLC) cell line (Bertram and Janik, 1980). LLC cells arose spontaneously in the lungs of C57BL/6 mice and a clonal cell line was created. This cell line is highly metastatic and migrates to the lungs and the liver (Bertram and Janik, 1980). Notably, the response of LLC cells to treatment with SMCs and TNF-α has not been previously reported. However, when non-small cell lung cancer was studied, SMC treatment induced apoptosis and caspase-3 activity (Dean *et al*., 2010). Based on these findings, we propose to explore if LLC cells are sensitive to SMC treatment. In addition, we will assess the impact of SMC treatment in the LLC model on the atrophy of skeletal muscle.

1.42 Characteristics of Melanoma Cancer

Melanoma cancer is a skin cancer that affects fewer Canadians than does lung cancer but is becoming increasingly more prevalent. Between 1970 and 2007, the incidence for developing a melanoma has increased 2.3% for males and 0.8% for females

(Kachuri *et al*., 2013). Melanoma cancer begins in the melanocytes and the number one cause of the disease is a mutation caused by overexposure to ultraviolet radiation. The treatments for this cancer include regular chemotherapy and radiation. In melanoma cancer, a mutation in the BRAF gene constitutes 60% of cases, resulting in constitutive activation of the mitogen-activated protein kinase (MAPK) and the phosphatidylinositol 3-kinase (PI3K) signalling pathways which may lead to improper signalling by Akt (or protein kinase B), NF-κB and p53 (Madonna *et al*., 2012; Vulture and Herlyn, 2013). B16F10 cells are a clonal cell line of melanoma cancer that is highly metastatic. The B16F10 cells are characterized as being capable of forming secondary pulmonary tumour colonies in C57BL/6 mice (Fidler, 1975). B16 melanoma cells have been analyzed *in-vitro* by Dr. Dougan and collegues in response to SMC (Dougan *et al*., 2010). SMC treatment of B16 cells *in-vitro* did not affect proliferation, apoptosis or caspases activity. Based on these results, an *in-vivo* model was tested to examine the synergy between irradiated B16 cells and SMC treatment. A suboptimal tumour cell vaccine composed of irradiated B16 cells was injected into C57BL/6 mice. The mice then received a dose of SMC and were implanted with B16 cells. The control groups, SMC treatment alone or B16 irradiated vaccine alone, showed no reduction in tumour growth and tumour sizes were comparable with mice that only received B16 tumours. The double treatment group of mice did show a 65% reduction in tumour growth rate (Dougan *et al*., 2010). Therefore, although the combination treatment of vaccine and SMC was shown to be effective in reducing tumour growth, the resistance factor was not determined in this study.

All in all, there is the potential to develop a personalized treatment plan for melanoma cancer. In order to study the sensitivity to Smac mimetic compounds, we have chosen to use the B16F10 cell line to decipher any differences in the activation of the NF-κB pathway compared to the LLC cells. In addition, we would like to investigate the effects of Smac mimetic compounds on skeletal muscle of mice bearing B16F10 tumours as B16F10 cells are known to induce cancer cachexia (Das *et al*., 2011).

1.5 Research Project Rational and Hypothesis

Cancer-induced cachexia is associated with a significant loss in skeletal muscle mass and adipose tissue and this process is partly mediated by the NF-κB pathway. SMCs target cIAP1/2, which are regulators of the NF-κB pathway. It could therefore be questioned if SMCs would have impact on cancer-induced cachexia. As previously indicated, SMCs induce the production of TNF-α or "cachectin" which is known to be a major mediator of skeletal muscle atrophy. Therefore, it is important to determine if SMC therapy will exacerbate cachexia in the mouse model.

Cancer cells can be characterized as having four different categories of responses when treated with SMCs. The level of sensitivity of cancer cells include cell death in response to SMC treatment alone, SMC and TNF-α co-treatment, SMC and TNF-α co-treatment only when c-FLIP is down-regulated and lastly, complete resistance (Cheung *et al*., 2009).

We have found that LLC cells fall into the category whereby they are sensitized to death by the addition of SMC and TNF-α treatment, whereas B16F10 cells die in the presence of SMC and TNF-α addition only when c-FLIP is down-regulated. We hypothesize that an extrinsic method to knock-down c-FLIP, such as siRNA, is required

to sensitize the cells such that the ripoptosome will be formed and the caspase cascade will lead to caspase-8 mediated cell death. Comparatively, we expect that LLC cells are sensitive to SMC and TNF-α co-treatment because c-FLIP is endogenously being down-regulated.

1.6 Objectives

The goal of our research project is to investigate the effect of the loss of cIAP1 and cIAP2 expression mediated by SMC on tumour development and skeletal muscle. In order to obtain this goal, the primary objective is to characterize the response of LLC and B16F10 cells to SMC and TNF-α treatment *in-vitro* and to determine the method of cell death. Since B16F10 cells are not sensitive to this treatment as LLC cells are, we want to determine the reason for B16F10 resistance to SMC and TNF-α co-treatment and provide a mechanism to sensitize this cell line. Finally, the *in-vivo* characterization of SMC treatment in mice bearing either LLC or B16F10 tumours will be looked at in terms of the impact on skeletal muscle as well as the impact on tumour regression.

The importance of this research project is that SMCs are currently in clinical trials as anti-cancer therapy drugs and if we can extend the studies of SMC treatment to either the treatment of cancer-induced cachexia or to additional cancer cell lines, we can help to provide further evidence of their widespread efficacy.

CHAPTER 2: MATERIALS & METHODS

2.1 Reagents and Antibodies

The Smac mimetic compound LCL161 was provided to us by Novartis (Dorval, QC, Canada). The Smac mimetic compound OICR720 was provided to us by the Ontario Institute of Cancer Research (Toronto, ON, Canada). Dr. John Bell (Ottawa Hospital Research Institute, Ottawa, ON, Canada) kindly provided the oncolytic virus (VSVΔ51) used in these studies. Mouse TNF-α was obtained from R & D Systems (410MT) (Burlington, ON, Canada). Primary antibodies: GAPDH (Advanced Immuno Chemical Inc.; 10-G4-C5), p100/52 (Cell Signaling Technology; 4882), RIAP1 (internally produced), cIAP1 (Enzo Life Sciences; 1E1-1-10), caspase-8 (Enzo Life Sciences; IG12), cleaved caspase-3 (Cell Signaling Technology; 9661) and PARP (Cell Signaling Technology; 9532). Secondary antibodies: AlexaFluor 680 (Molecular Probes) and IRDye800 (Rockland).

2.2 Cell Lines

2.21 Lewis Lung Carcinoma Cells

LLC cells were kindly provided to us by Dr. Nadine Wiper-Bergeron (University of Ottawa, ON, Canada) and purchased from ATCC (Manassas, VA, USA). LLC cells were kept in an incubator with settings of 37°C and 5% CO_2. The cells were grown in Dulbecco's modified Eagle medium (DMEM) media supplemented with 10% heat-inactivated fetal bovine serum (FBS), penicillin, streptomycin, glutamine and 1% non-essential amino acids (all from Invitrogen, Burlington, ON, Canada).

2.22 B16F10 Melanoma Cells

The B16F10-LacZ cells (hereafter referred to as B16F10) were kindly provided to us by Dr. John Bell (Ottawa Hospital Research Institute, ON, Canada). B16F10 cells were kept in an incubator at 37°C and 5% CO_2 in DMEM media supplemented with 10% heat-inactivated FBS, penicillin and streptomycin (all from Invitrogen, Burlington, ON, Canada).

2.3 Cell Culture Experiments

2.31 Transfection of small interfering RNA

B16F10 cells were seeded at a density of 128 500 cells/well in a 6-well plate. Cells were reverse transfected to have a final transfection concentration of 10nM. Reverse transfections were done in antibiotic-free DMEM media using Opti-MEM and transfection reagent Lipofectamine RNAiMax (Invitrogen) for 48 hours. The siRNA used was either a non-targeting siRNA (Dharmacon, Lafayette, CO, USA) or an siRNA targeting c-FLIP (Dharmacon, ON-TARGET plus SMARTpool). Cells were then either collected for Western immunoblotting, for RT-PCR or were treated with SMC and TNF-α for an additional 24 hours and then collected for Western immunoblotting or for cell viability assays.

2.32 Cell Viability Assays

LLC cells were seeded at a density of 7000 cells/well in a 96-well plate in growth media for 24 hours. Appropriate wells were then treated with either dimethyl sulfoxide (DMSO) as the vehicle or varying concentrations of LCL161 or OICR720 and 1ng/mL of TNF-α for another 24 hours. B16F10 cells were seeded at a density of 5000 cells/well in a 96-well plate in antibiotic free media containing either a non-targeting siRNA or an

siRNA targeting c-FLIP as described previously. Appropriate wells were then treated with either vehicle (DMSO), 10ng/mL TNF-α, 5μM LCL161 or 500nM OICR720 or a combination thereof for an additional 24 hours. After 24 hours of treatment of both LLC and B16F10 cells, Alamar Blue vital dye (resazurin, Sigma) used at a concentration of 1:7 was added to cells. Cell viability was then read using the Gen5 Data Analysis Software (BioTek Instruments Inc., Winooski, Vermont, USA) and graphs were created using GraphPad Prism 5.0.

2.4 Protein

2.41 Cell Protein Extraction

Cells were collected by scraping the wells and rinsing with PBS followed by centrifugation. Samples were frozen as pellets at -80°C until needed. Samples were thawed on ice and lysed in cold whole cell lysis buffer consisting of 50mM Tris-HCl, pH 8.0 containing 1% Triton X-100, 150mM NaCl, 1mM NaF, 0.1mM phenylmethylsulfonyl fluoride, 5μg/mL pepstatin A and 10μg/mL of both leupeptin and aprotinin. If samples were not lysed completely, they were further lysed by being passed through a syringe tip a minimum of 5 times. Protein quantification was determined using the Bio-Rad Protein Assay (Mississauga, ON, Canada) where bovine serum albumin was used as a standard. Once protein was quantified, samples were frozen at -80°C.

2.42 Tissue Protein Extraction

Muscle, tumour or spleen was extracted from C57BL/6 mice and flash frozen in liquid nitrogen. Samples were stored in a -80°C freezer and when needed, allowed to thaw on ice. Cold whole cell lysis buffer consisting of 50mM Tris-HCl, pH 8.0 containing 1% Triton X-100, 150mM NaCl, 1mM NaF, 0.1mM phenylmethylsulfonyl

fluoride, 5µg/mL pepstatin A and 10µg/mL of both leupeptin and aprotinin was added to each sample. The tissue was then lysed using either the Polytron Tissue Homogenizer or the TissueLyser II (Qiagen). Samples sat in ice for 30 minutes to fully lyse and were then centrifuged at 4°C for 10 minutes. Debris was removed from the sample and protein was quantified using Bio-Rad DC Protein Assay and stored in a -20°C freezer.

2.43 Western Immunolotting

Protein samples were allowed to thaw on ice. Protein aliquots were made using 20ug of protein and diluted 1:1 in Laemmli Sample Buffer (Bio-Rad) containing β-mercaptoethanol. Aliquots were boiled for five to ten minutes and were then loaded equally onto a polyacrylamide gel (10-15%) and run in running buffer at 120V for 1.5 hours. The separated proteins on the gel were transferred onto a nitrocellulose membrane of 0.1µM or 0.45µM by either semi-dry transfer (15V for 1.5 hours) or wet transfer (400mA for 1.5 hours). Membranes were then incubated on a shaker overnight with a primary antibody in phosphate-buffered saline (PBS) and Licor at a 1:1 ratio at 4°C. The primary antibody was then removed and the membrane was washed five times with tris-phosphate buffered saline with tween (TBS-T) for 7 minutes and subsequently washed twice with PBS for 7 minutes. Membranes were then incubated on a shaker with a secondary antibody in PBS and Licor (1:1) for 1 hour at room temperature in the dark. The secondary antibody was discarded and the membrane again washed in the same way as previously described. Membranes were then transferred to the Odyssey Infrared Imaging System (LI-COR) for scanning and analysis.

2.5 mRNA

2.51 RNA Extraction

Total mRNA was isolated from cells that were treated with siRNA against c-FLIP. These samples were pelleted and kept at -80°C until needed. The mRNA extraction process was performed using the RNeasy Mini Kit (Qiagen Inc., Mississauga, ON) according to the manufacturer's protocol. The RNA was eluted from spin column membranes with 40µL RNase-free water, collected at first elution. The RNA was quantified using a spectrophotometer (Eppendorf Biophotometer, Hamburg, Germany) with an OD reading of 260nm.

2.52 Reverse Transcription Polymerase Chain Reaction (RT-PCR)

mRNA was extracted as per described and samples were kept at -80°C until needed and then allowed to thaw on ice. A master mix was then prepared using the QuantiTect SYBRGreen RT-PCR reagents (Qiagen) according to the manufacturer's instructions and modified based on primer optimization. The RT-PCR was then performed using 100ng of total RNA mixed with gene-specific primers. c-FLIP primers: Forward 5'- GAT GTG ACT GAG AAC CTG GC-3', Reverse 5'- CTG GAG CCT TGA CTT ATA CTT GA-3' (Integrated DNA Technologies).

2.6 Animal Models

2.61 Animal Models

Mice were ordered from Charles River Laboratories Inc. (Montreal, Canada) with specifications of being 6 weeks old, male and C57BL/6 background. The only exception is the experiment using oncolytic virus which used 4 week old female C57BL/6 mice also ordered from Charles River Laboratories Inc. Mice were housed in the University of

Ottawa Animal Care and Veterinary Services Facility. The mice were housed in proper accordance with the Institutional Animal Care and Use Committee guidelines with access to pellet food and sterile water.

2.62 In-vivo Tumours with SMC Treatment

C57BL/6 mice were put under anesthetics and were subcutaneously injected with either 3 x 10^5 B16F10 or LLC cells (>90% viable) in the right flank. Tumours were allowed to grow and once visible (approximately 100mm^3), mice were gavaged once with the SMC, LCL161 or vehicle and were sacrificed 16 hours or 48 hours post-SMC treatment. The tibialis anterior muscle, spleen and tumour were collected from each mouse and flash frozen in liquid nitrogen before being transferred to a -80°C freezer.

C57BL/6 mice were put under anesthetics and were subcutaneously injected with either 3 x 10^5 B16F10 or LLC cells (>90% viable) in the right flank. Tumours were allowed to grow and once measurable, mice received four treatments of SMC LCL161 (50mg/kg) or vehicle, with each treatment being 3 days apart to allow recovery time for the mice. Endpoint was defined as the tumour reaching 2000mm^3 based on the formula $\pi r^2 h$, the volume of a cylinder, (where r = ½ the diameter of the tumour, h = length of the tumour) unless additional complications arose to require euthanization prior to this defined endpoint.

C57BL/6 mice were put under anesthetics and were intravenously injected with 3 x 10^5 B16F10 cells (>90% viable) and tumours migrated to locate in the lungs. Mice received gavage treatments of the SMC LCL161 or vehicle four times, beginning day 2 post-tumour implantation. Mice were sacrificed on day 14 and their lungs preserved for tumour nodule analysis.

2.63 In-vivo Tumours with SMC and Oncolytic Virus Treatment

C57BL/6 mice were subcutaneously injected with 3 x 10^5 LLC cells (>90% viable) in the right flank. On day 8 post-tumour implantation, the mice were treated with VSVΔ51 (IV: 5x 10^5 PFU; IT: 1 x 10^5 PFU) or vehicle followed by gavage of LCL161 (50mg/kg) on day 9. This two day treatment plan was performed a total of four times on consecutive days. Mice were sacrificed when their tumour reached 2000mm^3 based on the formula $\pi r^2 h$ (where r = ½ the diameter of the tumour, h = length of the tumour).

2.7 Histology

2.71 Histological Muscle Sectioning

Muscle tissues were removed from mice and were embedded in optimal cutting temperature compound (OCTC) and flash frozen in isopentane cooled in liquid nitrogen or dry ice. Samples were stored in a -80°C freezer until needed. Samples were then embedded to a cutting plate using OCTC and sectioned using a cryostat. Sections of muscle were taken from the middle of the muscle at a thickness of 10μm and put on a microscope slide. Slides were frozen and kept at -80°C.

2.72 Hematoxylin and Eosin Staining

Slides were removed from the -80°C freezer and thawed in room-temperature water. The slides were then placed in a coplin jar and stained in Mayer's hematoxylin for 3 minutes. Slides were then rinsed in distilled water for approximately 3 minutes, until the dye became purple and slides were then stained in eosin for 30 seconds. Slides were then dipped 8 times in 95% ethanol followed by 8 times in 100% ethanol and allowed to dehydrate for 2 minutes in 100% ethanol. Finally, slides were equilibrated 3 times for 2 minutes each time in xylenes. Once slides were dry, the mounting medium, DPX

mountant for histology, was added and a cover slip was glued to the slide. The slides were allowed to dry and sit in a dark location for 24 hours until images of muscle sections were captured with a microscope.

2.73 Determining Fibre Cross-Sectional Area

Microscope pictures were taken with a Zeiss digital camera on an Olympus microscope at a 10x magnification with the Cell Sens Entry program. The microscope images were imported into the programs Panorama Maker and Northern Eclipse to be formatted. Finally, the Image J program was used to trace the muscle fibres and calculate the area of each fibre. From this data, the average cross-sectional area and the histogram graphs were created using the program GraphPad Prism 5.0.

2.8 Statistical Analysis

2.81 One-way ANOVA

Data in bar graphs was analyzed in GraphPad Prism 5.0 using the test one-way ANOVA. A Dunnett's Multiple Comparison Test determined statistical significance between each category with respect to vehicle. Statistical significance was defined for data with a P value lesser than 0.05 or 0.001.

2.82 Survival Analysis

Survival data was analyzed in GraphPad Prism 5.0 using the Log Rank Mantel-Cox Test. Statistical significance was defined for data with a P value lesser than 0.001.

CHAPTER 3: RESULTS

3.1 *In-vitro* Analysis of LLC and B16F10 Cells in Response to SMC Treatment

3.11 SMCs are Active in LLC and B16F10 Cells

LLC and B16F10 cells were chosen for this research project for the purposes of studying the effect of cIAP1 and cIAP2 loss of expression on tumour development and skeletal muscle. LLC and B16F10 cells were analyzed for their response to LCL161, a monomeric SMC and to OICR720, a bivalent SMC. The latter SMC has two AVPI tetra-peptide sequences as opposed to one, allowing SMC to bind both the BIR2 and BIR3 domain of the IAPs, thus resulting in more effective antagonism (Flygare and Fairbrother, 2010). The expression of a number of different proteins can be monitored to confirm SMC activation. First, SMCs induce the proteosomal degradation of cIAP1 and 2, which is visible via Western blot analysis. In addition, the loss of IAP expression causes p100 to be partially processed into p52 allowing for a quantitative measure of SMC activation of the alternative NF-κB pathway (Wu *et al*., 2007). To confirm SMC activation in LLC and B16F10 cells, Western blots were performed to look at cIAP1/2 and p100/p52 protein expression levels. As seen by the Western blots in Figure 5A, cIAP1 and cIAP2 are being knocked down by the Smac mimetics in LLC cells and there is greater suppression with increasing concentrations of both LCL161 and OICR720. Furthermore, with increasing amounts of SMC, there is a gradual decrease in p100 protein levels and a corresponding gradual increase in p52 protein levels. This is in accordance with research showing that SMCs activate the alternative NF-κB pathway as indicated by a change in the p100 to p52 ratio (Ashwell, 2008). Glyceraldehyde phosphate dehydrogenase (GAPDH) was used as a loading control. Overall, since LLC cells respond in a dose

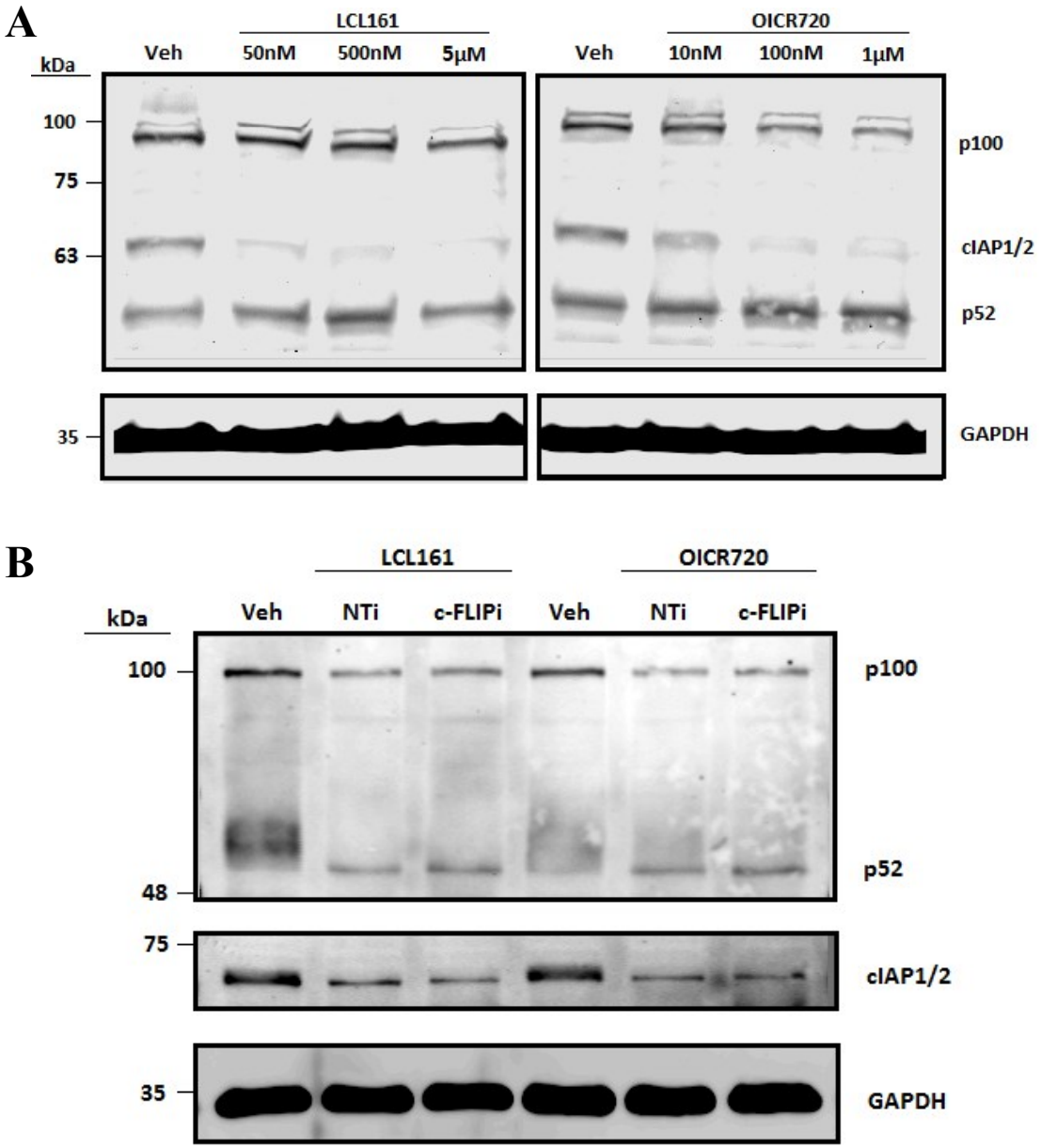

Figure 5. Smac mimetics are active in LLC and B16F10 cells.

Loss of cIAP1/2 expression by SMC treatment results in activation of the alternative NF-κB pathway as evidenced by the p100 to p52 expression levels and the down-regulation of cIAP1/2. LLC cells (A) were treated with indicated concentrations of either LCL161 or OICR720 for 24 hours. Cells were then harvested and subjected to Western immunoblotting. B16F10 cells (B) were reverse transfected with non-targeting siRNA or siRNA targeting c-FLIP for 48 hours. LCL161 (5μM) or OICR720 (500nM) was added for an additional 24 hours. Cells were then harvested and subjected to Western immunoblotting. GAPDH was used as a loading control.

dependent manner to SMCs, this information was used to formulate a standard concentration of SMC to use in all of the following experiments. This Western blot confirms that Smac mimetics function as expected in LLC cells. Similarly, the confirmation that the Smac mimetics are being activated in B16F10 cells can be found in Figure 5B, showing down-regulation of the cIAP1/2 genes and a change in the p100 to p52 ratio.

3.12 LLC Cells are Sensitive to SMC and TNF-α Co-treatment

The next step involved performing cell viability assays to look at the response of LLC cells to SMC alone and to SMC and TNF-α co-treatment. TNF-α, which is induced by Smac mimetics has been shown to synergize with SMCs and is very effective at inducing cell death in certain cancer cell lines (Cheung et al., 2009). As seen in Figure 6, the addition of LCL161 alone to LLC cells does not result in cell death, suggesting that there is not enough endogenous TNF-α to synergize with LCL161. However, with the addition of exogenous TNF-α, the synergy with LCL161 causes nearly 100% cell death at a concentration of 200nM LCL161 (Figure 6A). Similar to the monomer, OICR720 does not cause cell death on its own. Conversely, 100% cell death is triggered by the addition of TNF-α and 500nM OICR720 (Figure 6B). Subsequently, cell viability assays were used to analyze the response of LLC cells to a constant SMC concentration but a varying TNF-α concentration. With increasing amounts of TNF-α added, there was a resulting increase in cell death levels. Approximately 50% cell death occurred in LLC cells with 5pg/mL of TNF-α in the presence of LCL161 (Figure 7A) and 10pg/mL of TNF-α in the presence of OICR720 (Figure 7B). In the presence of the monomer and the dimer SMC, LLC cells reached 100% cell death by 1ng/mL and 2ng/mL TNF-α, respectively.

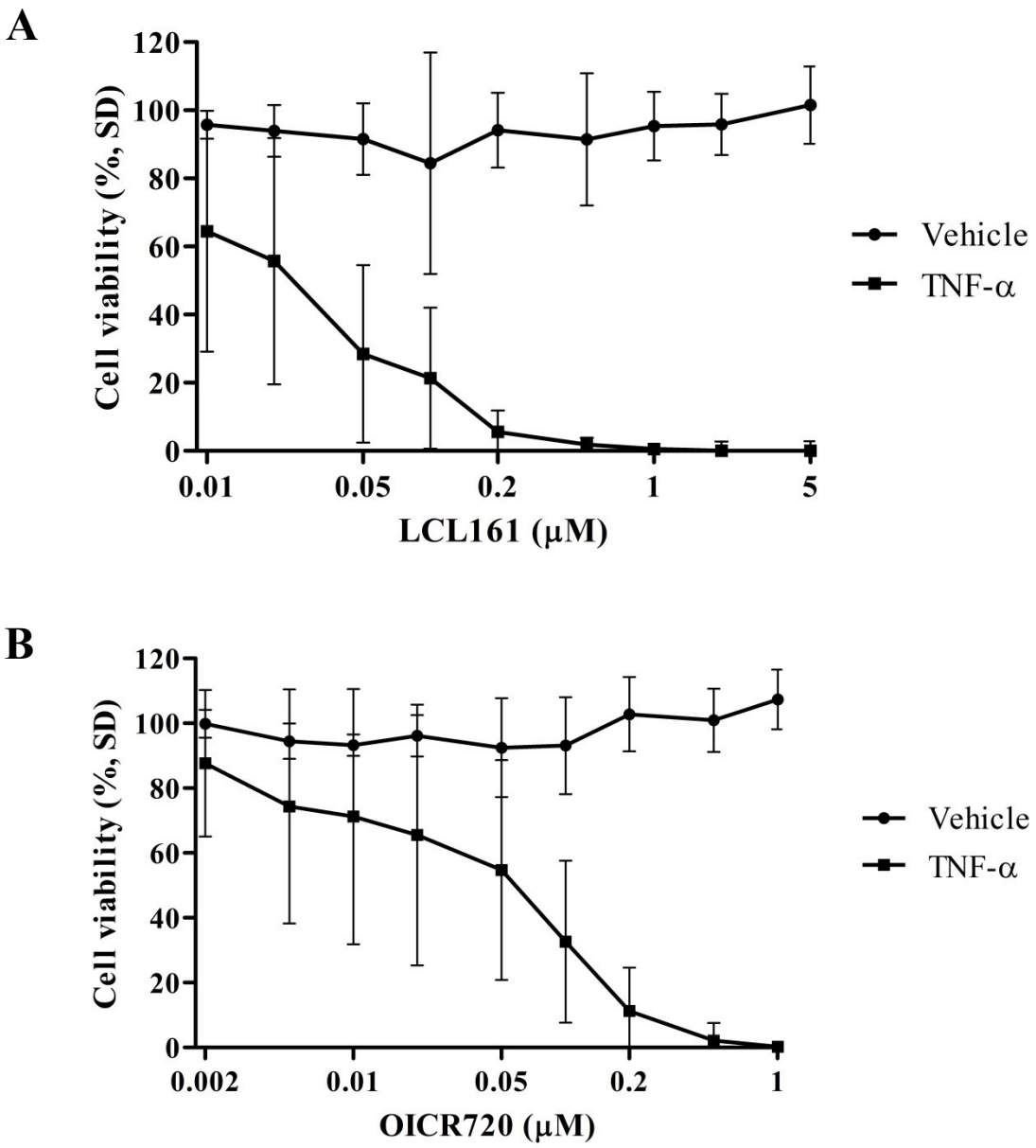

Figure 6. LLC cells are sensitive to SMC and TNF-α co-treatment.

The combination treatment of LCL161 or OICR720 with TNF-α results in the synergistic killing of LLC cells. At 48 hours post-seeding, LLC cells were treated with the indicated concentrations of LCL161 (A) or OICR720 (B) with or without 1ng/mL TNF-α. Cell viability was determined 24 hours after drug exposure by Alamar Blue analysis. Percentage viability representative of eight independent experiments with standard deviation (n = 6) was plotted. SD = standard deviation.

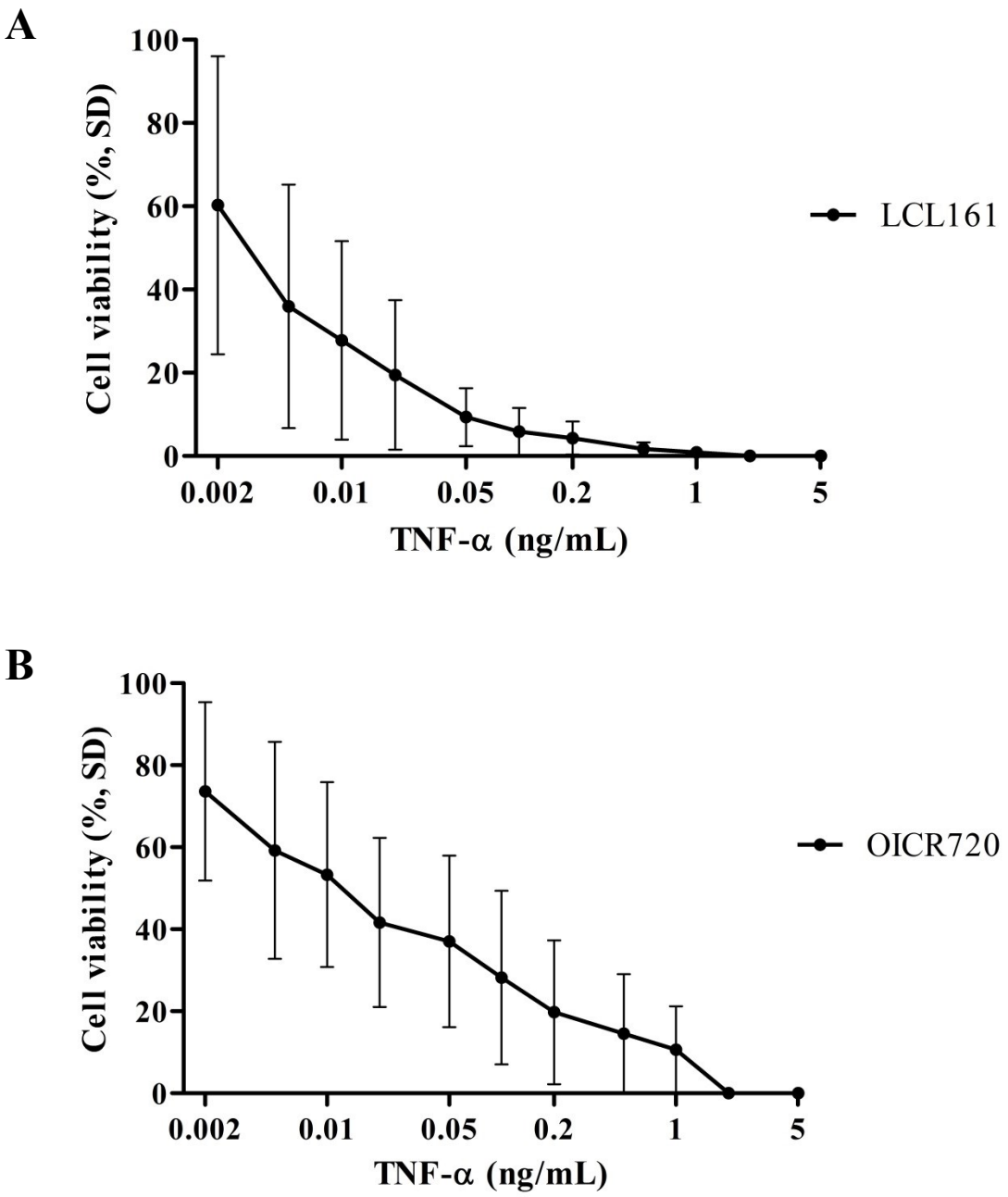

Figure 7. LLC cells are killed by TNF-α treatment in presence of SMC.

At 48 hours post-seeding, LLC cells were treated with the indicated concentrations of TNF-α and co-treated with 2μM LCL161 (A) or 500nM OICR720 (B). Cell viability was determined 24 hours after drug exposure by Alamar Blue analysis. Percentage viability representative of eight independent experiments with standard deviation (n = 6) was plotted. SD = standard deviation.

Overall, these results indicate that LLC cells are only sensitive to SMCs when exogenous TNF-α is added.

3.13 B16F10 Cells are Resistant to SMC and TNF-α Co-treatment

A cell viability assay was performed using B16F10 cells whereby results show non-sensitivity to LCL161 alone (Figure 8A) or to OICR720 alone (Figure 8B). Furthermore, compared to LLC cells, B16F10 cells remained nearly completely viable in response to the double combination treatment of SMC and TNF-α. Only 0 – 15% cell death occurred regardless of the concentration of LCL161 (Figure 9A) or OICR720 (Figure 9B). Therefore, this suggested the presence of an inhibitory factor in the B16F10 cells that provide them further resistance against the synergy between SMCs and TNF-α.

3.14 The Resistance Factor in B16F10 Cells Appears to be the Inhibition of Apoptosis by c-FLIP

Based on Dr. Cheung's Cancer Research paper, we hypothesized that the cell death inhibitor in B16F10 cells is c-FLIP (Cheung *et al*., 2009). In doing so, we made the assumption that all of the components of the extrinsic apoptotic pathway were present and functional. Therefore, if c-FLIP is the inhibitor, cell death should occur when this protein is down-regulated. A short interfering RNA (siRNA) targeting c-FLIP or a non-targeting siRNA was added to the B16F10 cells. At 48 hours post-transfection, the B16F10 cells were then treated with LCL161 and TNF-α for an additional 24 hours. Non-targeted cells treated with LCL161 alone, TNF-α alone or LCL161 and TNF-α had comparable cell viability to the vehicle treated cells, with the viability maintained at approximately 100% ± 15% (Figure 9A). However, in the absence of c-FLIP, the cells became sensitive to the treatment of TNF-α and the viability dropped to approximately

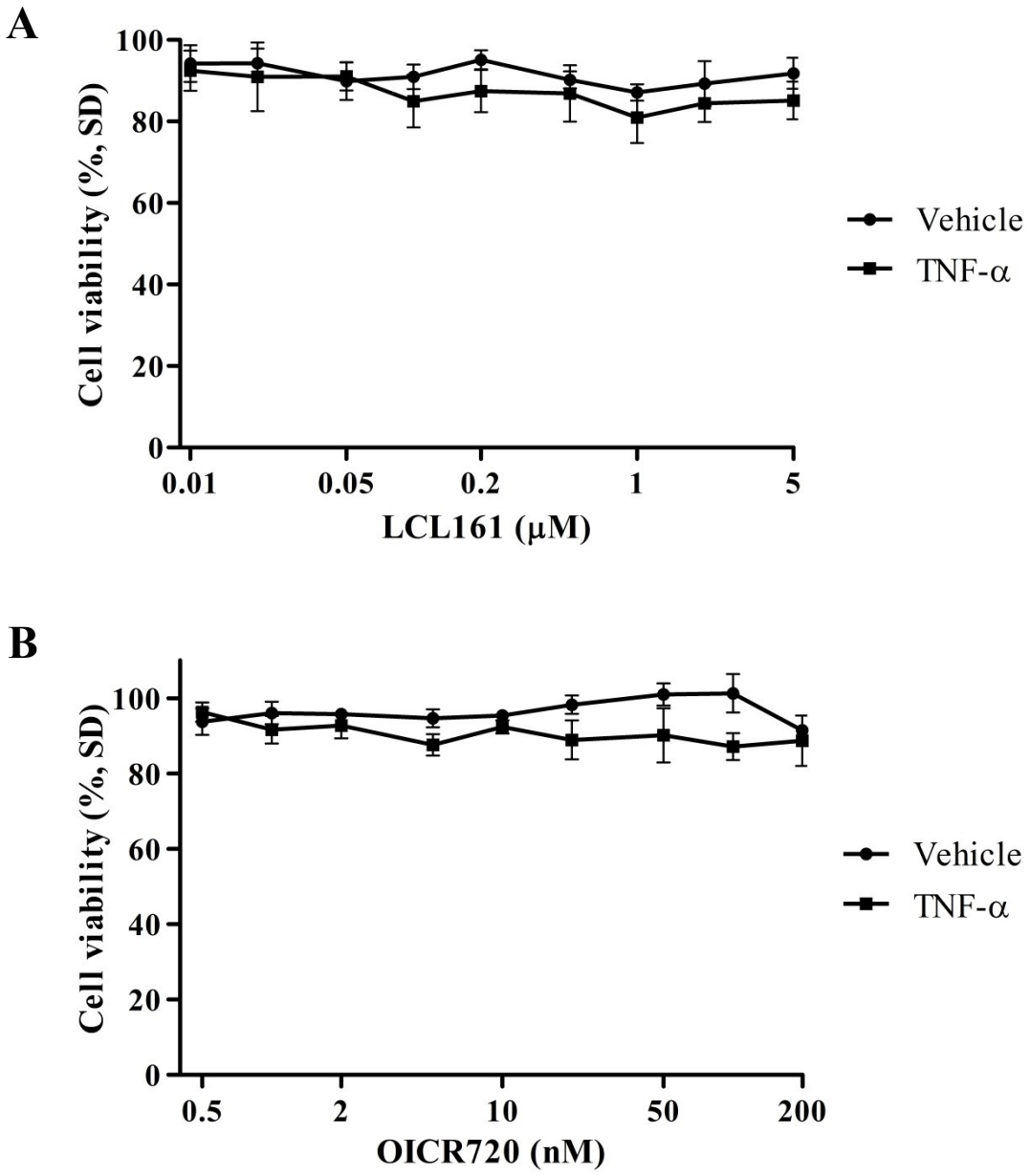

Figure 8. B16F10 cells are not sensitive to SMC mediated cell death.

B16F10 cells were treated with LCL161 (A) or OICR720 (B) at indicated concentrations with or without 10ng/mL TNF-α. Cell viability was determined 24 hours after drug exposure by Alamar Blue analysis. Percentage viability relative to control with standard deviation (n = 3) was plotted. SD = standard deviation.

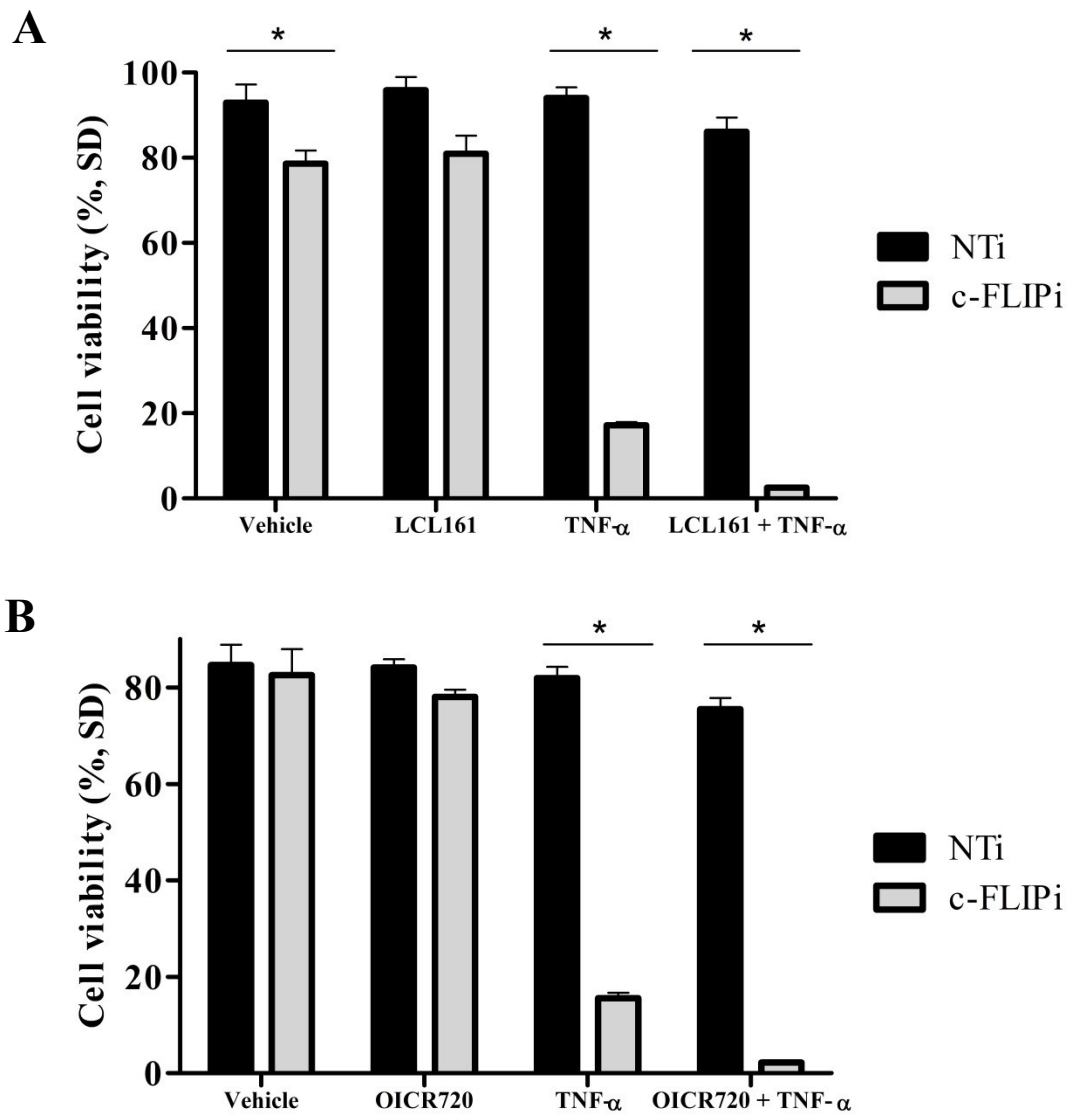

Figure 9. Down-regulation of c-FLIP sensitizes B16F10 cells to SMC mediated cell death.

B16F10 cells are resistant to SMC and TNF-α treatment but are sensitized when c-FLIP is down-regulated. B16F10 cells were reverse transfected with non-targeting siRNA or siRNA targeting c-FLIP for 48 hours. B16F10 cells were then treated with 5μM LCL161 (A) or 500nM OICR720 (B) with or without 10ng/mL TNF-α. Cell viability was determined 24 hours after drug exposure by Alamar Blue analysis. Percentage viability relative to control with standard error (n = 3) was plotted. SD = standard deviation. One-way ANOVA, Dunnett's Multiple Comparison Test: *, $P < 0.001$.

20%. Albeit, the addition of LCL161 appeared to synergize with exogenous TNF-α in the absence of c-FLIP and this co-treatment resulted in approximately 0% cell viability (Figure 9A). Very similar results were obtained using OICR720. When c-FLIP was present, none of the categories of treatment resulted in a decrease in cell viability (Figure 9B). However, in the absence of c-FLIP, TNF-α alone caused cell killing of approximately 80% of cells and cell viability dropped to near 0% with the double therapeutic treatment of OICR720 and TNF-α (Figure 9B). The results of this section indicate that B16F10 cells are not sensitive to the co-treatment of SMC and TNF-α and c-FLIP may be the barrier to cell death.

In order to correlate the cell death in the B16F10 cells to the absence of c-FLIP, it was important to confirm that c-FLIP was in fact being down-regulated. Samples were collected of B16F10 cells that were transfected with either non-targeting siRNA or siRNA targeting c-FLIP. The c-FLIP primers spanned all four of the pooled siRNAs from Dharmacon (Figure 10A). RT-PCR samples were run on an agarose gel and imaged under ultra violet light (Figure 10B). The results of this experiment show that the siRNA targeting c-FLIP is working effectively at knocking-down its target. With all of the proper controls used, there appeared to be no off target effects. In conclusion, in the presence of c-FLIP, SMC and TNF-α co-treatment in B16F10 cells does not result in cell death. However, when c-FLIP is down-regulated, TNF-α alone induces some cell death and the co-treatment of SMC and TNF-α results in the complete death of the B16F10 cells.

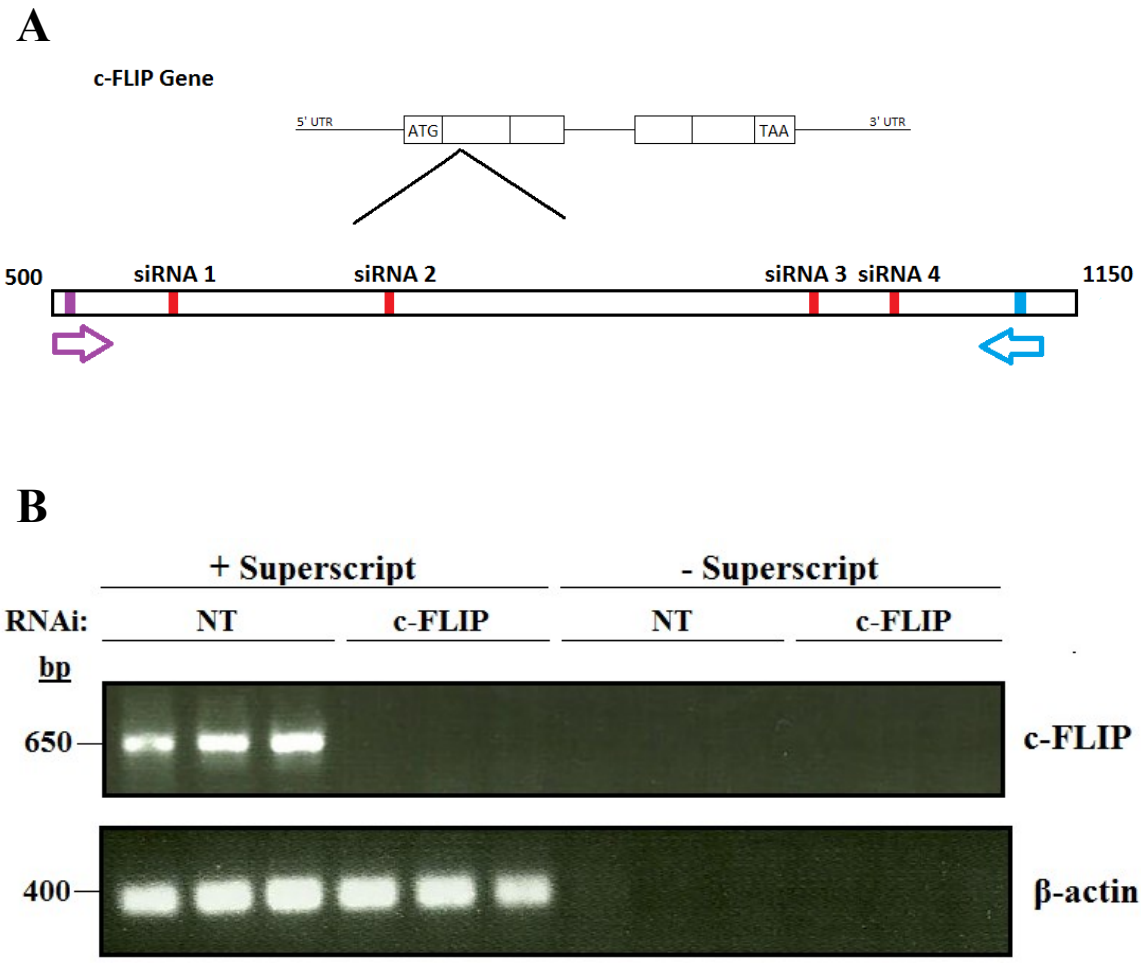

Figure 10. c-FLIP transcript levels are decreased by targeted siRNA treatment in B16F10 cells.

Complete loss of c-FLIP transcripts was achieved with siRNA treatment and is correlated with B16F10 sensitivity to TNF-α treatment alone and SMC and TNF-α co-treatment. B16F10 cells were reverse transfected with either non-targeting siRNA or siRNA targeting c-FLIP for 72 hours. Cells were then harvested, RNA was extracted and samples subjected to RT-PCR to look at the presence or absence of the c-FLIP gene. Placement of primers is shown in (A) and the agarose gel results are shown in (B). β-actin was used as a loading control.

3.15 The Cell Death Incurred by SMC and TNF-α Co-treatment Follows the Extrinsic Apoptotic Pathway

SMCs have been proposed to induce cell death via the caspase-8 dependent extrinsic apoptotic pathway (Lu *et al*., 2008). In order to analyze the method of cell death of LLC cells that are co-treated with SMC and TNF-α, a time course was performed. In LLC cells, the expression levels of cIAP1 and cIAP2 decreased dramatically in the presence of LCL161 after one hour of treatment and are almost completely depleted by seven hours and remain consistently so at 16 hours (Figure 11). Caspase-8, an initiator caspase, is activated by seven hours of LCL161 and TNF-α co-incubation and remains so at 16 hours as indicated by the processing of caspase-8 into its cleaved counterparts. Further downstream, effector caspase, cleaved caspase-3, is activated at 4 hours post-SMC and TNF-α addition. The Western blot indicates that the extrinsic apoptotic pathway is being activated by the treatment of LCL161 and TNF-α in LLC cells although other cell death pathways cannot be ruled out in playing a role as well.

To provide some mechanistic insight into how c-FLIP is functioning in the B16F10 cells, the method of cell death was analyzed. The literature proposes that c-FLIP antagonises caspase-8 and inhibits the formation of the ripoptosome, the mediator of the extrinsic apoptotic pathway (Fulda, 2013). In order to test this, a time course was performed to see if any consequential processing was occurring. In B16F10 cells, the time course was run for six hours with or without c-FLIP down-regulation. The pre-treatment of LCL161 is able to suppress the expression of cIAP1/2 for the length of the time course (Figure 12). Caspase-8 begins to be processed four hours post-treatment in

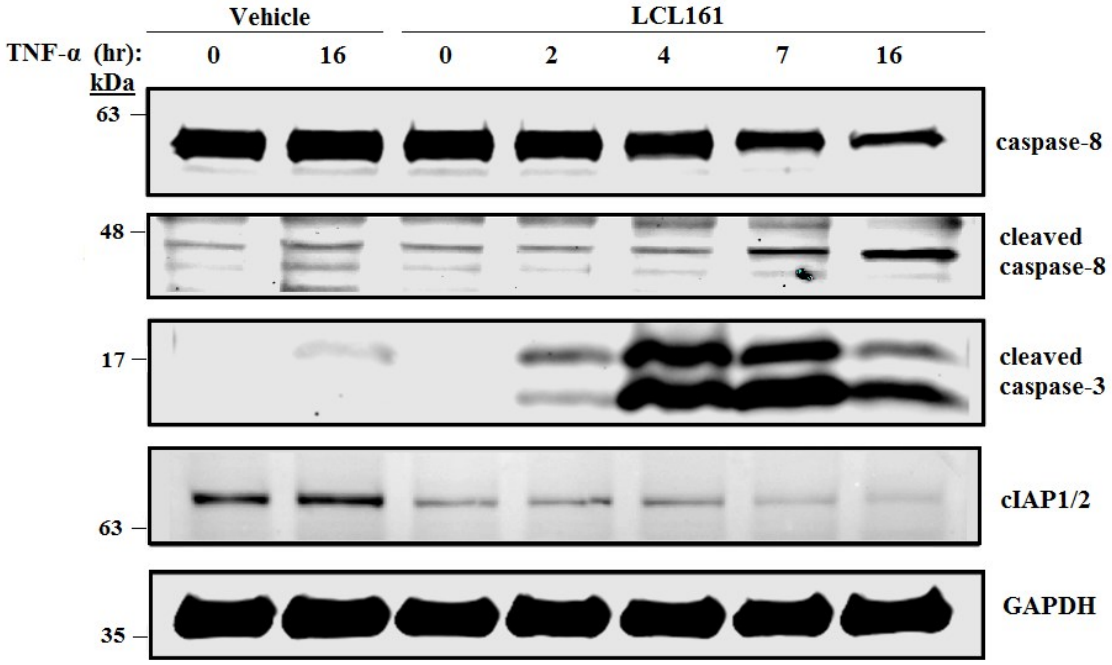

Figure 11. SMC and TNF-α co-treatment sensitizes LLC cells to caspase-8 mediated cell death.

LCL161 and TNF-α co-treatment results in loss of cIAP1/2 expression followed by the appearance of cleaved (activated) caspase-3 and -8, indicative of programmed cell death. LLC cells were pre-treated with 200nM LCL161 for 1 hour and then 1ng/mL TNF-α was added for indicated time points. Cells were then harvested and subjected to Western immunoblotting with antibodies against SMC targets (cIAP1/2) and components of the extrinsic apoptotic pathway (caspases). GAPDH was used as a loading control.

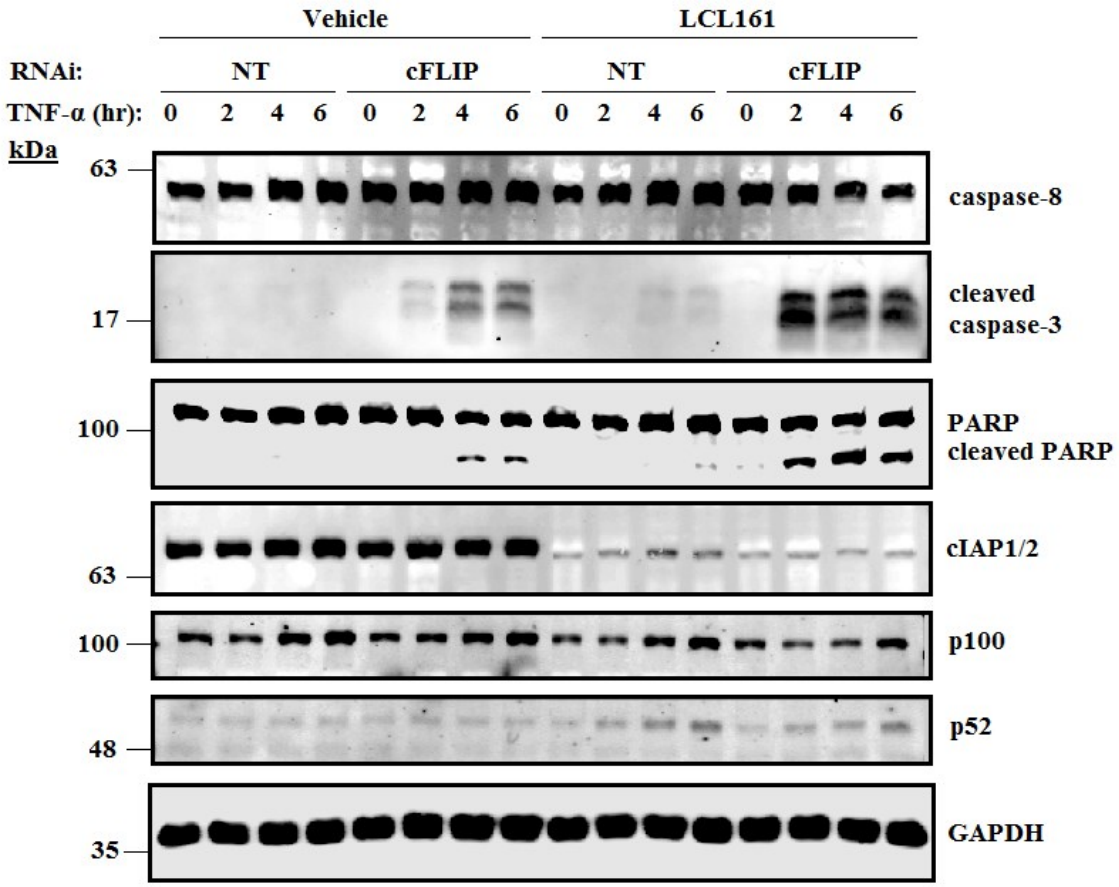

Figure 12. B16F10 cells treated with siRNA targeting c-FLIP are sensitized to caspase-8 mediated cell death.

LCL161 and TNF-α co-treatment results in loss of cIAP1/2 expression followed by the appearance of cleaved (activated) caspase-3 and -8, and PARP, indicative of programmed cell death. B16F10 cells were reverse transfected with either non-targeting siRNA or siRNA targeting c-FLIP for 48 hours. The cells were then pre-treated with LCL161 at 5μM for 1 hour and then 10ng/mL TNF-α was added for indicated time points. Cells were then harvested and subjected to Western immunoblotting with antibodies against SMC targets (cIAP1/2) and components of the extrinsic apoptotic pathway (caspases and PARP). GAPDH was used as a loading control.

the cells that have been treated with LCL161 and TNF-α in the absence of c-FLIP. This correlates with the cell viability data, thus suggesting activation of the extrinsic apoptotic pathway. Cleaved caspase-3 is slightly activated beginning at two hours in the c-FLIP down-regulated cells treated with TNF-α. Also correlated with the cell viability assay results, we see a greater activation of cleaved caspase-3 beginning at two hours in the cells that have received siRNA targeting c-FLIP along with LCL161 and TNF-α treatment. In addition, poly (ADP-ribose) polymerase (PARP) cleavage indicates that the final step of the extrinsic apoptotic pathway is activated. In Figure 12, B16F10 cells in the absence of c-FLIP, undergo PARP cleavage with the addition of TNF-α alone or TNF-α and LCL161 co-treatment. Although other pathways of cell death cannot be ruled out, these results do suggest that cell death is occurring, at least to some degree, via the extrinsic apoptotic pathway.

3.2 *In-vivo* Analysis of LLC Cells in Response to SMC Treatment

3.21 LLC Tumour Bearing Mice Treated with SMC Show Slowed Tumour Growth Rate

The initial LLC *in-vivo* experiment was performed to see the response of these cells to SMC in a mouse model. SMC induces TNF-α production, which is produced by the innate immune system; therefore, in an animal model with an immune system, it is possible that treating mice with SMC alone may be able to sensitize the tumour cells. The activation of SMC was tested *in-vivo* by analyzing cIAP1/2 knockdown in the tumour and in the spleen at 16 and 24 hours post-SMC treatment. cIAP1/2 is down-regulated in LLC tumours at 16 hours post-treatment and remains down-regulated at 24 hours (Figure 13A). The spleens from mice bearing LLC tumours show rapid

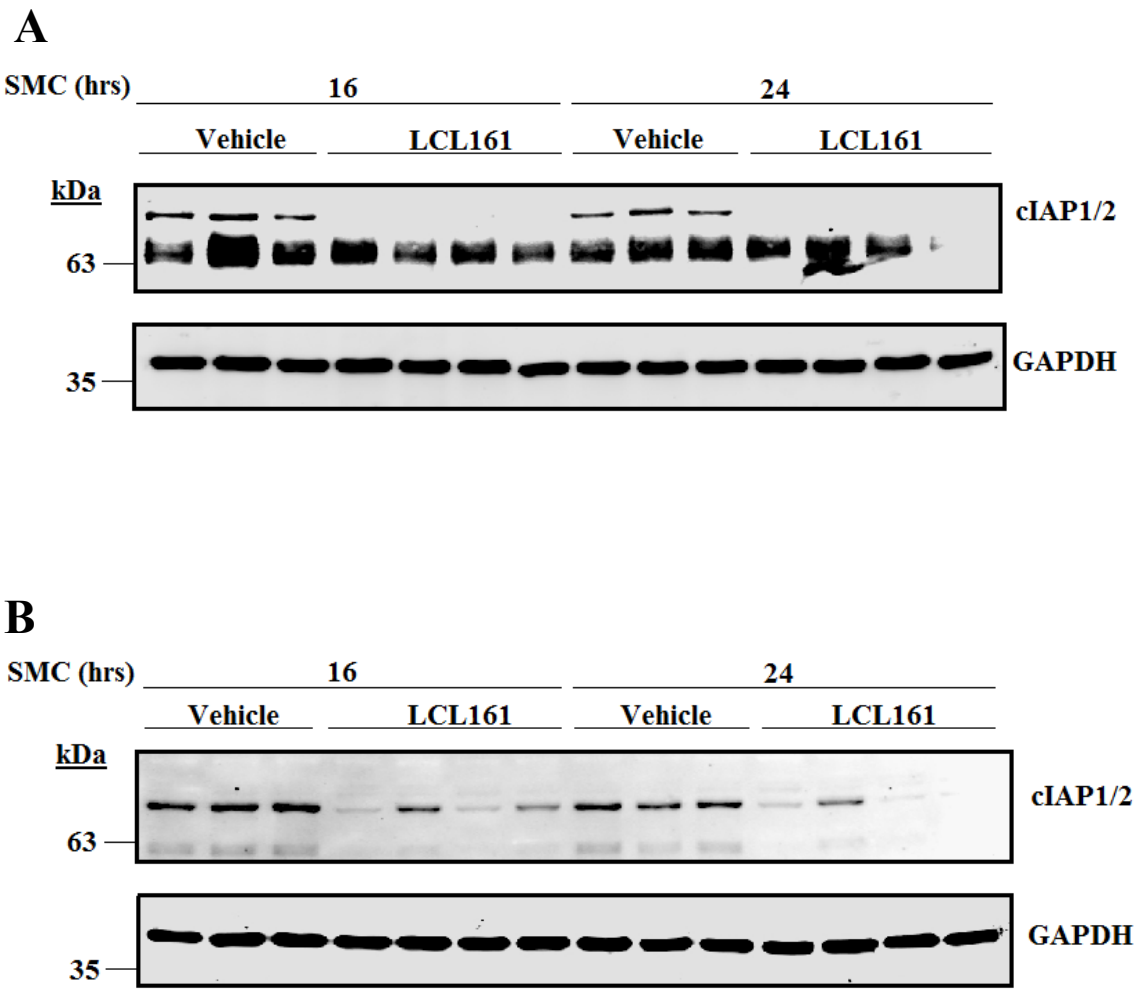

Figure 13. cIAP1/2 are targeted by LCL161 in the tumour and spleen of LLC tumour bearing mice.

The loss of cIAP1/2 occurs with the addition of SMC thus stimulating the activation of the alternative NF-κB pathway. Mice were injected with 3 x 10^5 LLC cells. Once tumours were established, mice were gavaged once with 50mg/kg LCL161 and sacrificed at either 16 hours or 24 hours post-treatment. The tumours (A) and spleens (B) were harvested and subjected to Western immunoblotting with antibodies against SMC targets. GAPDH was used as a loading control.

knock-down of cIAP1/2, however the IAPs are beginning to re-bound by 16 and 24 hours post-SMC treatment (Figure 13B). In a separate experiment, tumours that had been excised at variable times post-LCL161 treatment show no decrease in cIAP1/2 expression levels according to Figure 14. The reason for this is due to re-bound effects that generally occur by 72 hours post-SMC treatment in the tumour.

Since SMC activation is possible *in-vivo* in LLC tumour bearing mice, a complete study was performed in order to see if there are longer term impacts of SMC treatment on LLC lung carcinoma. In order to test this, mice were subcutaneously injected with LLC cells and given 12 days for the tumour to become established and palpable. Mice were gavaged four times, three days apart. Results indicated no significant difference between the average tumour size of vehicle versus LCL161 treated mice (Figure 15A). The mice treated with LCL161 tend to show an inclination toward a smaller tumour size (Figure 15B) but no conclusive statements could be made. We next looked at the tumour growth rate of vehicle versus LCL161 treated mice. LLC tumour bearing mice treated with LCL161 show a consistent decrease in average tumour growth rate of approximately $400mm^3$ (Figure 16A). In order to view the data as a relative tumour growth rate, mouse tumour sizes were compared to each corresponding mouse's tumour size on day 14 and then averaged based on the day post-treatment (Figure 16B). LLC tumour bearing mice treated with LCL161 do not appear to have a significant increase in survival time compared to vehicle treated mice (Table 2). Overall, it appears as though SMC treatment alone is able to mildly reduce LLC tumour burden *in-vivo*. There were two limitations to this study that most likely impacted the results. Firstly, the LCL161 was administered once the tumours became measurable and therefore had time to establish a niche; which

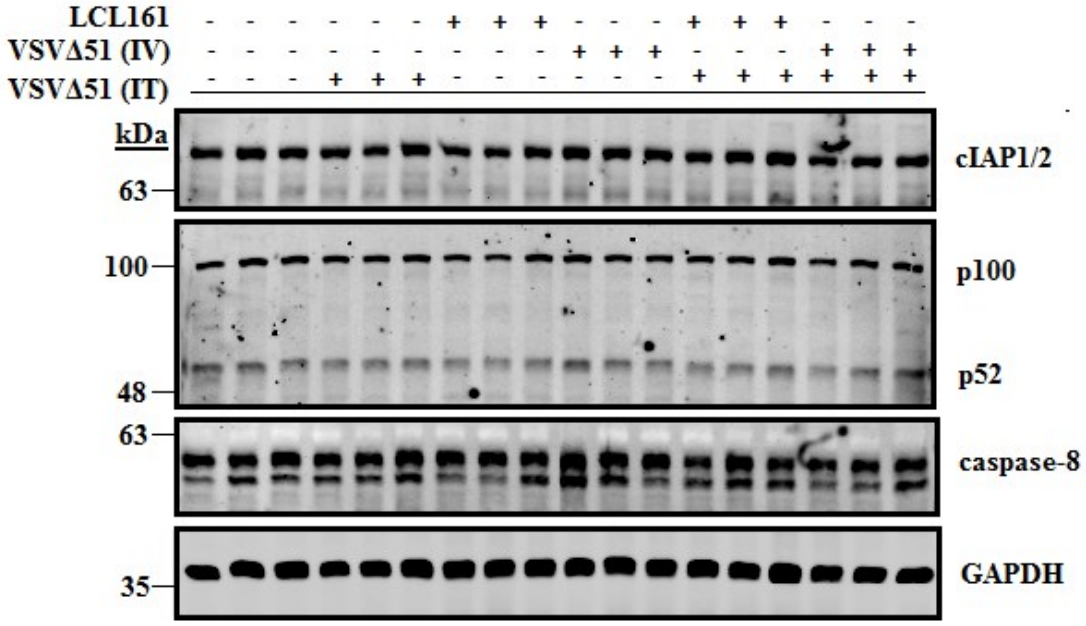

Figure 14. cIAP1/2 re-bound after more than 72 hours post-SMC treatment in the tumour of LLC tumour bearing mice.

The loss of cIAP1/2 occurs with the addition of SMC thus stimulating the activation of the alternative NF-κB pathway. However, down-regulation of the IAPs cannot be seen after more than 72 hours post-SMC treatment. Mice with LLC tumours were treated with VSVΔ51 and LCL161. When tumours reached 2000mm^3, the tumours were collected and subjected to Western immunoblotting and probed with antibodies against SMC targets and components of the extrinsic apoptotic pathway. GAPDH was used as a loading control.

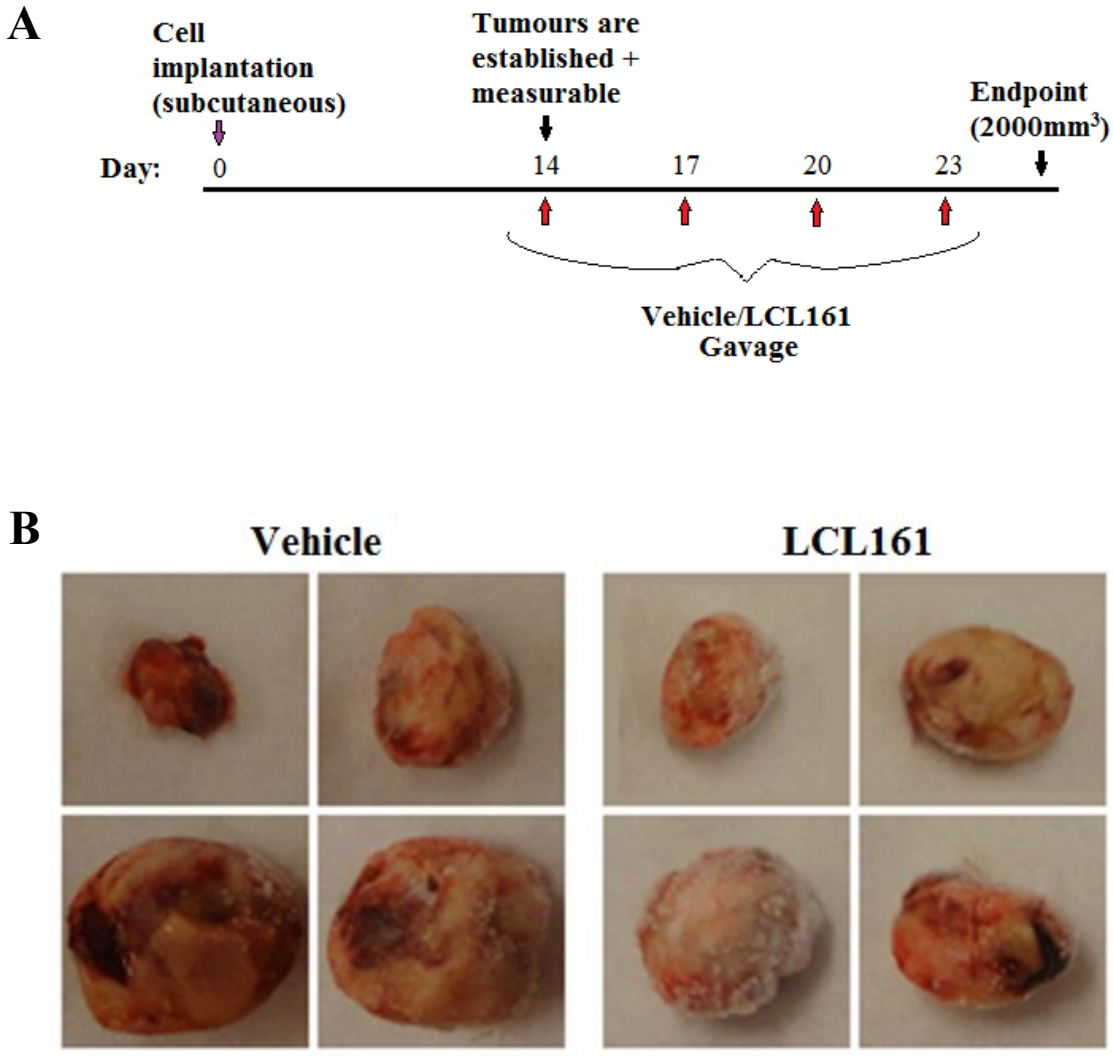

Figure 15. LLC tumour bearing mice are subjected to a treatment plan involving LCL161.

LLC cells respond to SMC and TNF-α co-treatment *in-vitro*, therefore, this treatment model was developed to test the efficacy of SMC treatment in a mouse model bearing LLC tumours. C57BL/6 mice were subcutaneously injected with 3 x 10^5 LLC cells and received four treatments of 50mg/kg LCL161 as seen in (A). Mice were sacrificed when tumours reached 2000mm^3 and the tumours dissected (B) to compare vehicle (n = 6) versus LCL161 treated mice (n = 6).

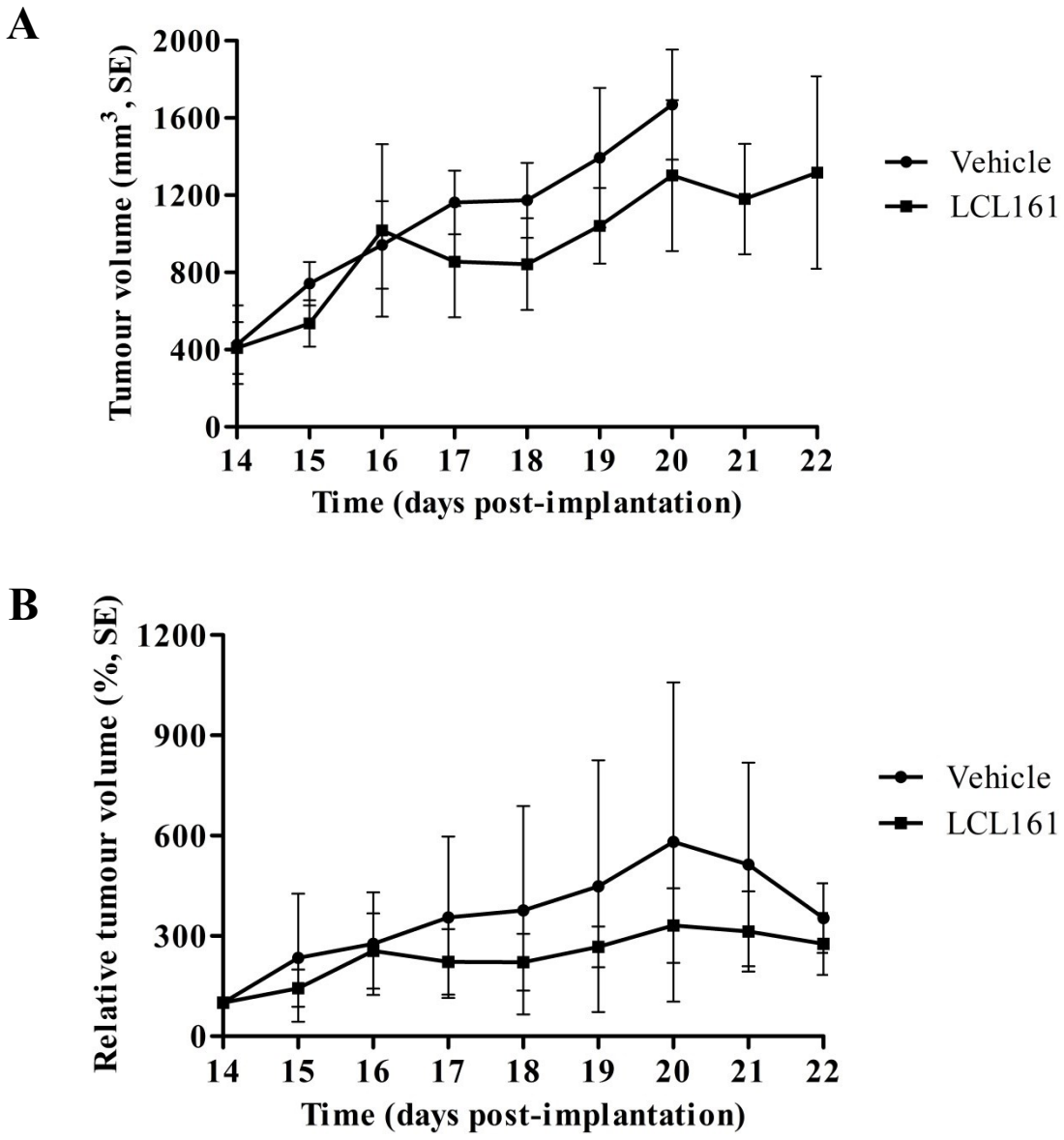

Figure 16. Mice bearing LLC tumours are mildly sensitive to LCL161 treatment.

The impact of SMC treatment was tested *in-vivo* on LLC tumour bearing mice. C57BL/6 mice were subcutaneously injected with 3 x 10^5 LLC cells and received four treatments of 50mg/kg LCL161. Mice were sacrificed when tumours reached a volume of 2000mm^3. An average tumour volume graph (A) or relative tumour volume graph (B) with standard error (n = 6/category) is plotted. Average tumour volume is calculated by the total tumour volume of each mouse on a particular day divided by the number of mice. Relative tumour volume is calculated by the total difference in tumour volume of each mouse on a given day compared to its own tumour volume on day 14. SE = standard error.

Table 2

Survival Time Comparisons of LLC Tumour Bearing Mice

ENDPOINT ($2000mm^3$)	VEHICLE (n = 6)	LCL161 (n = 6)
DAY	24+	24+
DAY	23	22
DAY	22	24+
DAY	24+	24+
DAY	20	24+
DAY	24+	24+

involves the recruitment of macrophages, the production of growth factors and the establishment of vasculature. If the mice were treated with the Smac mimetics sooner than day 14, it would be expected that a larger difference in tumour growth would occur between vehicle and LCL161 treated mice. Secondly, we may not be seeing as dramatic results as we did *in-vitro* because there may not be a great enough concentration of TNF-α *in-vivo*. Therefore, knowing that VSVΔ51 is an oncolytic virus that stimulates the immune system to produce a large amount of TNF-α, we decided to use VSVΔ51 *in-vivo* with the expectation that it would synergize with SMC in LLC cells based on its ability to synergize with SMC in EMT6 cells (Beug *et al*., 2014).

3.22 Oncolytic Virus and SMC Co-treatment Sensitizes LLC Tumours in Mice

We performed a similar experiment to the one above in which mice were treated with SMC alone. However, we added VSVΔ51 treatment in between each LCL161 treatment and began all treatments considerably earlier, at day 8, the first sign of tumour establishment (Figure 17A). LLC tumour bearing mice treated with SMC alone showed a slight increase in survival time of approximately four days (Figure 17B). Mice treated with VSVΔ51 (intratumoral or intravenous) alone experienced a survival time difference of zero and five days, respectively. All in all, using these agents as single therapeutic treatments does not seem to provide any benefit against lung cancer. Conversely, the most notable results were the 11 and eight day increase in survival time increase for the double treated, LCL161 and VSVΔ51 (intravenous and intratumoral respectively) mice. There proved to be a significant difference between the survival time between vehicle treated mice and the double treated mice that received either intravenous (Figure 18A) or intratumoral (Figure 18B) treatement (p- value < 0.001).

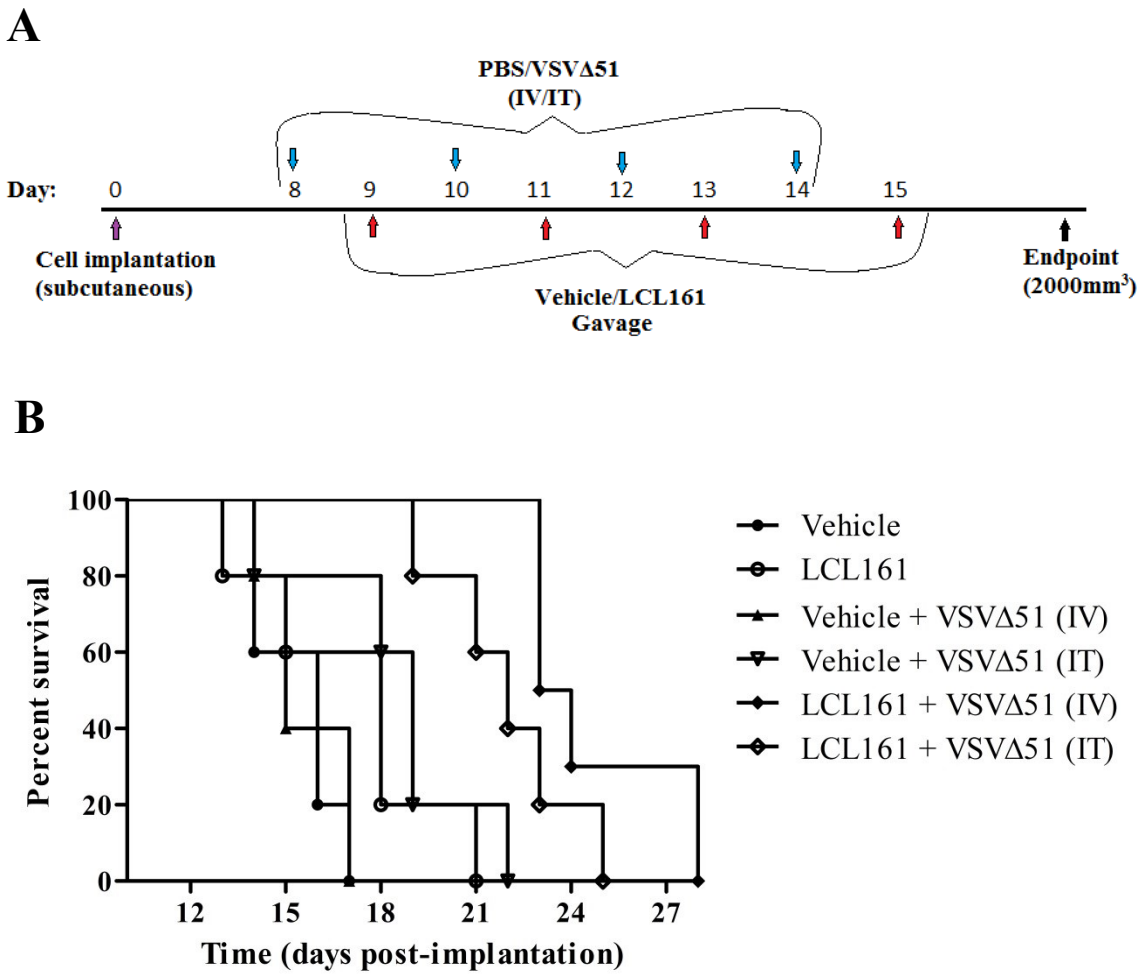

Figure 17. LLC tumour bearing mice are co-treated with LCL161 and a trigger, VSVΔ51.

In-vivo, mice require a trigger such as VSVΔ51 to induce the production of TNF-α which can then synergize with SMC to induce killing of LLC tumour cells. C57BL/6 mice were subcutaneously injected with 3 x 10^5 LLC cells and received four treatments of both VSVΔ51 (IV: 5 x 10^8 PFU, IT: 1 x 10^8 PFU) and LCL161 (50mg/kg) on opposite days as seen in (A). Mice were sacrificed when tumours reached a volume of 2000mm^3. A survival curve (B) was created to compare control untreated mice to single and double treated mice. n = 5 per category with the exception of n = 4 for LCL161 + VSVΔ51 treatment group . IV = intravenous, IT = intratumeral.

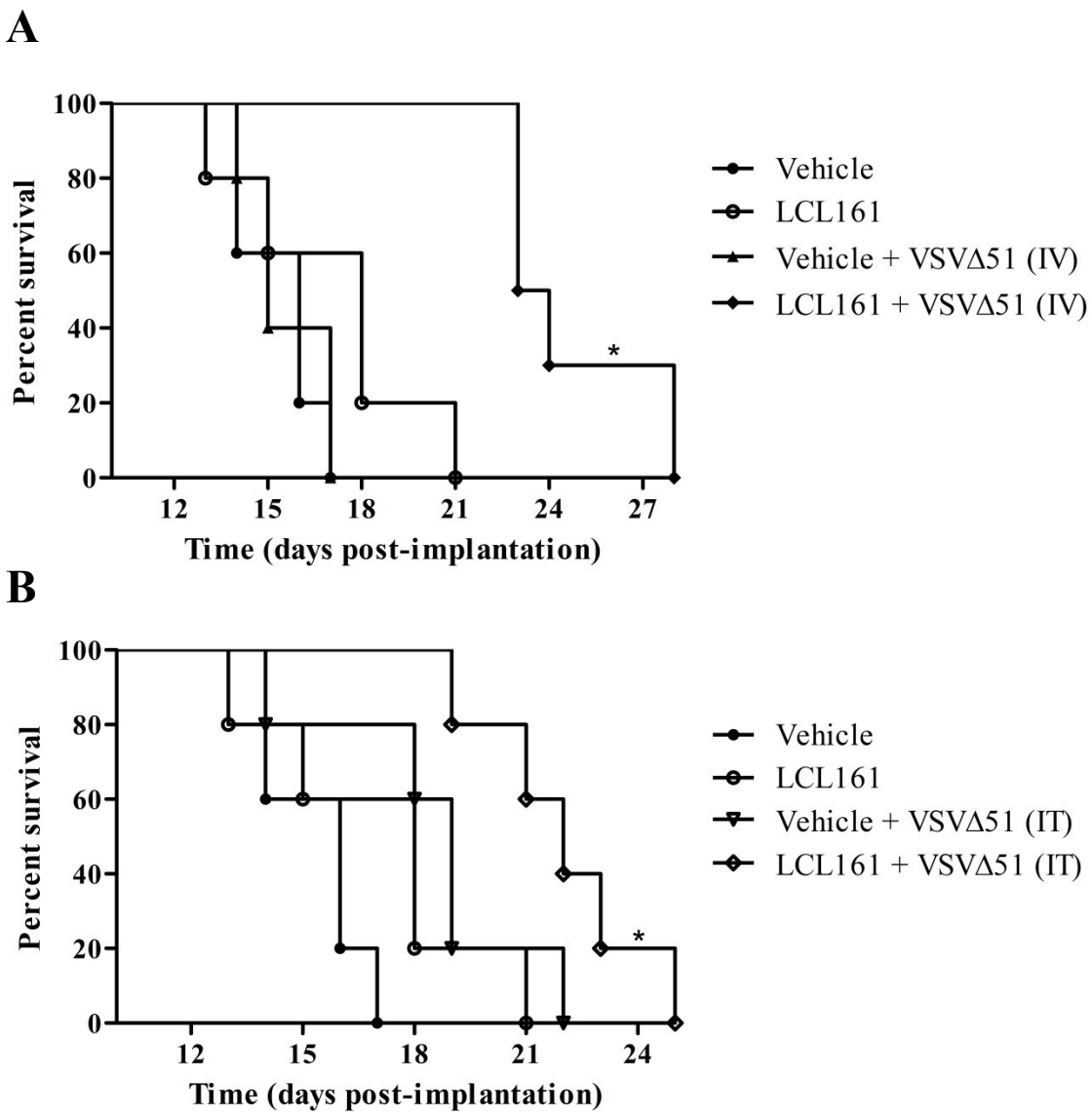

Figure 18. LCL161 and VSVΔ51 co-treated LLC tumour bearing mice see significant increase in survival time.

SMC and VSVΔ51 synergize to kill LLC cells which results in a statistically significant extended survival time for double treated mice. C57BL/6 mice were subcutaneously injected with 3 x 10^5 LLC cells and received four treatments of both VSVΔ51 (IV: 5 x 10^8 PFU, IT: 1 x 10^8 PFU) and LCL161 (50mg/kg) on opposite days. A survival curve was created to compare control mice and mice treated with VSVΔ51 (IV: 5 x 10^8 PFU) (A) and to compare control mice and mice treated with VSVΔ51 (IT: 1 x 10^8 PFU) (B). n = 5 per category with the exception of LCL161 + VSVΔ51 treatment group where n = 4. IV = intravenous, IT = intratumeral. Survival Analyses, Log Rank Mantel-Cox Test: *, $P < 0.001$.

As expected, the pattern of the results for the average tumour growth followed that of the survival time. The single therapy of LCL161, VSVΔ51 intratumoral or VSVΔ51 intravenous show no more than an 800mm^3 difference with vehicle treated mice on day 6 post-treatment (Figure 19A). Mice that received LCL161 and VSVΔ51 (intravenous and intratumoral) combination therapy show a 1300 - 1500mm^3 decrease in tumour volume on day 6 post-treatment (Figure 19A). The relative tumour volume (Figure 19B) clearly shows a significant drop in relative tumour volume in LCL161 and VSVΔ51 (IV) treated mice. As indicated by these results, VSVΔ51 is presumably able to produce a greater concentration of TNF-α which can then synergize with LCL161 and induce cell death of the LLC cells. An interesting result to note is that the difference between tumour volumes in vehicle treated compared to LCL161 treated mice in the first LLC *in-vivo* experiment is approximately 400mm^3. The second *in-vivo* LLC experiment shows a difference of 800mm^3 between vehicle and LCL161 treated mice. We propose that the reason for this difference is the fact that treatment was started four days earlier in the second *in-vivo* experiment so that the SMCs could start to work even before the tumour had time to develop a fully established niche.

3.3 In-vivo Analysis of B16F10 Cells in Response to SMC Treatment

3.31 Mice with B16F10 Tumours Show no Difference with SMC Treatment

We next looked at how established B16F10 tumours responded to SMCs. The activation of SMC was tested *in-vivo* by analyzing cIAP1/2 knockdown in the tumour and in the spleen at 16 and 24 hours post-SMC treatment. cIAP1/2 is down-regulated in B16F10 tumours at 16 hours post-treatment and remain down-regulated at 24 hours post-SMC treatment (Figure 20A). The IAPs show a rebound in the expression levels in the

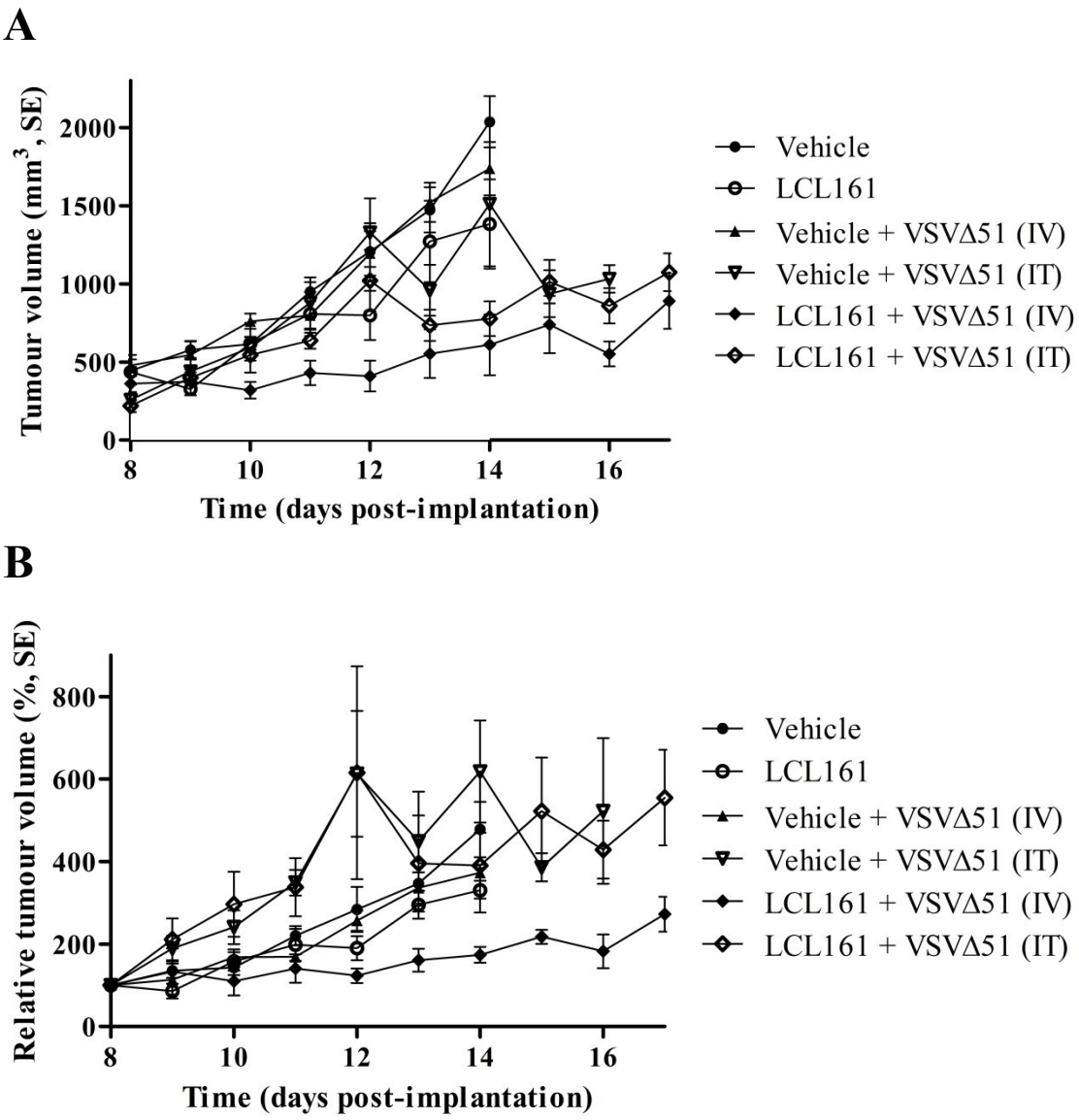

Figure 19. LLC tumour bearing mice experience decrease in tumour volume when co-treated with LCL161 and VSVΔ51.

The production of TNF-α by VSVΔ51 synergizes with SMC to induce tumour regression in double treated LLC tumour bearing mice. C57BL/6 mice were subcutaneously injected with 3 x 10^5 LLC cells and received four treatments of both VSVΔ51 (IV: 5 x 10^8 PFU, IT: 1 x 10^8 PFU) and LCL161 (50mg/kg) on opposite days. Mice were sacrificed only when tumours reached a volume of 2000mm^3. Plotted is the average tumour volume with standard error (A). A relative tumour volume graph (B) is plotted where, for example, the tumour volume of mouse 1 on day 2 is relative to its own tumour volume on day 1. n = 5 per category. SE = standard error, IV = intravenous, IT = intratumeral.

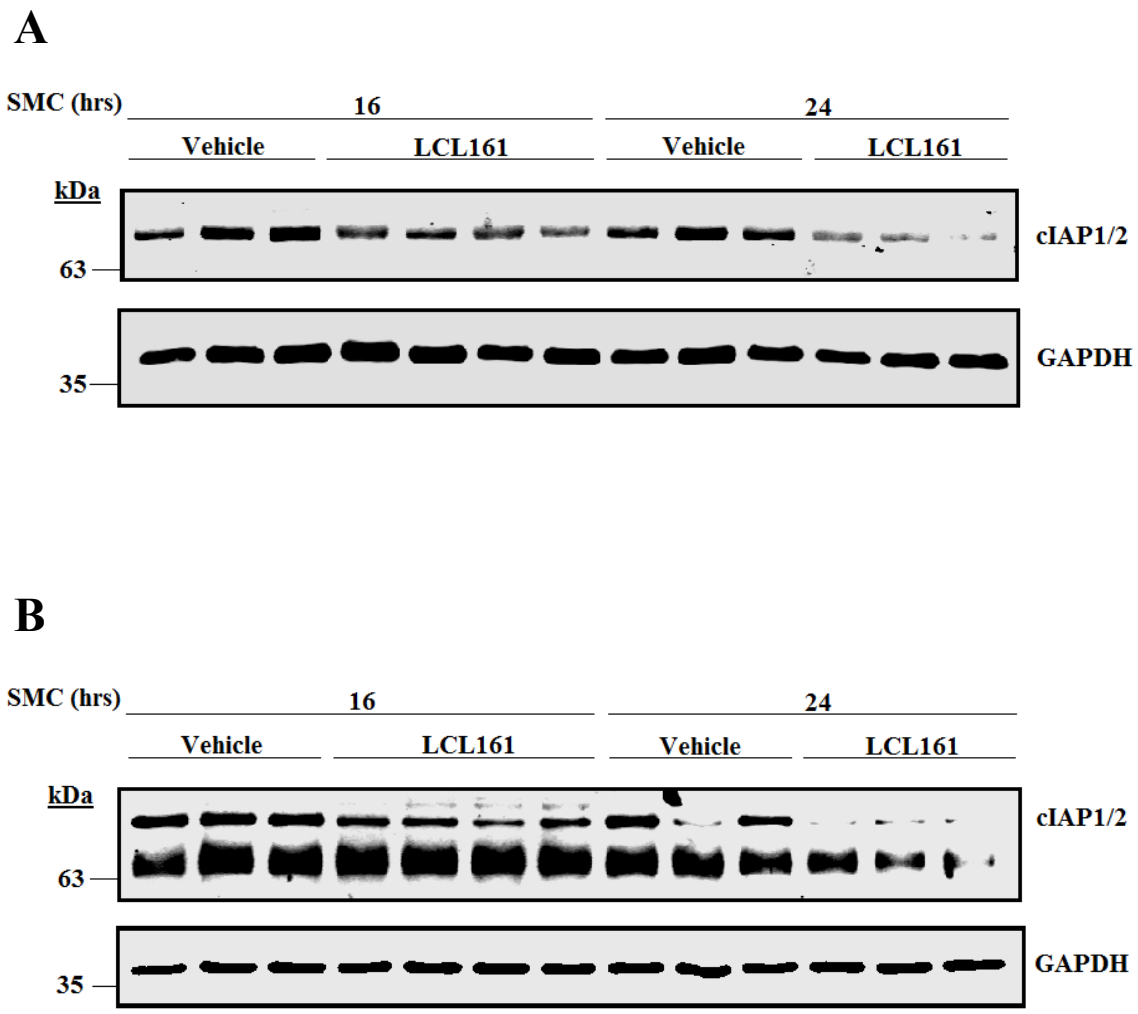

Figure 20. cIAP1/2 are targeted by LCL161 in the tumour and spleen of B16F10 tumour bearing mice.

The loss of cIAP1/2 occurs with the addition of SMC thus stimulating the activation of the alternative NF-κB pathway. Mice were injected with 3 x 10^5 B16F10 cells. Once tumours were established, mice were gavaged once with 50mg/kg LCL161 and sacrificed at either 16 hours or 24 hours post-treatment. The tumours (A) and spleens (B) were harvested and subjected to Western immunoblotting with antibodies against SMC targets. GAPDH was used as a loading control.

spleen at 16 and 24 hours post-SMC treatment (Figure 20B). Based on *in-vitro* data, we expected that the B16F10 cells would not be sensitized by SMC treatment in the mouse model. In order to confirm this hypothesis, mice were subcutaneously injected with B16F10 cells and as performed with LLC tumour bearing mice, were treated with LCL161 four times, three days apart (Figure 21A). Figure 21B is a visual of a sample of tumour sizes in vehicle versus LCL161 treated mice with B16F10 tumours. The average tumour growth rate of mice treated with LCL161 increases in comparable increments to the mice treated with vehicle (Figure 22A). When the relative tumour volume is graphed, it becomes even more evident that there is no difference in the average tumour growth rate of B16F10 tumour bearing mice (Figure 22B). In addition, the LCL161 treated mice with B16F10 tumours showed an earlier drop in survival rate compared to the vehicle treated mice (Table 3).

3.32 Oncolytic Virus and SMC Co-treatment Does Not Sensitize B16F10 Tumours in Mice

In-vitro data shows that B16F10 cells are resistant to SMC and TNF-α treatment unless c-FLIP is down-regulated. The lungs represent one of the most immunogenic locations in the body; the B16F10 cells were tested for reactivity to SMC in this environment. The macrophages of the innate immune system in the lung environment identify foreign bodies and will induce phagocytosis and the production of inflammatory mediators such as TNF-α (Zaas and Schwartz, 2005). If SMCs were to be able to synergize with TNF-α in the *in-vivo* B16F10 model, then one would expect that this could occur in the lungs. Mice were intravenously injected with B16F10 cells and tumour nodules embedded themselves in the lung tissue (Appendix I). The lungs were

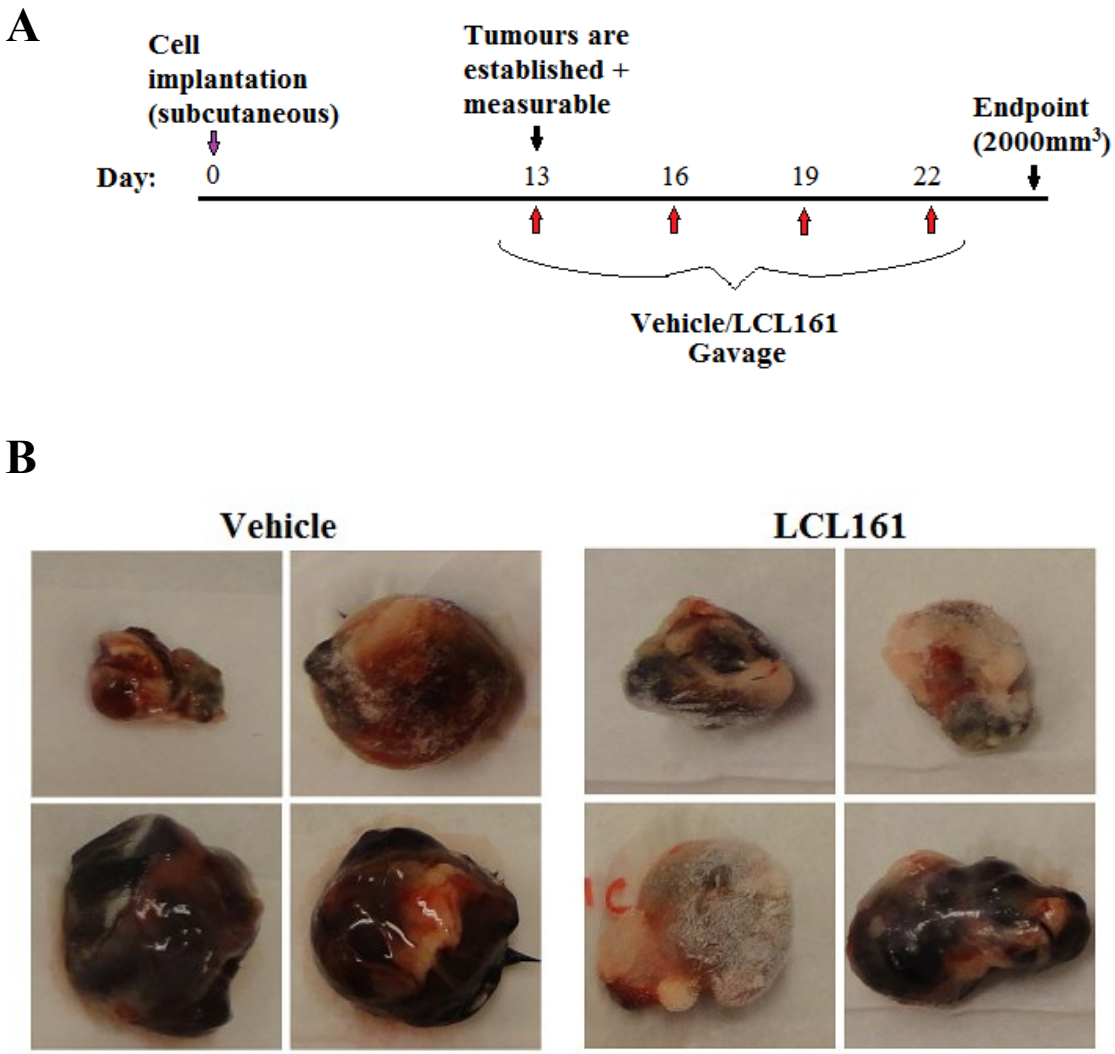

Figure 21. B16F10 tumour bearing mice are subjected to a treatment plan involving LCL161.

B16F10 cells are resistant to SMC and TNF-α co-treatment *in-vitro*, however, this treatment model was developed to test the efficacy of SMC treatment in a mouse model bearing B16F10 tumours. C57BL/6 mice were subcutaneously injected with 3 x 10^5 B16F10 cells and received four treatments of 50mg/kg LCL161 as seen in (A). Mice were sacrificed when tumours reached 2000mm^3 and the tumours dissected (B) to compare vehicle (n = 7) versus LCL161 treated mice (n = 8).

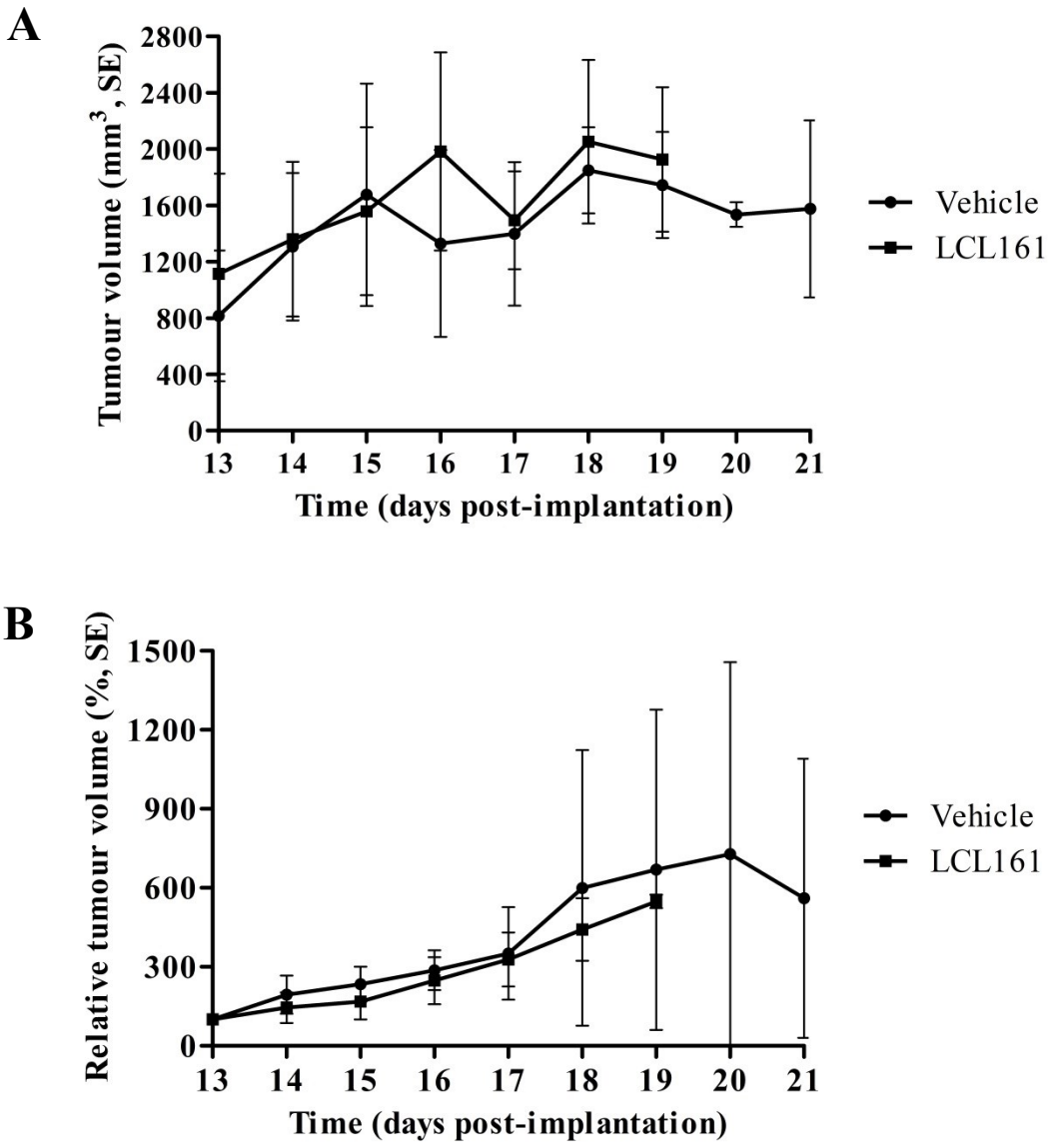

Figure 22. B16F10 tumour bearing mice are not sensitive to stand-alone LCL161 treatment.

The impact of SMC treatment was tested *in-vivo* on B16F10 tumour bearing mice. C57BL/6 mice were subcutaneously injected with 3 x 10^5 B16F10 cells and received four treatments of 50mg/kg LCL161. Mice were sacrificed only when tumours reached a volume of 2000mm^3. An average tumour volume graph with standard error (A) is plotted as well as a graph comparing the relative tumour volume (B) is plotted. Average tumour volume is calculated by the total tumour volume of each mouse on a particular day divided by the number of mice. Relative tumour volume is calculated by the total difference in tumour volume of each mouse on a given day compared to its own tumour volume on day 14. Vehicle (n = 7), LCL161 (n = 8). SE = standard error.

Table 3

Survival Time Comparisons of B16F10 Tumour Bearing Mice

ENDPOINT ($2000mm^3$)	VEHICLE (n = 7)	LCL161 (n = 8)
DAY	15	16
DAY	23+	22
DAY	18	19
DAY	15	16
DAY	21	16
DAY	19	18
DAY	15	15
DAY		16

dissected, stained with X-gal and the number of individual surface growths counted. Mice treated with LCL161 do not show any significant decrease in the number of tumour growths that developed compared to mice treated with vehicle (Appendix I). Visually, there is tremendous variation between and within the two categories, vehicle and LCL161 treated lungs (Appendix II). The lung model shows a greater degree of variability than did the subcutaneous model hence making results more difficult to interpret. In contrast to LLC experimental data, Dr. Beug's experimental data showed that using VSVΔ51 and LCL161 co-treatment, did not result in the sensitization of the B16F10 cells to death (data not shown). Mice that received VSVΔ51 alone, whether dosed intranasally or intravenously, did not have fewer numbers of tumour nodules in the lungs than the control. SMC alone was not effective either and even tended to show an increase in the number of individual surface growths compared to vehicle treated mice (data not shown).

Overall, as to be further reviewed in the discussion, we believe that for the B16F10 *in-vivo* model, c-FLIP would need to be down-regulated either by shRNA or a drug targeting c-FLIP in order to see cell death in response to SMC and VSVΔ51 co-treatment.

3.4 Cancer-induced Cachexia and the Impact of SMC Treatment

3.41 SMC Treatment Induces Skeletal Muscle Wasting in LLC Tumour Bearing Mice

Since cancer-induced cachexia affects approximately 30% of Canadian cancer patients, this remains a very important area of study (Tan and Fearon, 2008). As such, we decided to determine whether the SMC treatment of tumour bearing mice would negatively impact skeletal muscle (atrophy), positively impact skeletal muscle (protection) or have no effect whatsoever on skeletal muscle. In comparison to denervation models where significant atrophy is documented, cancer-induced cachexia

models are not as robust and have proved much more difficult to identify. Thus, it is important to be aware while analyzing results that small changes or differences may go unidentified and more specific atrophy identification methods may be required. However, we theorized that if SMC is negatively impacting skeletal muscle to a significant degree, we would be able to see signs of atrophy or wasting in the muscle fibres of tumour bearing mice. In contrast, if SMC is positively impacting skeletal muscle to a significant degree, there should not be any signs of atrophy in the muscle fibres of treated mice.

Firstly, the TA muscle of LLC tumour bearing mice that had been gavaged with LCL161 was collected to ensure that SMC was active in the muscle. Figure 23 shows that cIAP1/2 is down-regulated in the TA at 16 and 24 hours post-SMC treatment, thus the LCL161 is active.

In order to test how SMC was impacting skeletal muscle on LLC tumour bearing mice, the tibialis anterior muscle of mice from the experiment where LLC tumour bearing mice received either LCL161 gavage or LCL161 gavage in conjunction with VSVΔ51 delivered either intravenously or intratumerally (IV/IT) was collected. As cancer-induced cachexia impacts type II skeletal muscle fibres more so than type I skeletal muscle fibres, the tibialis anterior (TA) muscle, made up of mostly type II fibres, was collected from mice, sectioned and stained with hematoxylin and eosin. Microscope images were taken of the muscle and the muscle fibres were traced to be able to determine if atrophy was induced in the treated conditions. Figure 24 shows an example of the cross-sectional images of the TA muscle fibres in each condition. The average whole muscle cross-sectional area (Figure 25A) and the average fibre cross-sectional area

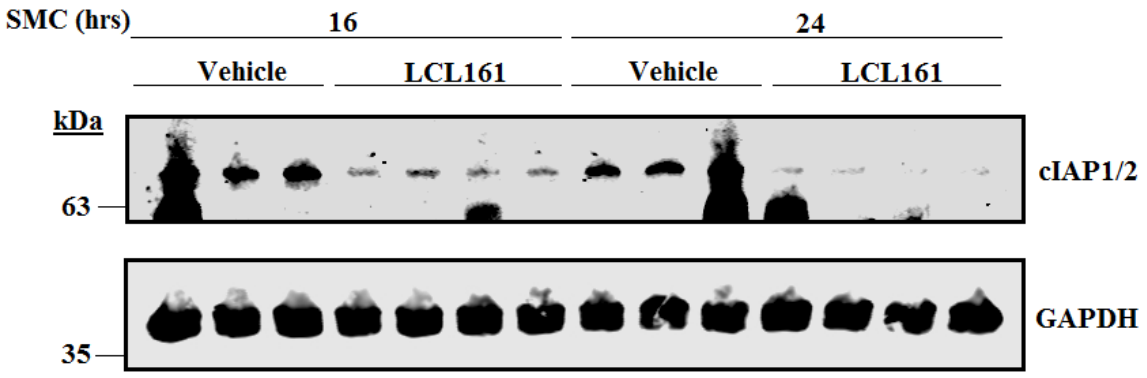

Figure 23. LCL161 targets cIAP1/2 in the tibialis anterior muscle of LLC tumour bearing mice.

The loss of cIAP1/2 occurs with the addition of SMC thus stimulating the activation of the alternative NF-κB pathway. Mice were injected with 3 x 10^5 LLC cells. Once tumours were established, mice were gavaged once with 50mg/kg LCL161 and sacrificed at either 16 hours or 24 hours post-treatment. The TA muscles were harvested and subjected to Western immunoblotting with antibodies against SMC targets. GAPDH was used as a loading control.

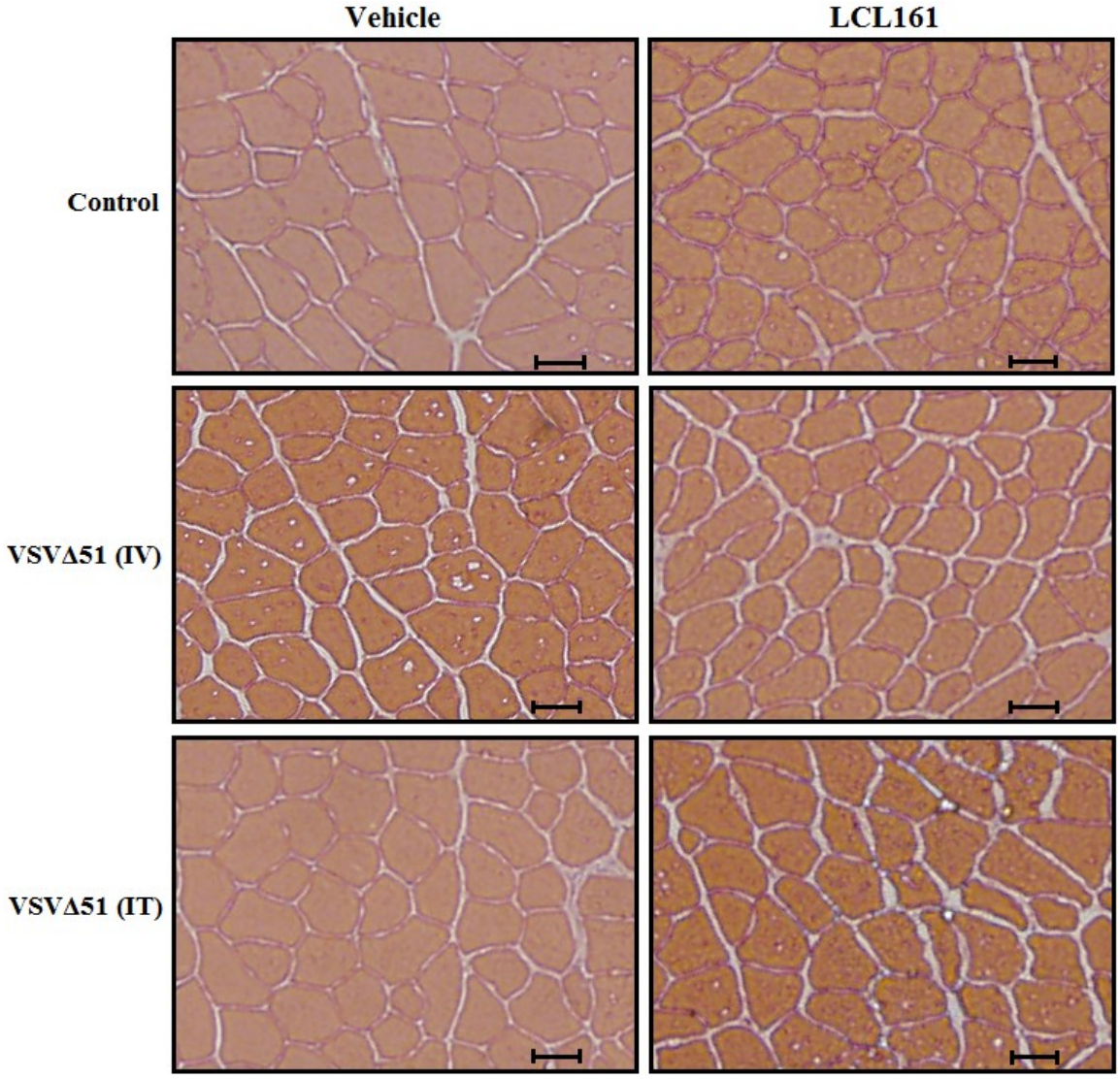

Figure 24. The impact of SMC and VSVΔ51 co-treatment on skeletal muscle of LLC tumour bearing mice.

With SMC depleting the cIAPs and VSVΔ51 inducing the production of TNF-α, which is known to induce skeletal muscle atrophy, the impact of SMC and VSVΔ51 treatment was investigated. C57BL/6 mice were subcutaneously injected with 3 x 10^5 LLC cells and received four treatments of both VSVΔ51 (IV: 5 x 10^8 PFU, IT: 1 x 10^8 PFU) and LCL161 (50mg/kg) on opposite days. Mice were sacrificed when tumours reached a volume of 2000mm^3. The tibialis anterior muscles were dissected from the mice. Shown here are cross-sections of the tibialis anterior muscle stained with hematoxylin and eosin comparing the muscle sections of control mice versus mice treated with LCL161 alone, VSVΔ51 alone or the double treatment. IV = intravenous, IT = intratumeral.

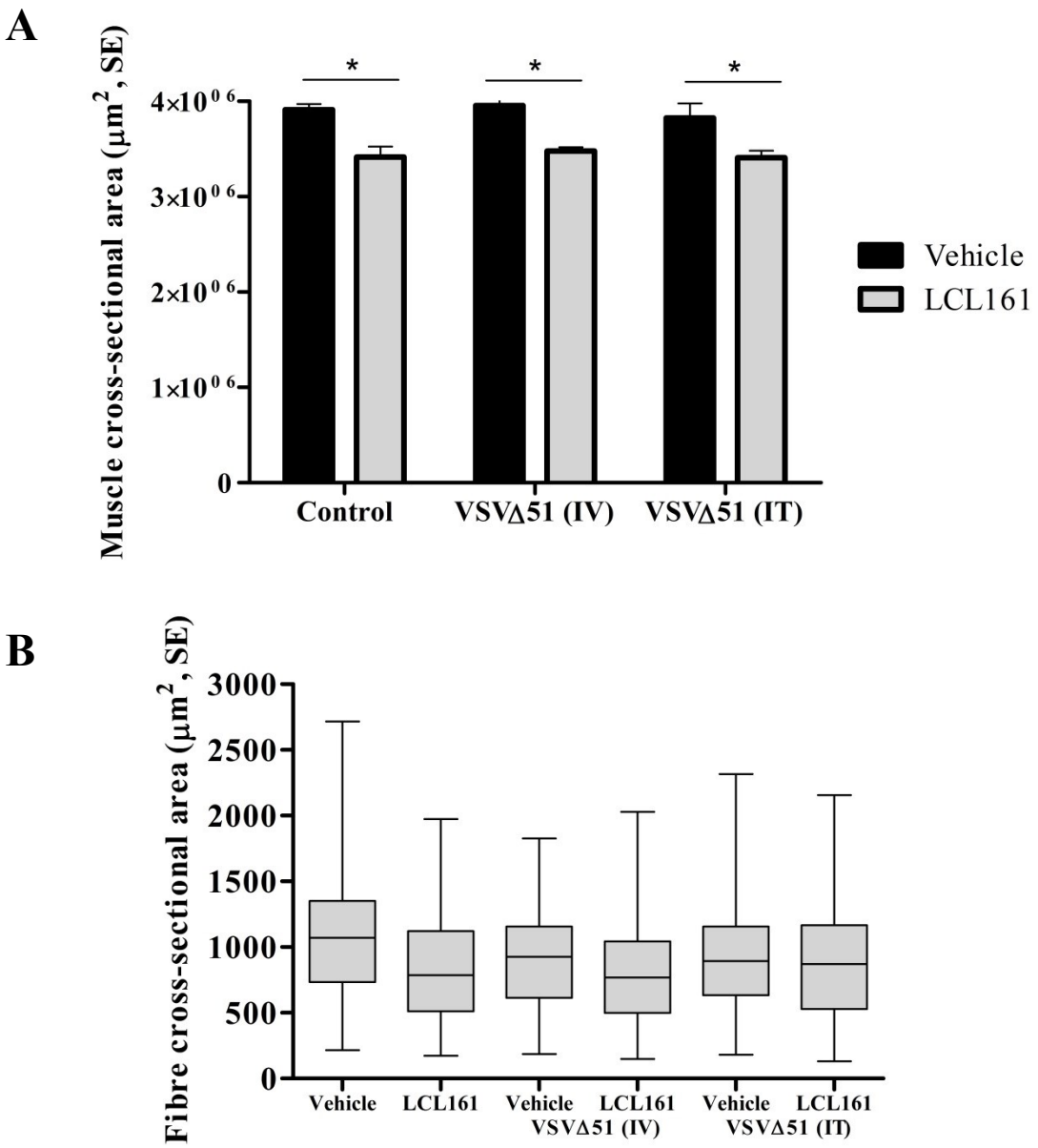

Figure 25. SMC treatment causes decrease in whole muscle and fibre cross-sectional area of TA of LLC tumour bearing mice.

Skeletal muscles that experience wasting or atrophy will show a decrease in whole muscle and fibre cross-sectional areas. TA muscles were collected from LLC tumour bearing mice treated with LCL161 and/or VSVΔ51. Whole muscle cross-sectional area (A) and fibre cross-sectional area (B) were averaged to look for effects of the drugs on skeletal muscle. Muscle: n = 3 per category, fibre: n = 300 per category. SE = standard error, IV = intravenous, IT = intratumeral. One-way ANOVA, Dunnett's Multiple Comparison Test: *, $P < 0.05$.

(Figure 25B) were quantified and compared mice treated with vehicle, VSVΔ51 (IV) or VSVΔ51 (IT) in the absence or presence of LCL161. The muscle area of mice treated with LCL161 compared to vehicle is significantly lower with $p < 0.05$ (Figure 25A). Mice co-treated with VSVΔ51 (IV/IT) and LCL161 also showed a statistical difference in average muscle size compared to vehicle treated mice. The average fibre cross-sectional graph shows a trend in that, mice that received LCL161 have decreased muscle fibre areas (Figure 25B). Another indication of skeletal muscle wasting is when the muscle contains an increased number of smaller fibres and a decreased number of larger fibres. LLC tumour bearing mice treated with LCL161 show a greater number of small muscle fibres and a correlated decrease in the number of large fibres (Figure 26). These results remain similar for mice treated with VSVΔ51 (IV) whereby the LCL161 treated mice possess an increased number of smaller muscle fibres compared to mice treated with vehicle (Figure 27). Finally, the distribution of fibre sizes for mice treated with VSVΔ51 (IT) does not appear to follow as defined a trend as the previous two categories of mice (Figure 28). The LCL161 and VSVΔ51 (IT) treated mice have a higher number of muscle fibres under $400\mu m^2$ but then mice receiving vehicle show increased numbers of muscle fibres between $400\mu m^2$ and $1400\mu m^2$. All in all, this study suggests that SMCs induce skeletal muscle wasting regardless and independently of oncolytic virus treatment. However, this study is not capable of dissecting out any role of cancer-induced cachexia as additional parameters would have had to have been monitored such as food intake and the presence of cytokines. Results from the western blot analysis (Figure 29) reveal that there are no differences between any category, contradicting the result that any wasting or atrophy is occurring. Antibodies against MHC, a muscle specific protein were not

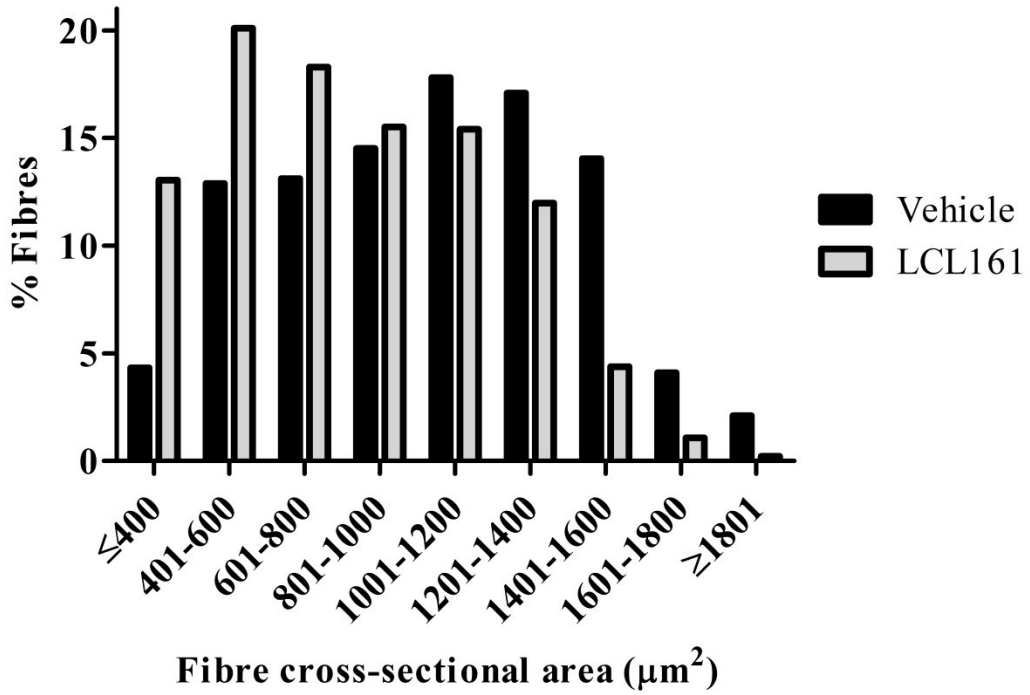

Figure 26. LLC tumour bearing mice treated with LCL161 show an increased number of smaller TA muscle fibres compared to those of vehicle treated mice.

An indication of skeletal muscle atrophy is to have an increase in the number of small fibre cross-sectional areas. Mice bearing LLC tumours were treated with vehicle or LCL161. The TA muscles were isolated and fibre cross-sectional areas calculated. Shown here is the percentage of vehicle versus SMC treated muscle fibres that fit into the indicated size categories. Muscle: n = 3 per category, fibre: n = 300 per category.

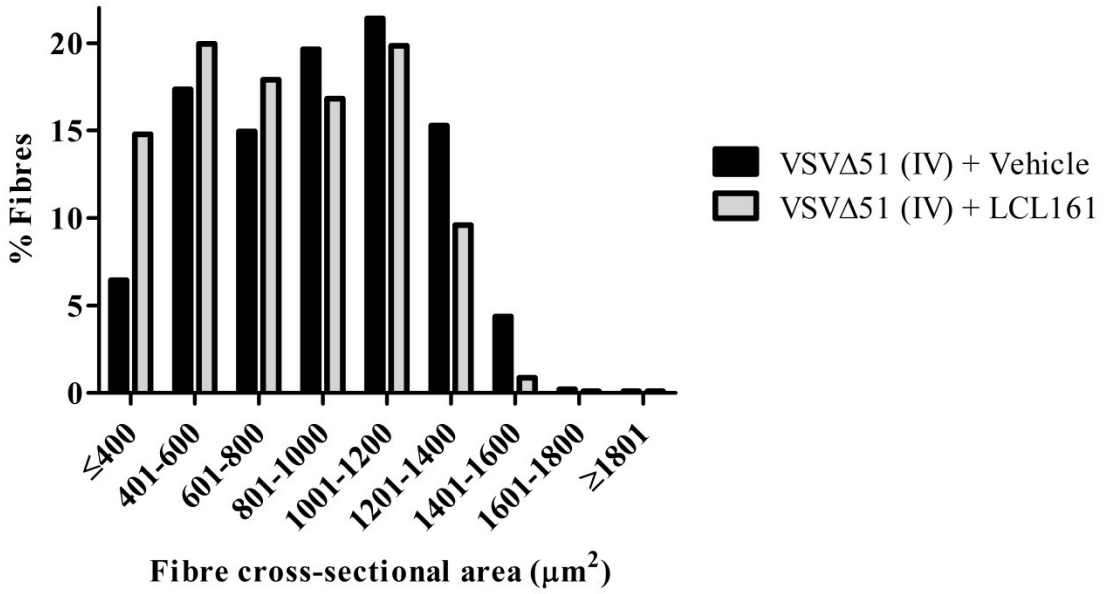

Figure 27. Increase in smaller TA muscle fibre areas of LLC tumour bearing mice co-treated with SMC and VSVΔ51 (IV) compared to those co-treated with vehicle and VSVΔ51.

An indication of skeletal muscle atrophy is to have an increase in the number of small fibre cross-sectional areas. Mice bearing LLC tumours were treated with VSVΔ51 (IV) and either vehicle or LCL161. The TA muscles were isolated and fibre cross-sectional areas calculated. Shown here is the percentage of vehicle and VSVΔ51 (IV) versus SMC and VSVΔ51 (IV) treated muscle fibres that fit into the indicated size categories. Muscle: n = 3 per category, fibre: n = 300 per category. IV = intravenous.

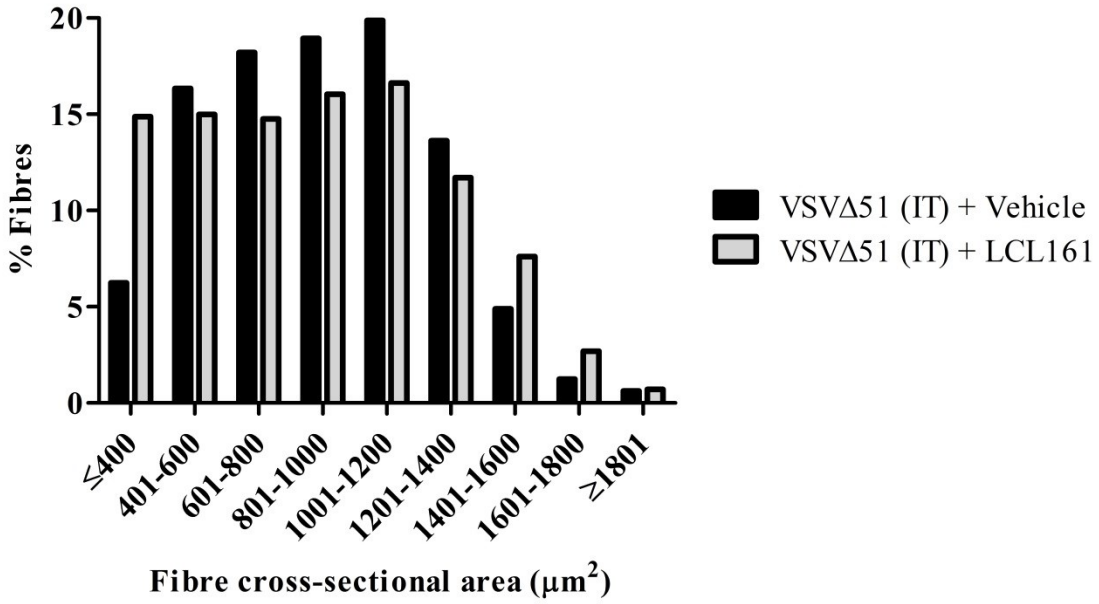

Figure 28. Higher percentage of smaller muscle fibre areas in LLC tumour bearing mice treated with SMC and VSVΔ51 (IT) compared to vehicle and VSVΔ51 treated mice.

An indication of skeletal muscle atrophy is to have an increase in the number of small fibre cross-sectional areas. Mice bearing LLC tumours were treated with VSVΔ51 (IT) and either vehicle or LCL161. The TA muscles were isolated and fibre cross-sectional areas calculated. Shown here is the percentage of vehicle and VSVΔ51 (IT) versus SMC and VSVΔ51 (IT) treated muscle fibres that fit into the indicated size categories. Muscle: n = 3 per category, fibre: n = 300 per category. IT = intratumoural.

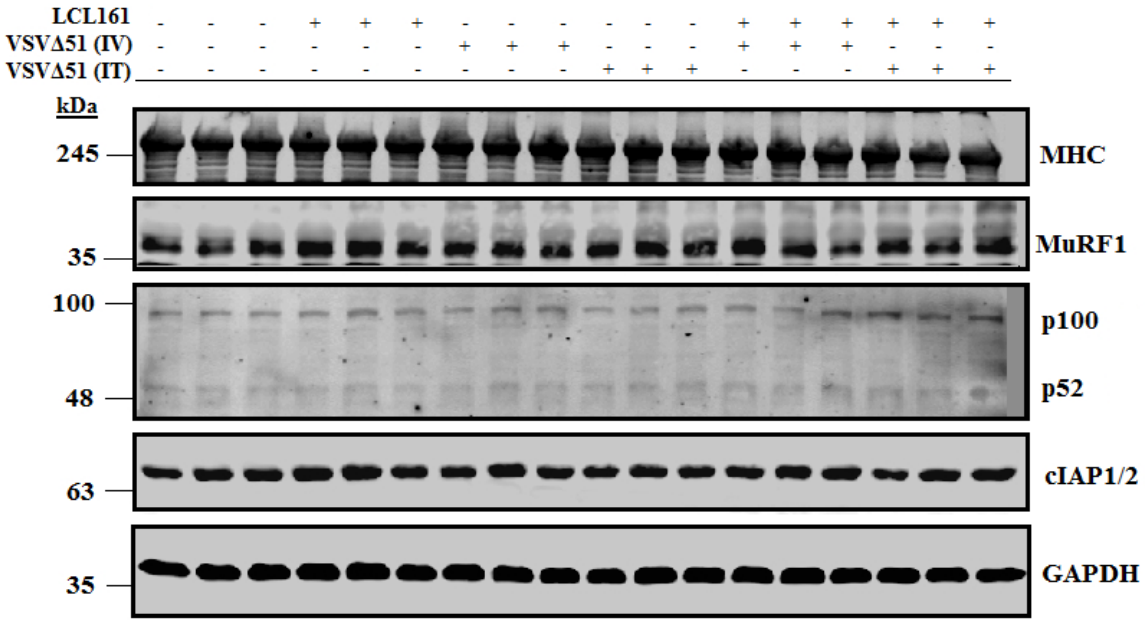

Figure 29. Atrophy markers are not activated in TA of LLC tumour bearing mice receiving SMC.

Skeletal muscle atrophy is indicated by the decrease in MHC, a muscle specific protein and the increase in MuRF1, a muscle specific E3 ligase. C57BL/6 mice were subcutaneously injected with 3 x 10^5 LLC cells and received four treatments of both VSVΔ51 (IV: 5 x 10^8 PFU, IT: 1 x 10^8 PFU) and LCL161 (50mg/kg) on opposite days as seen in (A). Mice were sacrificed when tumours reached a volume of 2000mm^3. Shown here are antibodies against skeletal muscle atrophy markers (MHC, MuRF1) and direct and indirect targets of SMC (cIAP1/2, p100/52). GAPDH was used as a loading control. IV = intravenous, IT = intratumoural.

decreased as would be expected should atrophy be induced. MuRF1, a muscle specific E3 ligase, should have been increased in the presence of skeletal muscle atrophy but does not change in the western blot analysis. In addition, the SMC targets were unaltered at the time of dissection suggesting the re-bound effect of the IAPs had already occurred. Regardless, western blot data is not as reliable as the fibre cross-sectional area data in terms of identifying skeletal muscle area because the former does not have the capability to pick up subtle differences that may arise. Nevertheless, the study suggests SMC can induce skeletal muscle atrophy, albeit minor, in LLC tumour bearing mice. In order for this statement to be validated, another experiment would have to be performed while taking into account the limitations of the current experiment. Overcoming these limitations would include having a larger sample size per category; analyzing more than one muscle type; and dissecting muscles at a number of specified time points.

CHAPTER 4: DISCUSSION

4.1 Effects of SMC Treatment on Lewis Lung Carcinoma and B16F10 Melanoma

Many cancers have been found to over-express the cIAP and/or XIAP proteins. Patients bearing this tumour type show a decreased response to anti-cancer therapy and have a poor prognosis due to increased aggressiveness of the tumour. This prompted research towards the development of therapeutic drugs that could target and antagonize the IAP proteins. Smac mimetic compounds (SMCs) are small molecule IAP antagonists that induce the down-regulation of cIAP1 and cIAP2, and to a lesser extent, XIAP, thus stimulating cell death in sensitive cancer cell lines or triggering TNF-α sensitization in others (Reviewed in Dubrez *et al*., 2013). We chose to study the effects of SMC therapy on Lewis Lung Cancer (LLC) and B16F10 melanoma cancer cell lines. We found that LLC cells are sensitive to the co-treatment of exogenous TNF-α with SMC. B16F10 cells, however, remain resistant. We discovered c-FLIP to be the resistance factor in non-sensitizing B16F10 melanoma cells. When c-FLIP is down-regulated, B16F10 cells can then be sensitized to SMC and TNF-α caspase-mediated cell death. Our discovery, along with the work done by Cheung and team, shows that c-FLIP is a resistance factor in a number of cancer cell lines, including ovarian, lung, glioblastoma and melanoma cells (Cheung *et al*., 2009).

4.11 c-FLIP is the Resistance Factor to SMC-mediated Cell Death in B16F10 Melanoma Cells

B16F10 melanoma cells are resistant to the double treatment of SMC and TNF-α *in-vitro*. When c-FLIP is down-regulated, the melanoma cells are then sensitized to SMC and TNF-α double treatment. These results further validate Dr. Cheung's finding that the down-regulation of c-FLIP sensitizes resistant cancer cell lines to TNF-α mediated cell

death (Cheung *et al*., 2009). Based on this *in-vitro* data, we decided to investigate the effect of SMC treatment on B16F10 cells in an animal model setting. Not unexpectedly, we found that B16F10 tumours do not respond to SMC treatment *in-vivo*. Additional data collected from our lab shows that B16F10 cells remain resistant even when co-treated with SMC and an oncolytic virus (data not shown). Together, this data suggests that c-FLIP is the main resistance factor and once targeted, the melanoma cancer cells can become sensitized to SMC and TNF-α co-treatment.

For the purposes of treating resistant cancer cells, it would be important to find out what is responsible for the regulation of c-FLIP expression given that LLC cells are sensitive to SMC therapy whereas B16F10 cells require an exogenous source to target c-FLIP for down-regulation. Previous studies have suggested that tumour cells that become resistant to death ligands, such as TRAIL, develop the ability to become less 'visible' to the immune system (Zhang and Fang, 2005). With the same principal idea, Medema and co-workers studied tumour cells engineered to over-express c-FLIP or to be depleted of c-FLIP. They found that tumour cells not expressing c-FLIP can be more readily eliminated by the immune system whereas tumour cells expressing c-FLIP appear to evade detection by the immune system (Medema *et al*., 1999). Therefore, if endogenous levels of c-FLIP are maintained in treated B16F10 cells, then they should display increased resistance to cell death mediated by SMC and TNF-α co-treatment.

In addition, research has shown that in several types of cancer, there is a correlation between the amount of c-FLIP expression levels and the resistance to TRAIL or other ligands, and melanoma is one such example (Zhang and Fang, 2005). Therefore, although the endogenous c-FLIP expression level in LLC and B16F10 cancer cells is

unknown, we would predict that LLC cells possess a lower endogenous level of c-FLIP protein compared to B16F10 cells, thus providing LLC cells with increased chance of being detected by the immune system and less resistance in response to TRAIL or TNF-α. Contrary to LLC cells, B16F10 cells, which likely have increased c-FLIP expression levels would have increased malignant potential and strategies for evasion of the immune system.

An interesting result revealed from the cell viability assay in B16F10 cells was that a considerable amount of cell death occurs upon the addition of TNF-α alone once c-FLIP has been down-regulated. Interestingly, over-expression of c-FLIP has been shown to lead to the increased activation of the NF-κB pathway as well as the extracellular signal-regulated kinase (ERK) pathway. c-FLIP successfully activates these pathways by interacting with TRAF1, TRAF2, RIP and Raf1 (Safa, 2012). Moreover, Raf1 is a downstream effector of the Ras pathway, a pathway responsible for regulating cell growth, proliferation and survival (Oceandy *et al*., 2009). Generally, Ras-association domain-containing protein 1 isoform A (RASSF1A), a tumour suppressor, inhibits the signalling between Ras and Raf1 which in turn shuts down the signalling pathway that otherwise would have activated ERK1/2, and led to proliferation. Notably, 15% of human cancers are affected by RASSF1 modifications and in 41% of melanoma cancers, specifically, RASSF1 is silenced due to epigenetic changes such as methylation (Donninger *et al*., 2007). A theory could be proposed whereby B16F10 cells, being a melanoma cancer, does not possess a functional RASSF1A protein and therefore cannot inhibit the proliferation induced by the activation of the ERK1/2 pathway. If this were to be the case, then a dual resistance in B16F10 cells caused by the over-expression of c-

FLIP could be proposed to be affecting both NF-κB (survival) and ERK (proliferation) signalling. This model would also be consistent with the results of a study that demonstrates that the loss of function of RASSF1A induces resistance to TNF-α induced apoptosis (van der Weyden and Adams, 2007). Hence, when c-FLIP is down-regulated via siRNA, the NF-κB and ERK pathways are suppressed, and proliferation and survival are inhibited. The addition of TNF-α, therefore, would induce cell death.

All in all, determining that c-FLIP is the resistance factor in B16F10 cells gives direction for future objectives to find a drug to target and down-regulate c-FLIP levels to overcome the resilience of the cancers such as melanoma.

4.12 LLC Cells are Sensitized to SMC and VSVΔ51 Double Treatment

We found that LLC cells are sensitive to SMC and TNF-α co-treatment *in-vitro*. Therefore, LLC cells fall into the second category from Table 1 where they require a trigger such as TNF-α or TRAIL to synergize with SMCs but presumably, c-FLIP is not in any way inhibiting cell death from occurring.

We hypothesized that since LLC cells were sensitive to the double treatment *in-vitro*, LLC tumour bearing mice would be sensitive to SMC treatment *in-vivo* since SMC treatment can induce the production of TNF-α, which in turn could act as the death trigger. We found that LLC tumour bearing mice are only mildly sensitive to SMC alone *in-vivo*, suggesting that there is not enough endogenous TNF-α being produced in order to synergize with SMC and induce cell death. Therefore, we postulated that an oncolytic virus, which could robustly stimulate the production of TNF-α, would allow sensitization of the cancer cells to SMC (Beug *et al*., 2014). Oncolytic viruses stimulate RIG-I-like receptors (RLR) and toll-like receptors (TLR), which then signal through the IFN

response factor (IRF) 3/7 and NF-kB pathway to increase the concentration of IFN and IFN responsive genes. This in turn induces the production of chemokines and cytokines such as TRAIL and TNF-α (Beug *et al*., 2014). We discovered that by using VSVΔ51, an oncolytic rhabdovirus, as a trigger for SMC *in-vivo*, LLC cells become much more responsive to LCL161, suggesting that VSVΔ51 is stimulating the production of additional TNF-α which can then synergize with SMC to kill the cancer cells. The importance of these results is that we have shown LLC cells to be sensitive to SMC and oncolytic virus treatment in a mouse model which further validates the *in-vitro* data.

Overall, since progress in cancer therapy development for lung cancer has not advanced as rapidly as in other domains, these results have the ability to optimize lung cancer treatments in the near future as both SMCs and oncolytic viruses are in clinical trials.

4.2 Effects of SMC Treatment on Skeletal Muscle Wasting

SMCs have reached stage II in clinical trials, suggesting that the drug is generally well tolerated and is showing positive results in the battle against cancer (Fulda, 2014). SMCs, when used as a single agent, are not as effective as when used with a trigger such as TNF-α. However, TNF-α is known to induce skeletal muscle atrophy (Petersen *et al*., 2007; Vince *et al*., 2008). We chose to study LLC lung cancer and B16F10 melanoma cancer cell lines partly for the reason that they are widely characterized as being highly cachectic tumour models. Cancer-induced cachexia is the wasting of skeletal muscle due to the presence of cancer in the body (Nedergaard *et al*., 2013). As previously mentioned, SMCs induce the production of TNF-α and therefore, it was important to ask what effects SMC treatment would have on skeletal muscle. Based on previous studies, it

seems reasonable to hypothesize that SMC treatment, followed by IAP depletion, would induce atrophy of the skeletal muscles. Another possibility would be that SMC treatment will not have any significant impact on skeletal muscle. However, since SMC is known to regulate the IAPs and muscle cells express cIAP1, it is very likely that the addition of SMC would have an impact on skeletal muscle one way or another. Lastly, a final possibility is that SMC treatment would be, in fact, protective against atrophy. The rationale behind SMC being protective is from unpublished data from the Korneluk lab whereby Mdx mutant mice crossed with cIAP1$^{-/-}$ mice tend to have less diaphragm damage, do not deplete their pool of satellite cells as rapidly and therefore have overall less skeletal muscle atrophy in response to exercise (Enwere *et al*., 2013). Although DMD is clearly very different from cancer-induced cachexia, we questioned whether this type of "protection" could be possible in tumour bearing mice that are treated with SMC.

4.21 SMC Treatment Induces Skeletal Muscle Wasting in LLC Tumour Bearing Mice

For the analysis of the skeletal muscle from LLC tumour bearing mice treated with SMC, repeated experiments would be required for definitive conclusions to be made. However, we found suggestive evidence that SMC treatment causes limited skeletal muscle atrophy in LLC tumour bearing mice independent of co-treatment with an oncolytic virus. The increase in the number of smaller muscle fibres indicates that SMC is inducing atrophy to a small degree in skeletal muscle.

In contrast, the Western blot data does not support this evidence. A possible explanation as to why we do not see a difference in atrophy marker expression in Western blots is because whole lysate samples are used. The implication of this is that there could be a large pool of cells that have undergone atrophy but an even larger

number of cells that have not. Therefore, the differences are much too subtle to detect when analyzing protein lysate. Another limitation to this study includes the fact that mice were sacrificed when their tumour reached 2000mm^3, which means that not all mice were sacrificed on the same day. Hence, some mice will have been exposed to atrophic factors for longer than other mice and therefore a direct comparison, as we have shown, is not truly representative of an analogous degree of atrophy in each mouse.

4.3 Overall Conclusions and Future Directions

4.31 The Potential for SMC Therapy against B16F10 Melanoma

B16F10 cells are resistant to the double treatment of SMC and TNF-α *in-vitro*. These cells become sensitized only when apoptosis inhibitor, c-FLIP, is down-regulated. Notably, mice bearing B16F10 tumours show no difference in survival time or tumour volume when receiving SMC versus vehicle treatment. Mice bearing B16F10 tumours do not respond to the co-treatment of VSVΔ51 and LCL161 either, indicating that c-FLIP must be exogenously targeted in order to induce cell death. The importance of these results is that c-FLIP is clearly implicated as a key factor that should be targeted to sensitize cancer cell lines to caspase-8 mediated cell death.

Future studies can be performed in order to validate these findings. These could include creating an shRNA stable B16F10 cell line with c-FLIP that is down-regulated, which could then be used in the *in-vivo* models. If sensitization to SMC treatment is confirmed, the next step would be to find a drug that targets c-FLIP for down-regulation (reviewed in Shirley and Micheau, 2013). Dr. Cheung showed that the down-regulation of SMG1 and NIK induces a decrease in c-FLIP transcript levels and allows for cell death of cancer cells that were previously resistant to the double drug treatment (Cheung *et al*.,

2011). To further investigate this, we recently received an SMG1 inhibitor and we will be combining this with a SMC with and without TNF-α (Gopalsamy *et al*., 2012). Therefore, the mechanism would be that the SMG1 down-regulates c-FLIP in B16F10 cells and then SMC would be used to induce cell death. With SMC currently in clinical trials, it would be important to find a drug to target c-FLIP for those resistant cancer cell lines.

4.32 The Potential for SMC Therapy against LLC Cancer

LLC cells are sensitive to SMC and TNF-α co-treatment *in-vitro*, while *in-vivo*, SMC requires a trigger to produce a larger amount of TNF-α. We have found that the oncolytic virus, VSVΔ51, injected intravenously, synergizes with LCL161 to produce the most dramatic decrease in tumour volume and increase in survival time. VSVΔ51 dosed intratumerally also induces the same benefits against LLC tumours however, as the trigger is local, it synergizes to a slightly lesser degree with SMC compared to intravenous injection. The implication of these results is that sensitive cancer cell lines can targeted by co-treatment with LCL161 along with a trigger, such as VSVΔ51, both of which are progressing separately through clinical trials.

Further insight into LLC sensitivity to SMC treatment could be undertaken with non-viral immune stimulants. Specifically, LLC cells could be treated with a SMC along with a toll-like receptor (TLR) agonist such as polyinosine-polycytidylic (poly (I:C)) or CpG oligodeoxynucleotide (CpG) to determine if this results in cell death as it did in the mouse cell line EMT6 (Beug *et al*., 2014). poly(I:C) is an imitated equivalent of double stranded RNA and is used as a TLR3 agonist (Beck et al., 2011). TLR3 activates natural killer (NK) cells and dendritic cells of the immune system but is also often up-regulated

in malignant cells to increase the production of IFN. Friboulet and co-workers used poly(I:C) in combination with the Smac mimetic, RMT5265 to treat nasopharyngeal carcinoma. They found that the nasopharyngeal carcinoma cell line underwent apoptosis in response to the drug co-treatment (Friboulet *et al*., 2010). Another TLR agonist is CpG which is known to bind TLR 9. This in turn activates the NF-κB pathway thus inducing an inflammatory response by up-regulating IL-12 and -18, IFN-α and TNF-α (Kim *et al*., 2012). Beug and collegues showed that mice bearing EMT6 tumours could be cured with the double treatment of CpG and LCL161 (Beug *et al*., 2014). In essence, LLC tumours would very likely be responsive to both poly(I:C) and CpG double treatment with LCL161 *in-vitro*. In addition, this would allow cancer therapies to use innate immune stimulatory drugs rather than oncolytic viruses. Although both SMC and oncolytic viruses have proven to be safe for human use in cancer trials, the less drugs that need to be administered, the less chance of negative side effects.

4.33 Effect of SMC Treatment on Skeletal Muscle of Tumour Bearing Mice

LLC tumour bearing mice that received VSVΔ51 (IV or IT) did not undergo atrophy as indicated by the similar cross-sectional areas of the muscle fibres to those of the vehicle treated mice. However, mice that received LCL161 treatment experienced a decrease in the average muscle fibre cross-sectional area and an increase in the number of muscle fibres with a smaller cross-sectional area when compared to those of the vehicle treated mice. Although results would require confirmation, research suggests that SMC treatment induces skeletal muscle atrophy, to a limited degree, in LLC tumour bearing mice.

Moreover, these results bring up many further questions that would need to be addressed in future studies. Firstly, would SMC treatment induce skeletal muscle atrophy in non-tumour bearing mice? Here, we could hypothesize that SMC would still induce skeletal muscle atrophy as SMC treatment alone may induce TNF-α production. Likewise, would SMC treatment induce atrophy in skeletal muscle of mice bearing other tumours such as B16F10 cancer? Notably, we found B16F10 melanoma cells to be resistant *in-vitro* and *in-vivo* to SMC and TNF-α co-treatment. Although B16F10 cells are resistant to this treatment, we know that SMC is active regardless (Appendix III) and therefore we could predict that SMC would have an impact on the skeletal muscle of mice bearing B16F10 tumours as well. Finally, it would be important to ascertain if the limited skeletal muscle atrophy seen in the mouse models of cancer cachexia will be duplicated in human cancer and if it will be reversible once treatment is stopped.

REFERENCES

Acharyya S, Guttridge DC. 2007. Cancer cachexia signaling pathways continue to emerge yet much still points to the proteasome. *Clin Cancer Res*, 13:1356-61.

Acharyya S, Ladner KJ, Nelsen LL, Damrauer J, Reiser PJ, Swoap S, Guttridge DC. 2004. Cancer cachexia is regulated by selective targeting of skeletal muscle gene products. *J Clin Invest*, 114:370-8.

Ashwell JD. 2008. TWEAKing death. *J Cell Biol*, 182:15-7.

Bagnoli M, Canevari S, Mezzanzanica D. 2010. Cellular FLICE-inhibitory protein (c-FLIP) signalling: a key regulator of receptor-mediated apoptosis in physiologic context and in cancer. *Int J Biochem Cell Biol*, 42:210-3.

Bakkar N, Guttridge DC. 2010. NF-kappaB signaling: a tale of two pathways in skeletal myogenesis. *Physiol Rev*, 90:495-511.

Beck B, Dörfel D, Lichtenegger FS, Geiger C, Lindner L, Merk M, Schendel DJ, Subklewe M. 2011. Effects of TLR agonists on maturation and function of 3-day dendritic cells from AML patients in complete remission. *J Transl Med*, 9:151.

Bertram JS, Janik P. 1980. Establishment of a cloned line of Lewis Lung Carcinoma cells adapted to cell culture. *Cancer Lett*, 11:63-73.

Bertrand MJ, Milutinovic S, Dickson KM, Ho WC, Boudreault A, Durkin J, Gillard JW, Jaquith JB, Morris SJ, Barker PA. 2008. cIAP1 and cIAP2 facilitate cancer cell survival by functioning as E3 ligases that promote RIP1 ubiquitination. *Mol Cell*, 30:689-700.

Beug ST, Cheung HH, LaCasse EC, Korneluk RG. 2012. Modulation of immune signalling by inhibitors of apoptosis. *Trends Immunol*, 33:535-45.

Beug ST, Tang VA, Lacasse EC, Cheung HH, Beauregard CE, Brun J, Nuyens JP, Earl N, St-Jean M, Holbrook J, Dastidar H, Mahoney DJ, Ilkow C, Le Boeuf F, Bell JC, Korneluk RG. 2014. Smac mimetics and innate immune stimuli synergize to promote tumor death. *Nat Biotechnol*, 32:182-90.

Bodine SC, Latres E, Baumhueter S, Lai VK, Nunez L, Clarke BA, Poueymirou WT, Panaro FJ, Na E, Dharmarajan K, Pan ZQ, Valenzuela DM, DeChiara TM, Stitt TN, Yancopoulos GD, Glass DJ. 2001. Identification of ubiquitin ligases required for skeletal muscle atrophy. Science, 294:1704-8.

Bonaldo P, Sandri M. 2013. Cellular and molecular mechanisms of muscle atrophy. *Dis Model Mech*, 6:25-39.

Bonetto A, Aydogdu T, Jin X, Zhang Z, Zhan R, Puzis L, Koniaris LG, Zimmers TA. 2012. JAK/STAT3 pathway inhibition blocks skeletal muscle wasting downstream of IL-6 and in experimental cancer cachexia. *Am J Physiol Endocrinol Metab*, 303:E410-21.

Brooks AD, Sayers TJ. 2005. Reduction of the antiapoptotic protein cFLIP enhances the susceptibility of human renal cancer cells to TRAIL apoptosis. *Cancer Immunol Immunother*, 54:499-505.

Buckingham M, Bajard L, Chang T, Daubas P, Hadchouel J, Meilhac S, Montarras D, Rocancourt D, Relaix F. 2003. The formation of skeletal muscle: from somite to limb. *J Anat*, 202:59-68.

Cai D, Frantz JD, Tawa NE Jr, Melendez PA, Oh BC, Lidov HG, Hasselgren PO, Frontera WR, Lee J, Glass DJ, Shoelson SE. 2004. IKKbeta/NF-kappaB activation causes severe muscle wasting in mice. *Cell*, 119:285-98.

Chen DJ, Huerta S. 2009. Smac mimetics as new cancer therapeutics. *Anticancer Drugs*, 20:646-58.

Cheung HH, Beug ST, St Jean M, Brewster A, Kelly NL, Wang S, Korneluk RG. 2010. Smac mimetic compounds potentiate interleukin-1beta-mediated cell death. *J Biol Chem*, 285:40612-23.

Cheung HH, Mahoney DJ, Lacasse EC, Korneluk RG. 2009. Down-regulation of c-FLIP Enhances death of cancer cells by smac mimetic compound. *Cancer Res*, 69:7729-38.

Cheung HH, St Jean M, Beug ST, Lejmi-Mrad R, LaCasse E, Baird SD, Stojdl DF, Screaton RA, Korneluk RG. 2011. SMG1 and NIK regulate apoptosis induced by Smac mimetic compounds. *Cell Death Dis*, 2:e146.

Croft M, Benedict CA, Ware CF. 2013. Clinical targeting of the TNF and TNFR superfamilies. *Nat Rev Drug Discov*, 12:147-68.

Darding M, Feltham R, Tenev T, Bianchi K, Benetatos C, Silke J, Meier P. 2011. Molecular determinants of Smac mimetic induced degradation of cIAP1 and cIAP2. *Cell Death Differ*, 18:1376-86.

Darding M, Meier P. 2011. IAPs: Guardians of RIPK1. *Cell Death Differ*, 19:58-66.

Das SK, Eder S, Schauer S, Diwoky C, Temmel H, Guertl B, Gorkiewicz G, Tamilarasan KP, Kumari P, Trauner M, Zimmermann R, Vesely P, Haemmerle G, Zechner R, Hoefler G. 2011. Adipose triglyceride lipase contributes to cancer-associated cachexia. *Science*, 333:233-8. Erratum in: *Science*, 2011, 333:1576.

Dean EJ, Ward T, Pinilla C, Houghten R, Welsh K, Makin G, Ranson M, Dive C. 2010. A small molecule inhibitor of XIAP induces apoptosis and synergises with vinorelbine and cisplatin in NSCLC. *Br J Cancer*, 102:97-103.

Donninger H, Vos MD, Clark GJ. 2007. The RASSF1A tumor suppressor. *J Cell Sci*, 120:3163-72.

Dougan M, Dougan S, Slisz J, Firestone B, Vanneman M, Draganov D, Goyal G, Li W, Neuberg D, Blumberg R, Hacohen N, Porter D, Zawel L, Dranoff G. 2010. IAP inhibitors enhance co-stimulation to promote tumor immunity. *J Exp Med*, 207:2195-206.

Dubrez L, Berthelet J, Glorian V. 2013. IAP proteins as targets for drug development in oncology. *Onco Targets Ther*, 9:1285-1304. Review.

Duiker EW, van der Zee AG, de Graeff P, Boersma-van Ek W, Hollema H, de Bock GH, de Jong S, de Vries EG. 2010. The extrinsic apoptosis pathway and its prognostic impact in ovarian cancer. *Gynecol Oncol*, 116:549-55.

Dutton A, Young LS, Murray PG. 2006. The role of cellular FLICE inhibitory protein (c-FLIP) in the pathogenesis and treatment of cancer. *Expert Opin Ther Targets*, 10:27-35.

Enwere EK, Boudreault L, Holbrook J, Timusk K, Earl N, LaCasse E, Renaud JM, Korneluk RG. 2013. Loss of cIAP1 attenuates soleus muscle pathology and improves diaphragm function in mdx mice. *Hum Mol Genet*, 22:867-78.

Enwere EK, Lacasse EC, Adam NJ, Korneluk RG. 2014. Role of the TWEAK-Fn14-cIAP1-NF-κB Signaling Axis in the Regulation of Myogenesis and Muscle Homeostasis. *Front Immunol*, 5:34. Review.

Fearon KC, Glass DJ, Guttridge DC. 2012. Cancer cachexia: mediators, signaling, and metabolic pathways. *Cell Metab*, 16:153-66.

Fidler IJ. 1975. Biological behavior of malignant melanoma cells correlated to their survival in vivo. *Cancer Res*, 35:218-24.

Flygare JA, Fairbrother WJ. 2010. Small-molecule pan-IAP antagonists: a patent review. *Expert Opin Ther Pat*, 20:251-67.

Friboulet L, Gourzones C, Tsao SW, Morel Y, Paturel C, Témam S, Uzan C, Busson P. 2010. Poly(I:C) induces intense expression of c-IAP2 and cooperates with an IAP inhibitor in induction of apoptosis in cancer cells. *BMC Cancer*, 10:327.

Fulda S. 2014. Molecular pathways: targeting inhibitor of apoptosis proteins in cancer--from molecular mechanism to therapeutic application. *Clin Cancer Res*, 20:289-95.

Fulda S. 2013. Targeting c-FLICE-like inhibitory protein (CFLAR) in cancer. *Expert Opin Ther Targets*, 17:195-201.

Fulda S, Vucic D. 2012. Targeting IAP proteins for therapeutic intervention in cancer. *Nat Rev Drug Discov*, 11:109-24. Erratum in: *Nat Rev Drug Discov*, 2012, 11:331.

Geserick P, Drewniok C, Hupe M, Haas TL, Diessenbacher P, Sprick MR, Schön MP, Henkler F, Gollnick H, Walczak H, Leverkus M. 2008. Suppression of cFLIP is sufficient to sensitize human melanoma cells to TRAIL- and CD95L-mediated apoptosis. *Oncogene*, 27:3211-20.

Ghosh G, Wang VY, Huang DB, Fusco A. 2012. NF-κB regulation: lessons from structures. *Immunol Rev*, 246:36-58.

Gopalsamy A, Bennett EM, Shi M, Zhang WG, Bard J, Yu K. 2012. Identification of pyrimidine derivatives as hSMG-1 inhibitors. *Bioorg Med Chem Lett*, 22:6636-41.

Guttridge DC, Mayo MW, Madrid LV, Wang CY, Baldwin AS Jr. 2000. NF-kappaB-induced loss of MyoD messenger RNA: possible role in muscle decay and cachexia. *Science*, 289:2363-6.

Gyrd-Hansen M, Darding M, Miasari M, Santoro MM, Zender L, Xue W, Tenev T, da Fonseca PC, Zvelebil M, Bujnicki JM, Lowe S, Silke J, Meier P. 2008. IAPs contain an evolutionarily conserved ubiquitin-binding domain that regulates NF-kappaB as well as cell survival and oncogenesis. *Nat Cell Biol*, 10:1309-17.

Ili CG, Brebi P, Tapia O, Sandoval A, Lopez J, Garcia P, Leal P, Sidransky D, Guerrero-Preston R, Roa JC. 2013. Cellular FLICE-like inhibitory protein long form (c-FLIPL) overexpression is related to cervical cancer progression. *Int J Gynecol Pathol*, 32:316-22.

Jackman RW, Cornwell EW, Wu CL, Kandarian SC. 2013. Nuclear factor-κB signalling and transcriptional regulation in skeletal muscle atrophy. *Exp Physiol*, 98:19-24.

Jackman RW, Kandarian SC. 2004. The molecular basis of skeletal muscle atrophy. *Am J Physiol Cell Physiol*, 287:C834-43.

Jiang Z, Clemens PR. 2006. Cellular caspase-8-like inhibitory protein (cFLIP) prevents inhibition of muscle cell differentiation induced by cancer cells. *FASEB J*, 20:2570-2.

Johns N, Stephens NA, Preston T. 2012. Muscle protein kinetics in cancer cachexia. *Curr Opin Support Palliat Care*, 6:417-23.

Kachuri L, De P, Ellison LF, Semenciw R; Advisory Committee on Canadian Cancer Statistics. 2013. Cancer incidence, mortality and survival trends in Canada, 1970-2007. *Chronic Dis Inj Can*, 33:69-80.

Katragadda L, Carter BZ, Borthakur G. 2013. XIAP antisense therapy with AEG 35156 in acute myeloid leukemia. *Expert Opin Investig Drugs*, 22:663-70.

Kim IY, Yan X, Tohme S, Ahmed A, Cordon-Cardo C, Shantha Kumara HM, Kim SK, Whelan RL. 2012. CpG ODN, Toll like receptor (TLR)-9 agonist, inhibits metastatic colon adenocarcinoma in a murine hepatic tumor model. *J Surg Res*, 174:284-90.

Krepler C, Chunduru SK, Halloran MB, He X, Xiao M, Vultur A, Villanueva J, Mitsuuchi Y, Neiman EM, Benetatos C, Nathanson KL, Amaravadi RK, Pehamberger H, McKinlay M, Herlyn M. 2013. The novel SMAC mimetic birinapant exhibits potent activity against human melanoma cells. *Clin Cancer Res*, 19:1784-94.

LaCasse EC, Mahoney DJ, Cheung HH, Plenchette S, Baird S, Korneluk RG. 2008. IAP-targeted therapies for cancer. *Oncogene*, 27:6252-75.

Ladner KJ, Caligiuri MA, Guttridge DC. 2003. Tumor necrosis factor-regulated biphasic activation of NF-kappa B is required for cytokine-induced loss of skeletal muscle gene products. *J Biol Chem*, 278:2294-303.

Liston P, Roy N, Tamai K, Lefebvre C, Baird S, Cherton-Horvat G, Farahani R, McLean M, Ikeda JE, MacKenzie A, Korneluk RG. 1996. Suppression of apoptosis in mammalian cells by NAIP and a related family of IAP genes. *Nature*, 379:349-53.

Lu J, Bai L, Sun H, Nikolovska-Coleska Z, McEachern D, Qiu S, Miller RS, Yi H, Shangary S, Sun Y, Meagher JL, Stuckey JA, Wang S. 2008. SM-164: a novel, bivalent Smac mimetic that induces apoptosis and tumor regression by concurrent removal of the blockade of cIAP-1/2 and XIAP. *Cancer Res*, 68:9384-93.

Madonna G, Ullman CD, Gentilcore G, Palmieri G, Ascierto PA. 2012. NF-κB as potential target in the treatment of melanoma. *J Transl Med*, 10:53.

Mahoney DJ, Cheung HH, Mrad RL, Plenchette S, Simard C, Enwere E, Arora V, Mak TW, Lacasse EC, Waring J, Korneluk RG. 2008. Both cIAP1 and cIAP2 regulate TNFalpha-mediated NF-kappaB activation. *Proc Natl Acad Sci U S A*, 105:11778-83.

Matthews GM, Newbold A, Johnstone RW. 2012. Intrinsic and extrinsic apoptotic pathway signaling as determinants of histone deacetylase inhibitor antitumor activity. *Adv Cancer Res*, 116:165-97.

Medema JP, de Jong J, van Hall T, Melief CJ, Offringa R. 1999. Immune escape of tumors in vivo by expression of cellular FLICE-inhibitory protein. *J Exp Med*, 190:1033-8.

Micheau O. 2003. Cellular FLICE-inhibitory protein: an attractive therapeutic target? *Expert Opin Ther Targets*, 7:559-73.

Micheau O, Lens S, Gaide O, Alevizopoulos K, Tschopp J. 2001. NF-kappaB signals induce the expression of c-FLIP. Mol Cell Biol, 21:5299-305.

Moses AG, Maingay J, Sangster K, Fearon KC, Ross JA. 2009. Pro-inflammatory cytokine release by peripheral blood mononuclear cells from patients with advanced pancreatic cancer: relationship to acute phase response and survival. *Oncol Rep*, 21:1091-5.

Nedergaard A, Karsdal MA, Sun S, Henriksen K. 2013. Serological muscle loss biomarkers: an overview of current concepts and future possibilities. *J Cachexia Sarcopenia Muscle*, 4:1-17.

Oceandy D, Cartwright EJ, Neyses L. 2009. Ras-association domain family member 1A (RASSF1A)-where the heart and cancer meet. *Trends Cardiovasc Med*, 19:262-7.

Oliff A, Defeo-Jones D, Boyer M, Martinez D, Kiefer D, Vuocolo G, Wolfe A, Socher SH. 1987. Tumors secreting human TNF/cachectin induce cachexia in mice. *Cell*, 50:555-63.

Op den Kamp CM, Langen RC, Snepvangers FJ, de Theije CC, Schellekens JM, Laugs F, Dingemans AM, Schols AM. 2013. Nuclear transcription factor κB activation and protein turnover adaptations in skeletal muscle of patients with progressive stages of lung cancer cachexia. *Am J Clin Nutr*, 98:738-48.

Oztürk S, Schleich K, Lavrik IN. 2012. Cellular FLICE-like inhibitory proteins (c-FLIPs): fine-tuners of life and death decisions. *Exp Cell Res*, 318:1324-31.

Perego P, Ciusani E, Gatti L, Carenini N, Corna E, Zunino F. 2006. Sensitization to gimatecan-induced apoptosis by tumor necrosis factor-related apoptosis inducing ligand in prostate carcinoma cells. *Biochem Pharmacol*, 71:791-8.

Petersen SL, Wang L, Yalcin-Chin A, Li L, Peyton M, Minna J, Harran P, Wang X. 2007. Autocrine TNFalpha signaling renders human cancer cells susceptible to Smac-mimetic-induced apoptosis. *Cancer Cell*, 12:445-56.

Piao X, Komazawa-Sakon S, Nishina T, Koike M, Piao JH, Ehlken H, Kurihara H, Hara M, Van Rooijen N, Schütz G, Ohmuraya M, Uchiyama Y, Yagita H, Okumura K, He YW, Nakano H. 2012. c-FLIP maintains tissue homeostasis by preventing apoptosis and programmed necrosis. *Sci Signal*, 5:ra93.

Pietanza MC, Ladanyi M. 2012. Bringing the genomic landscape of small-cell lung cancer into focus. *Nat Genet*, 44:1074-5.

Probst BL, Liu L, Ramesh V, Li L, Sun H, Minna JD, Wang L. 2010. Smac mimetics increase cancer cell response to chemotherapeutics in a TNF-α-dependent manner. *Cell Death Differ*, 17:1645-54.

Qin S, Yang C, Li S, Xu C, Zhao Y, Ren H. 2012. Smac: Its role in apoptosis induction and use in lung cancer diagnosis and treatment. *Cancer Lett*, 318:9-13.

Ranjan K, Surolia A, Pathak C. 2012. Apoptotic potential of Fas-associated death domain on regulation of cell death regulatory protein cFLIP and death receptor mediated apoptosis in HEK 293T cells. *J Cell Commun Signal*, 6:155-68.

Ricciardi S, Tomao S, de Marinis F. 2009. Toxicity of targeted therapy in non-small-cell lung cancer management. *Clin Lung Cancer*, 10:28-35.

Romanick M, Thompson LV, Brown-Borg HM. 2013. Murine models of atrophy, cachexia, and sarcopenia in skeletal muscle. *Biochim Biophys Acta*, 1832:1410-20.

Ruan H, Hacohen N, Golub TR, Van Parijs L, Lodish HF. 2002. Tumor necrosis factor-alpha suppresses adipocyte-specific genes and activates expression of preadipocyte genes in 3T3-L1 adipocytes: nuclear factor-kappaB activation by TNF-alpha is obligatory. *Diabetes*, 51:1319-36.

Russell SJ, Peng KW, Bell JC. 2012. Oncolytic virotherapy. *Nat Biotechnol*, 30:658-70.

Safa AR. 2012. c-FLIP, a master anti-apoptotic regulator. *Exp Oncol*, 34:176-84.

Schiaffino S, Reggiani C. 2011. Fiber types in mammalian skeletal muscles. *Physiol Rev*, 91:1447-531.

Schultz DR, Harrington WJ Jr. 2003. Apoptosis: programmed cell death at a molecular level. *Semin Arthritis Rheum*, 32:345-69.

Scudiero I, Zotti T, Ferravante A, Vessichelli M, Reale C, Masone MC, Leonardi A, Vito P, Stilo R. 2012. Tumor necrosis factor (TNF) receptor-associated factor 7 is required for TNFα-induced Jun NH2-terminal kinase activation and promotes cell death by regulating polyubiquitination and lysosomal degradation of c-FLIP protein. *J Biol Chem*, 287:6053-61.

Shirley S, Micheau O. 2013. Targeting c-FLIP in cancer. *Cancer Lett*, 332:141-50.

Silke J, Strasser A. 2013. The FLIP Side of Life. *Sci Signal*, 6:pe2.

Siomek A. 2012. NF-κB signaling pathway and free radical impact. *Acta Biochim Pol*, 59:323-31.

Stojdl DF, Lichty BD, tenOever BR, Paterson JM, Power AT, Knowles S, Marius R, Reynard J, Poliquin L, Atkins H, Brown EG, Durbin RK, Durbin JE, Hiscott J, Bell JC. 2003. VSV strains with defects in their ability to shutdown innate immunity are potent systemic anti-cancer agents. *Cancer Cell*, 4:263-75.

Sun SC. 2012. The noncanonical NF-κB pathway. *Immunol Rev*, 246:125-40.

Tan BH, Fearon KC. 2008. Cachexia: prevalence and impact in medicine. *Curr Opin Clin Nutr Metab Care*, 11:400-7.

Tan BH, Ross JA, Kaasa S, Skorpen F, Fearon KC; European Palliative Care Research Collaborative. 2011. Identification of possible genetic polymorphisms involved in cancer cachexia: a systematic review. *J Genet*, 90:165-77.

Tintignac LA, Lagirand J, Batonnet S, Sirri V, Leibovitch MP, Leibovitch SA. 2005. Degradation of MyoD mediated by the SCF (MAFbx) ubiquitin ligase. *J Biol Chem*, 280:2847-56.

Tisdale MJ. 2005. Molecular pathways leading to cancer cachexia. *Physiology*, 20:340-8.

Tornatore L, Thotakura AK, Bennett J, Moretti M, Franzoso G. 2012. The nuclear factor kappa B signaling pathway: integrating metabolism with inflammation. *Trends Cell Biol*, 22:557-66.

Tran T, Andersen R, Sherman SP, Pyle AD. 2013. Insights into skeletal muscle development and applications in regenerative medicine. *Int Rev Cell Mol Biol*, 300:51-83.

van der Weyden L, Adams DJ. 2007. The Ras-association domain family (RASSF) members and their role in human tumourigenesis. *Biochim Biophys Acta*, 1776:58-85.

Vince JE, Chau D, Callus B, Wong WW, Hawkins CJ, Schneider P, McKinlay M, Benetatos CA, Condon SM, Chunduru SK, Yeoh G, Brink R, Vaux DL, Silke J. 2008. TWEAK-FN14 signaling induces lysosomal degradation of a cIAP1-TRAF2 complex to sensitize tumor cells to TNFalpha. *J Cell Biol*, 182:171-84.

Vultur A, Herlyn M. 2013. SnapShot: melanoma. *Cancer Cell*, 23:706-706e1.

Wang S. 2011. Design of small-molecule Smac mimetics as IAP antagonists. *Curr Top Microbiol Immunol*, 348:89-113.

White SJ, Lu P, Keller GM, Voelkel-Johnson C. 2006. Targeting the short form of cFLIP by RNA interference is sufficient to enhance TRAIL sensitivity in PC3 prostate carcinoma cells. *Cancer Biol Ther*, 5:1618-23.

Wu H, Tschopp J, Lin SC. 2007. Smac mimetics and TNFalpha: a dangerous liaison? *Cell*, 131:655-8.

Xu Y, Zhou L, Huang J, Liu F, Yu J, Zhan Q, Zhang L, Zhao X. 2011. Role of Smac in determining the chemotherapeutic response of esophageal squamous cell carcinoma. *Clin Cancer Res*, 17:5412-22.

Yang JK. 2008. FLIP as an anti-cancer therapeutic target. Yonsei Med J, 49:19-27.

Yusuf F, Brand-Saberi B. 2012. Myogenesis and muscle regeneration. *Histochem Cell Biol*, 138:187-99.

Zaas AK, Schwartz DA. 2005. Innate immunity and the lung: defense at the interface between host and environment. *Trends Cardiovasc Med*, 15:195-202.

Zhang L, Fang B. 2005. Mechanisms of resistance to TRAIL-induced apoptosis in cancer. *Cancer Gene Ther*, 12:228-37.

Zhang G, Jin B, Li YP. 2011. C/EBPβ mediates tumour-induced ubiquitin ligase atrogin1/MAFbx upregulation and muscle wasting. *EMBO J*, 30:4323-35.

Zhang S, Li G, Zhao Y, Liu G, Wang Y, Ma X, Li D, Wu Y, Lu J. 2012. Smac mimetic SM-164 potentiates APO2L/TRAIL- and doxorubicin-mediated anticancer activity in human hepatocellular carcinoma cells. *PLoS One*, 7:e51461.

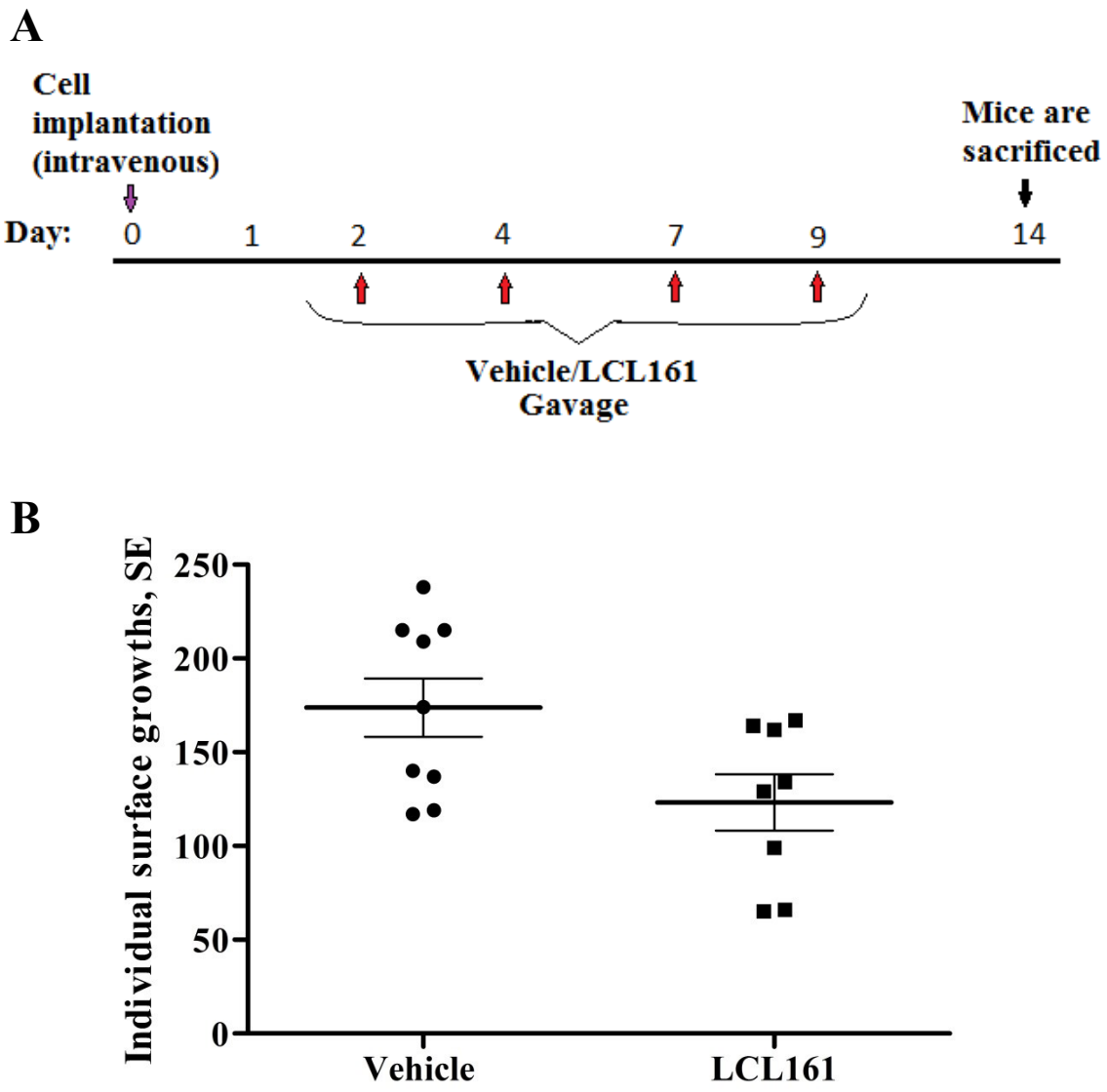

Figure 30. SMC treatment does not sensitize B16F10 lung nodules to caspase-8 mediated cell death.

B16F10 cells, which located to the immune reactive lung environment, remained resistant to SMC treatment. C57BL/6 mice were intravenously injected with 3 x 10^5 B16F10 cells and received four treatments of 50mg/kg LCL161 as seen in (A). Mice were sacrificed on day 14 and the number of surface lung nodules were counted, averaged and graphed to compare vehicle (n = 9) treated versus LCL161 (n = 8) treated mice (B). SE = standard error.

APPENDIX II

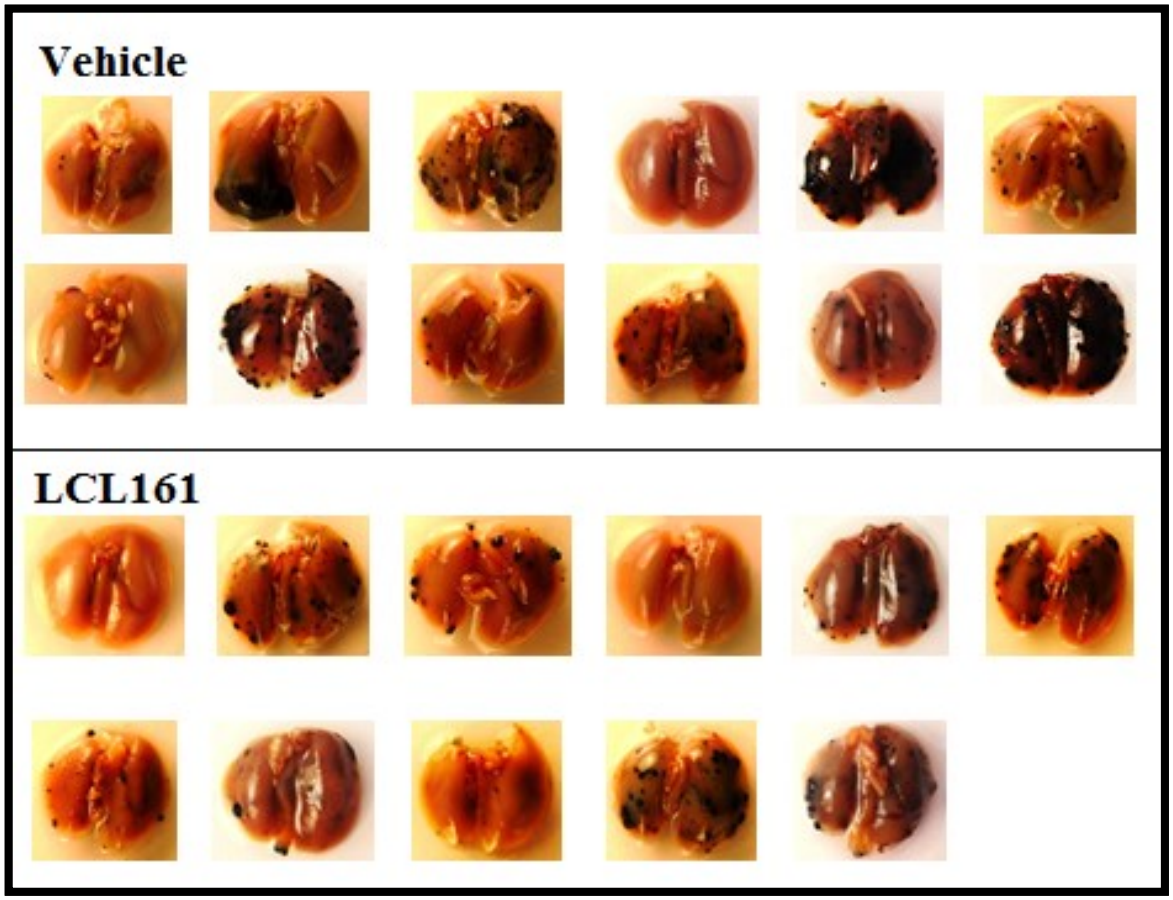

Figure 31. No significant difference in number of B16F10 lung nodules when mice are treated with SMC.

B16F10 cells, which located to the immune reactive lung environment, remained resistant to SMC treatment. C57BL/6 mice were intravenously injected with 3 x 10^5 B16F10 cells and received four treatments of 50mg/kg LCL161. Mice were sacrificed on day 14 and the lungs were dissected and preserved in paraformaldehyde. Shown here is the comparison of the number of lung nodules in the lungs of vehicle (n = 12) treated versus LCL161 (n = 11) treated mice.

APPENDIX III

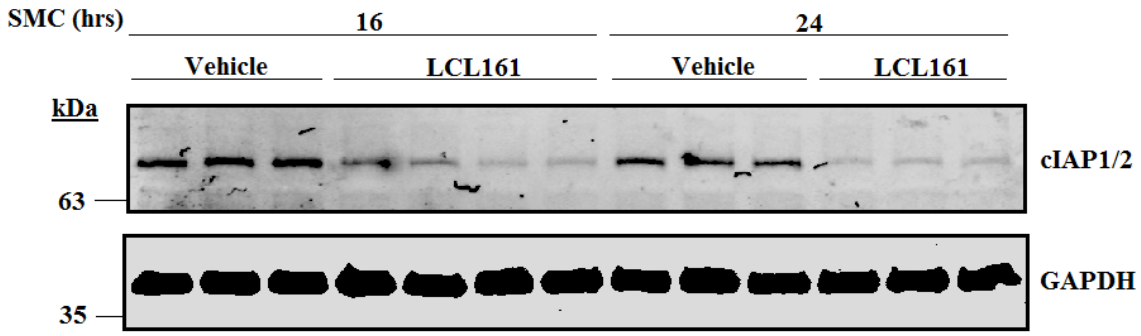

Figure 32. LCL161 targets cIAP1/2 in the tibialis anterior muscle of B16F10 tumour bearing mice.

The loss of cIAP1/2 occurs with the addition of SMC thus stimulating the activation of the alternative NF-κB pathway. Mice were injected with 3 x 10^5 B16F10 cells. Once tumours were established, mice were gavaged once with 50mg/kg LCL161 and sacrificed at either 16 hours or 24 hours post-treatment. The TA muscles were harvested and subjected to Western immunoblotting with antibodies against SMC targets. GAPDH was used as a loading control.